BIO-POLYMERIC HEAVY METAL ADSORBING MATERIALS FOR INDUSTRIAL WASTEWATER TREATMENT

Report to the

WATER RESEARCH COMMISSION

by

H W J P Neomagus

Research Group of Separation Science and Technology
North-West University (Potchefstroom Campus)

WRC Report No 1072/1/05
ISBN No 1-77005-341-7

AUGUST 2005

Disclaimer

This report emanates from a project financed by the Water Research Commission (WRC) and is approved for publication. Approval does not signify that the contents necessarily reflect the views and policies of the WRC or the members of the project steering committee, nor does mention of trade names or commercial products constitute endorsement or recommendation for use.

EXECUTIVE SUMMARY

BACKGROUND AND MOTIVATION

A clean supply of water is an essential requirement for the establishment of a healthy community. It acts not only as a source of potable water, but also supports the growth of aquatic life, thereby providing valuable food supplements. Nowadays, despite its importance, water throughout South Africa is polluted and a particular area of concern is the release of heavy metals by the industrial sector into sewage streams and natural waters. Impure water, containing excessive levels of metals such as copper, zinc, nickel and mercury, is hazardous to human, animal, aquatic and plant life. Due to their toxic and often carcinogenic nature, as well as the careless disposal of large quantities into the environment, heavy metals have been prioritised as leading contaminants in South Africa. Since heavy metal ions are often even toxic at low concentrations and are not biodegradable, they must be removed from the contaminated water. Due to the financial value of some heavy metals it is also important to recover these metals from wastewater. In this study, the removal and recovery of heavy metals using the biosorbent chitosan is investigated

EXPERIMENTAL APPROACH

In this study, different forms of chitosan have been prepared from chitin flakes, obtained from rock lobster waste from the seafood processing industry by BioSpec (Cape Town), in order to use the chitosan material for the adsorption of heavy metals from wastewater. Firstly, the chitin flakes were converted to chitosan flakes, and after characterisation of the material, large similarities with commercial chitosan (biopolymer engineering) were found. Since flakes do not have good adsorption characteristics and are difficult to use in large equipment, other configurations (beads, membranes and immobilised chitosan) were prepared for the experimental adsorption studies. All configuration techniques used, were based on the phase inversion method, in which chitosan is dissolved in acetic acid and later precipitated in a caustic soda bath. The adsorption experiments were carried out at a laboratory scale.

RESULTS

Technical results

Using the phase inversion method, a gel type of material is formed, which contains predominantly water (93-96%) and the balance chitosan (4 – 7%). Initial experiments showed, that chitosan in the gel form has much better adsorption characteristics than chitosan flakes (affinity parameter is at least a factor 10 higher for beads compared to flakes).

Beads

When using beads, a high adsorption capacity of 160 mg/g for copper was obtained, and the affinity parameter was 0.07 L/mg, values that are larger than reported values for activated carbon and measured values for ion exchange resins (in this study Amberlite 200C was used as reference). During adsorption column experiments using a 10 ppm copper solution, at least 550 Bed-volumes were processed to a < 1 ppm (WHO limit) effluent solution, in three cycles of adsorption and desorption. The copper could be recovered using an acid of pH = 1, obtaining a copper solution of 1200 ppm, which could be processed further to recover the metal in its pure form. The beads were stable to only 5 cycles, using the high acid concentration. When milder desorption conditions (pH = 2), the effluent copper solution only contained about 100 mg/g, making further processing more difficult. During the adsorption process, the diffusion inside the beads played an important role in the total mass transfer. An effort was therefore undertaken to reduce the size of the beads, which resulted in beads with an average diameter of 1.8 mm, a size that still results in a negligible pressure difference over the column.

For the chitosan beads, a novel adsorption model has been developed, which takes the acid base characteristics of the chitosan into account. The new model can therefore be used at any pH, for both adsorption and desorption. From this model, it could be concluded that the chitosan has the largest affinity to copper, followed by lead, nickel, zinc and cadmium

Membranes

Chitosan membranes have been prepared according to a method quite similar to the production of beads. The membranes were characterised and it was found that the membranes could be modelled as a porous hydrated membrane and showed large similarities with ultrafiltration membranes, both for the flux of clean water and salt solutions. The membranes showed large affinities to Zn (maximum adsorption capacity 135 mg/g and affinity parameter of 0.02 mg/L at a pH of 6). The adsorption could well be described with a Langmuir isotherm in the region from 20 – 40 °C. The adsorption capacity increased from 20 – 30 °C and remained constant between 30 and 40 °C. The increase of the capacity could be due to a better accessibility of sites, caused by an increase in free volume of the biopolymer. The affinity parameter also increased in temperature, indicating an exothermic adsorption process. The membranes could be recycled effectively (>95%) using sulphuric acid (pH = 2), but after 2 cycles of adsorption and desorption the membranes were damaged and could not be used anymore. This was possibly caused by the acid, which was pumped through the membrane during desorption (SEM analysis revealed that after crosslinking the edges of the membrane were more cross-linked than in the centre of the membrane).

Immobilised chitosan

Immobilised beads were prepared by the coating of a thin chitosan layer (around 20 μm) on an alumina support. Very high adsorption capacities (> 200 mg Cu/g) were obtained when a porogen was used. The porogen makes the active sides easily available.

Non - technical results

Since chitosan is only produced at a small scale, the prices on the world market are relatively high ($ 35/kg). Since the market for chitosan is rapidly growing (mainly for the application of fat absorber), price decreases are expected in the future. The production costs for the preparation of chitosan are largely determined by the conversion of chitin to chitosan; a process that uses an excess of caustic soda. Without reuse of the soda, a price of around $6/kg is estimated. This price can be reduced to an approximated $ 0.6/kg if the caustic soda is recycled effectively. The cost for cleaning contaminated water is then about $ 0.06/m^3, not taking into account the investment for an adsorption/desorption plant. Although excellent adsorption characteristics have been obtained for immobilised chitosan, the production of the ceramic support is still very expensive (> $ 200 / m^2), which makes this technique less applicable for water purification.

ADVANTAGES AND DISADVANTAGES

In general, we can conclude that chitosan (in the gel form) is a very effective adsorbent. It can adsorb the studied metals Cu, Zn, Pb, Ni and Cd to a very high degree, higher than their economical counterparts, such as activated carbon and ion exchange resins. A general disadvantage of chitosan is that the stability is not very good. In the case of beads, chitosan could be recycled 5 times and for membranes only 2 times, which makes a long-term use of the biopolymer impossible. The harsh conditions, under which the desorption process takes place, is the main reason for this. Milder desorption conditions, however, would result in a more dilute metal stream, which again is unfavourable for further processing and recovery of the metal.

In comparing the three configurations studied in this project, the following table can be presented, in which the three different configurations are compared on adsorption, flux, stability characteristics and costs.

	Beads	Membranes	Immobilised on alumina
Adsorption	+	+	++
Flux	+ / -	+	+
Stability	+ / -	-	Not studied
Costs	+	+	--

Chitosan immobilised on alumina shows excellent adsorption characteristics above beads and membranes, but is rather expensive because of the high production costs involved in the preparation of the ceramic supports; also the low capacity per volume requires large equipment (only a thin layer of chitosan is deposited). Comparing chitosan membranes with beads, it can be concluded that beads are more stable than membranes. However, the advantage of using chitosan membranes is that a pressure difference is used to induce convective flow through the membrane, which in turn results in a higher throughput, compared to the diffusive transport inside the bead, which is the rate determining step in the adsorption column. (Also, slightly higher adsorption capacities could be obtained with membranes, compared to beads).

RECOMMENDATIONS

An improved crosslinking technique for membranes should be found in order to solve the stability problems. If such a technique could not be found, the use of adsorption beads in an adsorption/desorption column would be the recommended process, which can process metal contaminated wastewater at relative low concentrations (< 10 ppm) to disposal water, meeting the most stringent legislation, against a price of about $ 0.06/m^3.

ACKNOWLEDGMENTS

- The author is grateful to the Water Research Commission (WRC) for its financial support without which this research would not have been possible

- Acknowledgments to the steering commission for the valuable input given at the annual meetings

- The research focus area Separation Science and Technology (SST) of the North-West University and the Chemical Engineering group of the Vaal University of Technology are acknowledged for their fiscal and infrastructure support

- Finally, a large project as this could never have been realised without the hard work of several students. Many thanks to these students and I hope you have learned a lot from the different projects you did

TABLE OF CONTENTS

EXECUTIVE SUMMARY I
ACKNOWLEDGMENTS V
LIST OF FIGURES VIII
LIST OF TABLES X
LIST OF SYMBOLS XI

1 INTRODUCTION 1
1.1 Chitosan 1
1.2 Applications of chitosan 3
1.3 Availability and prices of chitosan 4
1.4 Scope and objectives 5

2 CHITOSAN PREPARATION 7
2.1 Isolation of chitin 7
2.2 Deacetylation 8
2.3 Commercial chitosan 9

3 FORMULATION OF CHITOSAN 11
3.1 Chitosan beads 11
3.2 Chitosan membranes 12
3.3 Immobilised chitosan 13
3.3.1 Support Preparation 14
3.3.2 Preparation of the chitosan coating 14

4 CHITOSAN BEADS 16
4.1 Relevant theory for adsorption and desorption in chitosan beads 16
4.1.1 Proposed equilibrium model 16
4.1.2 Particle model 17
4.1.3 Column breakthrough simulations 19
4.1.4 Adsorber column simulation 21
4.2 Characterisation of chitosan beads 22
4.2.1 Chitosan stability/water content 22
4.2.2 Accessibility of metal ions in gel bead 23
4.2.3 Protonated Amino Sites 24
4.2.4 Total amount of amino sites obtained from titration data 27
4.2.5 Degree of deacetylation 30
4.3 Experimental Procedures (methodology) 30
4.3.1 Determination of metal-ion concentration in the water samples 30
4.3.2 Adsorption studies at lab scale 31
4.3.3 Desorption 31
4.3.4 Multiple adsorption – desorption cycles 32
4.3.5 Adsorption in a column with chitosan beads 32
4.3.6 Desorption in a column with chitosan beads 33
4.4 Results and discussion 33
4.4.1 Batch experiments 34
4.4.2 Column experiments 39
4.4.3 Comparison with other adsorbents 45
4.5 Conclusions 45

5 CHITOSAN MEMBRANES 47
5.1 Characterisation of membranes 47
5.1.1 Introduction 47
5.1.2 Characterisation techniques used 47
5.1.3 Results and discussion of characterisation 50
5.2 Transport through chitosan membranes 56
5.3 Relevant adsorption theory 58
5.3.1 General adsorption theory 58
5.3.2 Adsorption on chitosan 60
5.3.3 Desorption of ions from chitosan membranes 63
5.4 Experimental procedures 63
5.5 Results and discussion 64
5.5.1 The adsorption equilibrium of zinc ions 65
5.5.2 The effect of temperature on adsorption 67
5.5.3 Dynamics of zinc adsorption by chitosan membranes 68
5.5.4 Adsorption of other metal ions 69
5.5.5 Desorption and recovery 70
5.6 Conclusions 72

6 IMMOBILISED CHITOSAN 74
6.1 Characterisation of ceramic support and chitosan coating 74
6.1.1 Strength test of supports 74
6.1.2 Structure of support 74
6.1.3 Flux and adsorption experiments 74
6.2 Characterisation results 74
6.2.1 Support characterisation 74
6.2.2 Chitosan layer characterisation 76
6.3 Results and discussion adsorption 79
6.4 Conclusions 81

7 ECONOMIC CONSIDERATIONS 82

8 GENERAL CONCLUSIONS 84

9 REFERENCES 87

LIST OF FIGURES

Figure 1.1 Chitin molecular structure 1
Figure 1.2 Chitosan molecular structure 2
Figure 2.1 Schematic representation of the production of chitosan material and derivatives of chitosan 7
Figure 2.2 Production equipment for chitin and chitosan 9
Figure 3.1 Schematic representation of experimental set-up for the production of chitosan beads 12
Figure 4.1 Schematic representation of shrinking core model 18
Figure 4.2 Photo of bead. (After 1 hour adsorption, 300 ppm, diameter 3.8 mm) 18
Figure 4.3 hrinking core model overview 19
Figure 4.4 chematic representation of column 21
Figure 4.5 Excel simulation overview 21
Figure 4.6 Crosslinking mechanism of chitosan with glutaraldehyde 23
Figure 4.7 Titration curves for the crosslinked and non-crosslinked chitosan 24
Figure 4.8 IR spectra of non-crosslinked chitosan bead (NXLB) and crosslinked chitosan bead (XLB) 25
Figure 4.9 Titration curves for new and aged beads 26
Figure 4.10 The degree of protonation obtained from the titration data. 28
Figure 4.11 Curves for chitosan suspension and chitosan beads in acid solution 29
Figure 4.12 Curves of pH changes titrated with 1.0 M HCl against chitosan solutions without copper and with copper 29
Figure 4.13 Schematic representation of the used column set-up 32
Figure 4.14 Precipitation interval for the different metal ions studied 33
Figure 4.15 The logarithm of the adsorption constant (K or K_{ads}) as a function of pH (both adsorption and desorption have been taken into account here) 34
Figure 4.16 Percentage of desorption as a function of pH 35
Figure 4.17 Equilibrium constant multiple adsorption cycles 36
Figure 4.18 Equilibrium constant measurement for Cu^{2+}, Pb^{2+}, Zn^{2+}, Cd^{2+}, & Ni^{2+} ions 37
Figure 4.19 The adsorption of copper and zinc on in a binary mixture at pH = 5 38
Figure 4.20 The adsorption of copper and cadmium on in a binary mixture at pH = 5 38
Figure 4.21 Adsorption of Cu^{2+} on beads as a function of time using a diffusion constant 6×10^{-11} m2/s (initial concentration is varied from 50 – 100 ppm) 39
Figure 4.22 Breakthrough: 10 ppm, c vs Bed Volumes 40
Figure 4.23 Desorption with 0.2 M HCl 41
Figure 4.24 Desorption with 0.02 M HCl 41
Figure 4.25 Breakthrough curves for 2 cycles at different flow rates 42
Figure 4.26 Breakthough curve for copper adsorption for 5 cycles of adsorption and desorption 44
Figure 4.27 Copper concentration in the acid solution after desorption as a function of the bedvolume 44
Figure 5.1 Schematic drawing of a bubble-point test apparatus 49
Figure 5.2 Effect of chitosan concentration (Chitosan A) on the wet membrane density 50
Figure 5.3 Effect of chitosan concentration on the chitosan content (the % dry material in a membrane) of the membranes 51
Figure 5.4 Effect of chitosan concentration on the porosity of wet chitosan membranes 52
Figure 5.5 Effect of chitosan concentration (Chitosan A) on the maximum pore adius of the wet chitosan membranes 52
Figure 5.6 Effect of chitosan concentration (Chitosan A) on the total surface area of dried chitosan membranes 53

Figure 5.7 Dried Chitosan Membrane structures (Chitosan A) before zinc adsorption (a) and after zinc adsorption (b) (Surface view) 53
Figure 5.8 Effect of Chitosan Concentration (Chitosan A) on the dry membrane characteristics..... 54
Figure 5.9 Side view of chitosan membrane structure..... 55
Figure 5.10 Pure water flux as a function of the pressure difference (membrane thickness = 0.8 mm and T = 298K)..... 56
Figure 5.11 Schematic drawing of the relationship between flux and applied pressure for different zinc concentrations (Membrane thickness = 0.8 mm)..... 57
Figure 5.12 Limiting flux J plotted as a function of the logarithm of the bulk concentration..... 58
Figure 5.13 Formation of chitosan chelates with copper ions (as suggested by Kaminski et al., 1997 60
Figure 5.14 Equilibrium capacity after recirculation of zinc sorption onto a 0.8 mm chitosan membrane 65
Figure 5.15 Experimental data modelling using Langmuir equation for corrected concentration..... 66
Figure 5.16 Van der Waals plot of Zinc sorption onto a 0.8 mm chitosan membrane 67
Figure 5.17 The breakthrough profile of zinc solutions (Membrane thickness = 0.8 mm and 100 kPa pressure difference) compared to copper solutions..... 68
Figure 5.18 Schematic drawing of the breakthrough profile for zinc solutions 69
Figure 5.19 Schematic drawing of the regeneration of chitosan membranes using different acids..... 71
Figure 5.20 Schematic drawing of the regeneration cycles of chitosan membranes using sulphuric acid solution at a pH of 2..... 72
Figure 6.1 SEM picture of an inner surface of a centrifugal casted AKP-15 support sintered at 1150^{oC} 76
Figure 6.2 SEM micrograph of Chi-NaOH membrane before adsorption of $Cu2^{+}$ 77
Figure 6.3 SEM micrograph of Chi-Si-NaOH membrane after $Cu2^{+}$ adsorption..... 77
Figure 6.4 SEM micrograph of Chi-Si-NaOH-Cross membrane after $Cu2^{+}$ adsorption 78
Figure 6.5 Concentration of $Cu2^{+}$ ions in permeate as a function of the volume in the permeate..... 79
Figure 7.1 Different treatment techniques for different contaminant concentrations.....82

LIST OF TABLES

Table 1.1 Applications of chitosan.....4
Table 1.2 SABS standards for water quality 6
Table 2.1 Molecular weight determination using SEC.....10
Table 2.2 Molecular weight of chitosan.....10
Table 4.1 Solubility of chitosan in acidic solutions 22
Table 4.2 % metal ion accessibility in chitosan gel bead.....24
Table 4.3 Characterised chitosan parameters 26
Table 4.4 Results multiple adsorption cycles.....35
Table 4.5 Adsorption constant for different metal ions 37
Table 4.6 Experimental settings.....40
Table 4.7 Summary of initial column results 40
Table 4.8 Additional adsorption parameters at 8 ml/min.....43
Table 4.9 Additional adsorption parameters at 18 ml/min 43
Table 4.10 Specifications of Amberlyte 200C Na, as delivered by RHOM and HAAS.....45
Table 4.11 The adsorption characteristics of different adsorbent for copper.....45
Table 5.1 Composition of chitosan membrane 51
Table 5.2 Langmuir constants for zinc adsorption at different temperatures.....66
Table 5.3 Theoretical and experimental adsorption capacity for SA chitosan.....70
Table 5.4 Chitosan membrane adsorption compared to the highest adsorption capacities on other adsorbent materials for the metal ion zinc 70
Table 6.1 Properties of the different types of ceramic tubular supports.....75
Table 6.2 Liquid transport data of pure water, the $Cu2^{+}$-solution and the relative resistance of the chitosan coating for several alumina/chitosan membranes.....78
Table 6.3 Comparison of literature values with the value obtained in this study for the maximum adsorption of $Cu2^{+}$ ions by chitosan.....80
Table 8.1 Pros and Cons for different formulations of chitosan.....86

LIST OF SYMBOLS

Roman

Symbol	Description	Unit
a	Specific surface area	m^2/kg
b	Langmuir adsorption constant	L/mg
c_{final}	Final metal concentration	mol/L
$c_{initial}$	Initial metal concentration	mol/L
c_i	Bulk concentration	
C_B	Bulk metal concentration	mol/m^3
C_e	Equilibrium concentration	mol/m^3
C_S	Metal concentration at the bead surface	mol/m^3
d	Bead diameter (twice the radius)	m
D_{eff}	Effective diffusivity of metal ion within the bead	m^2/s
D_{water}	Diffusivity of metal ion in water	m^2/s
H	Adsorption enthalpy	J/mol
J	Flux	L/m^2 h
$J_{limiting}$	Limiting flux	L/m^2 h
K_a	Acid base equilibrium constant	m^3/mol
K_{ads}	Adsortion equilibrium constant	
K_F	Freundlich adsorption constant	mg/g
K_L	Langmuir adsorption constant	L/g
k_L	External mass transfer coefficient	m/s
$m_{dry\ chitosan}$	Mass of dry chitosan	g
$m_{emmbrane}$	Mass of membrane	g
M_n	Number averaged molecular weight	g/mol
M_w	Average molecular weight	g/mol
n	Freundlich adsorption constant	
P	Pressure	bar
Q	Adsorption loading	mol/kg
q_{ads}	Equilibrium adsorption loading	mg/g
qm	Maximum adsorption loading	mg/g
R	gas constant	J/mol K
R_S	Bead radius	m
r_p	Pore diameter	m
T	Temperature	K
t	Time	s
$V_{membrane}$	Volume of membrane	L
$V_{solution}$	Volume of metal solution	L
v_∞	bulk fluid velocity	m/s

Greek

Symbol	Description	Unit
α	Degree of protonation (DOP)	-
ε	porosity	-
γ	surface tension	N/m
μ, η	Viscosity of liquid	kg/m·s
?	Fractional adsorbent loading (Q/Qmax)	-
?	Bead density (dry mass/wet volume)	kg/m^3
$?_{membrane}$	Membrane density	kg/m^3
$?_f$	Fluid density	kg/m^3
τ	tortuosity	-

1 INTRODUCTION

Water pollution is a significant problem in South Africa. Almost all fresh water resources have already been utilised and the population growth and economical development will only increase the demand for fresh water, while pollution is threatening its availability. The mayor sources of water pollution in South Africa are industrial effluents, domestic and commercial sewage, acid mine drainage, agricultural runoff, and litter. Nutrients, sediments, acidic compounds, salts, heavy metals and biocides are considered the most important pollutants.

Especially industrial and mining effluents contribute to the pollution of water with heavy metals. There are several methods to remove heavy metals from wastewater. Examples are precipitation, oxidation and reduction, ion exchange, filtration, reverse osmosis, electrochemical removal and evaporative recovery. Besides these methods biosorption using either living or dead biomass has been proposed as an alternative method.

When heavy metals are present at trace concentrations, most available methods become inefficient and adsorption-processes are a good alternative in these cases.

1.1 Chitosan

Chitin (poly(beta-(1,4)-2-acetamido-2-deoxy-D-glucose, chemical formula see Figure 1.1) is one of the most naturally available biopolymers. It is widely available in the exoskeletons of anthropods, and can be manufactured from crab, lobster and shrimp shell wastes. The deacetylated form of chitin is poly(Beta-(1,4)-2-amino-2-deoxy-D-glucose) and is called chitosan (see Figure 1.2). In practice it is impossible to deacetylate chitin completely. If the substance has a degree of deacetylation of more than 50%, it is called chitosan. If the degree of deacetylation is less than 50%, it is called chitin. Chitin and chitosan are non-toxic and readily biodegradable [Chui et al., 1996].

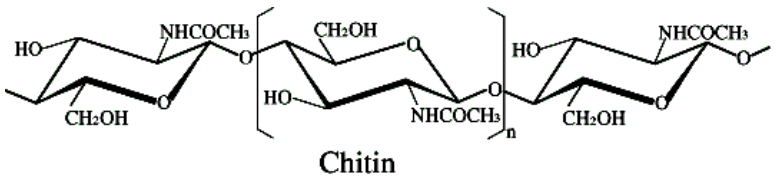

Chitin

Figure 1.1: Chitin molecular structure

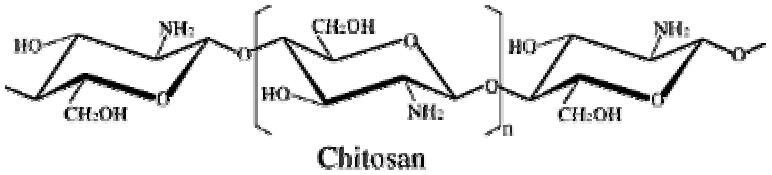

Figure 1.2: Chitosan molecular structure

Chitosan is not soluble in water or organic solvents. It does dissolve in water-ethanol, water-methanol, water-acetone and other mixtures if an amount of acid is added. Formic and acetic acid are also able to dissolve chitosan. At higher acid concentrations organic acids are also able to dissolve it [Muzarelli, 1973]. Muzarelli reported that chitosan is not soluble in sulphuric acid, because the insoluble salt chitosan sulphate is formed [Muzarelli, 1973]. According to Mcafee *et al.* [2001] chitosan dissolves in metal solutions adjusted to pH 2 with hydrochloric acid. They found that it also dissolves in metal solutions with a pH adjusted below 3 with H_2SO_4 as well as in 1N H_2SO_4.

Chitosan, having an amino group, is also a weak base. The acid constant (pKa) of chitosan is in the range of 6.2-7 depending on the degree of deacetylation [Guibal, 2001]. Juang *et al.* [1999] mention a pKa of 6.3. Ruiz *et al.* [2000] report 6.2-6.5. However, for polyelectrolytes (like chitosan), the acid constant depends on the net charge of the polymer. So the apparent acid constant varies with the pH [Rhazi *et al.*, 2002a & b].

For chitosan from crab shells, Muzarelli reported an average molecular weight (Mw) of $1.2 \cdot 10^5$. The molecular weight of chitosan decreases significantly during the production process. In the process of decalcification high concentrations of acid solutions are used. Hydroxide is used for deacetylation. In both acid and hydroxide solutions chain degradation occurs, however the effect of basic solutions is less pronounced than that of acid solutions [Muzarelli, 1977].

Isogai reported a degree of polymerisation (DP_w) for 4 chitin samples ranging from 7510-9050 and the polydispersity (DP_w/DP_n) ranging from 2.1 to 3.3. The chitosan derived from the same chitin sources had a degree of polymerisation of 2910-990. The polydispersity was between 3.6 and 5.9. These results show that some depolymerisation occurs during deacetylation [Isogai, 1997].

1.2 Applications of chitosan

There are many more applications for chitosan besides adsorption of heavy metals. Many potential products using chitosan have been developed, including flocculating agents for water and waste treatment, coatings to improve dyeing characteristics of glass fibers, wet strength additives for paper, adhesives, photographic and printing applications, thickeners, and fibers and films. Table 1.1 gives an overview of the most common applications (www.primex.no).

Unlike most polysaccharides, chitosan has a strong positive charge, which allows it to bind to negatively charged surfaces such as hair and skin. This makes it useful as an ingredient in skin and hair care products (www.seaborne.com/chitinguide.htm).

The reason for the explosive growth in the number of manufacturers and distributors of chitosan might be its newfound acceptance as a diet aide. The chitosan craze was triggered by a book, *The Fat Blocker Diet*, written by Dr. Arnold Fox and Brenda Adderly, and published in 1997. Variously called "the fat magnet," the "fat trapper," or a "sponge," chitosan is thought to inhibit fat digestion by dissolving in the stomach, emulsifying fat in the stomach contents, and forming a gel in the intestine, which entraps the fat and prevents intestinal absorption. Chitosan can be found in local drug stores and vitamin shops. Other health benefits like the promotion of the growth of Bifidobacteria (a healthy bacteria), inhibiting bad and promoting good cholesterol, controlling high blood pressure and preventing irritable bowel syndrome are also ascribed to chitosan. It is also reported to have anti-tumor properties. Besides the positive properties of chitosan there are also some bad properties mentioned. It is said to reduce the uptake of minerals and fat soluble vitamins. It might also block birth control pills (ntp-server.niehs.nih.gov/htdocs/Chem_Background/ExSumPdf /Chitosan.pdf, www.all-natural.com/binder.html).

Table 1.1: Applications of chitosan

HEALTHCARE:
- Wound-healing ointments
- Orthopedics
- Wound dressing
- Anticholesterol and fat-binding
- Surgical sutures
- Drug delivery
- Ophthalmology
- Skin treatments
- Dentistry
- Transportation of cells

WASTE AND WATER TREATMENT:
- Drinking water
- Recovering metals
- Pools and spas
- Treating food wastes

FOOD AND BEVERAGES:
- Anticholesterol and fat-binding
- Food stabilizer
- Flavors and tastes
- Food packaging
- Nutritional additives
- Fruit preservation

PRODUCT SEPARATION AND RECOVERY:
- Membrane separation
- Encapsulating adsorbents
- Chromatographic columns
- Coagulation

AGRICULTURE:
- Seed treatments
- Feed ingredients
- Nematocides
- Insecticides

COSMETICS AND TOILETRIES:
- Hair care
- Skin care
- Oral care

1.3 Availability and prices of chitosan

Chitosan is produced from chitin. Chitin is the second most available biopolymer (after cellulose). Nature synthesizes at least 10 gigatons of chitin each year, which is degraded in the biosphere. Chitin is a renewable resource and only a small fraction of the chitin available is used in industry (www.euchis.org). In 1994, the total world consumption of chitin and chitosan was estimated to be more than 1,000 tons with 800 tons being used in Japan. Since 1994 the production of chitin and chitosan has increased a lot. Whereas in 1997 only two US companies were producing chitosan, in 1999 it was manufactured or distributed by 45. And capacity is still growing rapidly (http://ntp-server.niehs.nih.gov/htdocs/Chem_Background/ExSumPdf/Chitosan.pdf).

Biopolymer Engineering (United States) has a chitosan plant in El Salvador producing 200 tons annually. This will have increased to 1,000 tons by the end of 2003 and is planned to increase to 2,000 tons per year, then being the largest chitosan plant in the world (www.biopolymer.com).

1.4 Scope and objectives

It is the scope of this project to study the possibility of manufacturing chitosan for the application in removal of heavy metals from wastewater. The following objectives can therefore be given

- Produce chitosan from a local source and compare the chitosan with commercially produced chitosan

- Prepare different formulations of chitosan in order to find an optimum adsorbent in terms of adsorption properties and economical considerations.

- Study the different formulations of chitosan for the removal of heavy metals from wastewater and compare the biomaterial with conventional adsorption (and other) techniques

- Determine whether it is economical profitable to use chitosan for the removal of heavy metals from wastewater and identify for what type of wastewater stream the novel technology could be used.

The experiments will be carried out in order to produce wastewater streams that follow the acceptable SABS levels as given in Table 1.2.

Chapter 1 gives an introduction about the importance of the removal of heavy metals and gives some background information about chitosan. In Chapter 2, the production of the raw material is reported, while in Chapter 3, the different formulations of chitosan are described. Chapter 4, 5 and 6 reports about the different formulations of chitosan: chitosan beads, chitosan membranes and immobilised chitosan respectively. In Chapter 7, some economical considerations around the novel separation technique are given. The general conclusions are listed in Chapter 8.

Table 1.2: SABS standards for water quality

Determinands	**Units**	**Upper limit Ranges**		
		Class 0 (Ideal)	**Class I (Acceptable)**	**Class II (Max. Allowable)**
Physical and organoleptic requirements				
Colour	mgPt/l	15	20	50
Conductivity at 25 ^{O}C	mS/m	70	150	370
Dissolved solids	mg/l	450	1 000	2 400
Odour	TON	1	5	10
pH value at 25 ^{O}C	pH units	6.0 - 9.0	5.0 - 9.5	4.0 - 10.0
Taste	FTN	1	5	10
Turbidity	NTU	0.1	1	10
Chemical requirements: Macro-determinands				
Ammonia as N	mg/l	0.2	1.0	2.0
Calcium as Ca	mg/l	80	150	300
Chloride as Cl	mg/l	100	200	600
Fluoride as Fl	mg/l	0.7	1.0	1.5
Magnesium as Mg	mg/l	30	70	100
Nitrate and nitrite as N	mg/l	6.0	10.0	20
Potassium as K	mg/l	25	50	100
Sodium as Na	mg/l	100	200	400
Sulphate as SO_4	mg/l	200	400	600
Zinc as Zn	mg/l	3.0	5.0	10.0
Chemical requirements: Micro-determinands				
Aluminium as Al	µg/l	150	300	500
Antimony as Sb	µg/l	5	10	50
Arsenic as As	µg/l	10	50	200
Cadmium as Cd	µg/l	3	5	20
Chromium as Cr	µg/l	50	100	500
Cobalt as Co	µg/l	250	500	1 000
Copper as Cu	µg/l	500	1 000	2 000
Cyanide (free) as CN	µg/l	70	70	70
Cyanide (recoverable) as CN	µg/l	70	200	300
Iron as Fe	µg/l	10	200	2 000
Lead as Pb	µg/l	10	50	100
Manganese as Mn	µg/l	50	100	1 000
Mercury as Hg	µg/l	1	2	5
Nickel as Ni	µg/l	50	150	350
Selenium as Se	µg/l	10	20	50
Vanadium as V	µg/l	100	200	500
Chemical requirements: Organic determinands				
Dissolved organic carbon as C	mg/l	5	10	20
Total trihalomethanes	mg/l	100	200	300
Phenols as phenol	mg/l	5	10	70

2 CHITOSAN PREPARATION

The preparation of chitosan consists of several steps (Figure 2.1). After the chitin is isolated from the raw material source, it is deacetylated to yield chitosan. After deacetylation, the chitosan is formulated in beads, membranes or immobilised on alumina pellets. Schematically the production of the chitosan material used in this project is schematically given in the following

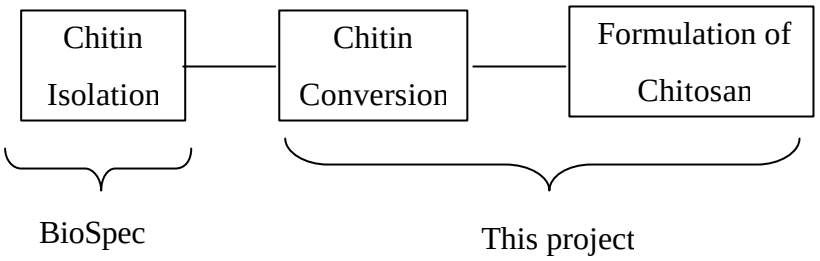

Figure 2.1: Schematic representation of the production of chitosan material and derivatives of chitosan

2.1 Isolation of chitin

Isolation of chitin from crustacean shell waste usually consists of three steps: protein separation – deproteinisation, calcium carbonate (and calcium phosphate) separation – demineralisation and removal of pigments – decolouration. Deproteinisation is usually carried out with a dilute sodium or potassium hydroxide solution (1-10%) at elevated temperature (65-110°C). The reaction time is usually 0.5 to 6 hours. Demineralisation can be performed with dilute hydrochloric acid at room temperature, for a period of 2 to 3 hours. To prevent depolymerisation, some researchers have used mild acids like EDTA or acetic acid. Different reagents have been reported for decolouration of chitin of different sources. Ethanol, ether, acetone, NaOCl and ethyl acetate are some of them [Kyoon No et al., 1997]. The raw material, chitin, used in this study was obtained from BioSpec (Cape Town). The following synthesis route was used:

1. Crushing of shells to small particle size (1 mm or less in diameter)
2. Water was heated in the heating tank to a temperature of 80°C. The water was then transferred into the reaction tank where the sodium hydroxide was added to a concentration of 8% aqueous sodium hydroxide. Adding the sodium hydroxide the heat produced increased the temperature in the tank to 100°C. Lastly, the crushed shells were transferred into the reaction tank for deproteinisation for 6 hours, under well-mixed conditions. A ratio of 0.5 kg of NaOH solution for every 1-kg shells was used.
3. The liquid was then drained from the reaction tank into the neutralisation tank where it was neutralised with hydrochloric acid under well-stirred conditions.

4. The shells were washed three times with water. It was washed by stirring for ten minutes in the reaction tank with five times the volume of water per volume of shells.
5. Demineralisation was carried out in the reaction tank by stirring in 10% hydrochloric acid for 6 hours.
6. The shells were washed by stirring for ten minutes in the reaction tank with five times the volume of water per volume of shells.
7. The chitin was then drained with the last washing cycle through a nylon mesh.
8. The chitin was dried in an oven at 50°C for 6 hours.

2.2 Deacetylation

Both acidic and basic solutions can deacetylise chitin. However, in acid solutions deacetylation is not possible without depolymerisation. Therefore base solutions are used for the synthesis of chitosan from chitin. Chitin monomers posses a hydroxyl group trans related to the acetamido group. These monomers are much harder to deacetylise than the ones possessing a cis group [Muzarelli, 1977]. Different methods of preparation of chitosan are reported in literature and most of them use potassium or sodium hydroxide to deacetylate chitin and reach a degree of deacetylation of 80-92% [Muzarelli, 1973]. Deacetylation to a degree higher than 80% is hardly possible without degrading the polymer. Because depolymerisation takes place during the treatment with hydroxide, the deacetylation should not be extended for too long (30 minutes is usually enough). Deacetylation in an inert atmosphere yields chitosan with a higher viscosity than deacetylation in air. Deacetylation in two stages of 30 minutes with washing in between is as effective as one step of 15 hours, while yielding chitosan with a higher viscosity [Muzarelli, 1977]. The concentration of the sodium hydroxide is usually 40-50%, the temperature around 100°C. Higher temperatures will increase the percentage of deacetylation but reduce the molecular size. The ratio chitin solids to alkali solution is usually between 1:10 and 1:100 [Kyoon No et al., 1997]. Some alternative methods are mentioned by Chui et al. [1996] and Kyoon No et al. [1997]. The production of chitosan from chitin was carried out according to the procedure as given by Huang et al. (1996). The equipment used for the conversion is given in Figure 2.2.

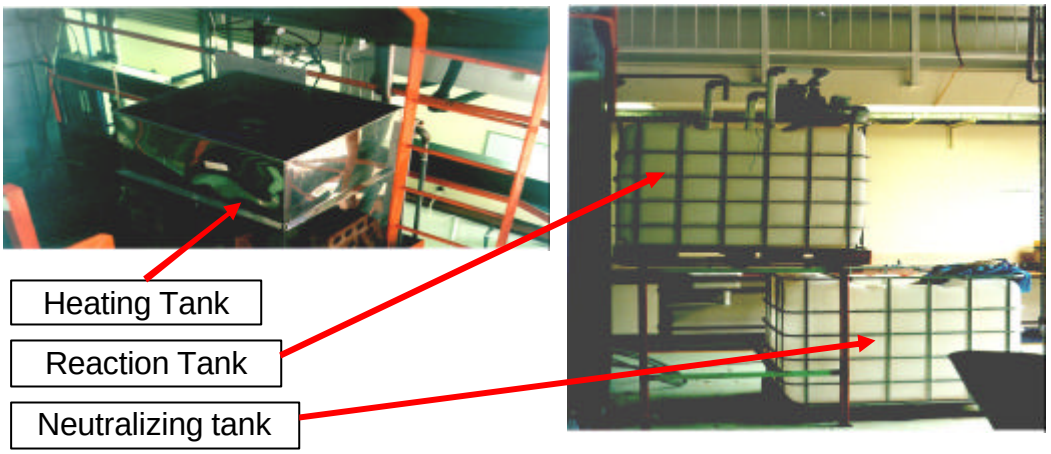

Figure 2.2: Production equipment for chitin and chitosan

1. Water was heated in the heating tank to a temperature of 80°C. The water was then transferred into the reaction tank where the sodium hydroxide was added to a concentration of 50% aqueous sodium hydroxide. On adding the sodium hydroxide the heat produced increased the temperature in the tank to 120°C. Lastly the chitin was transferred into the reaction tank for deacetylation (45 kg of sodium hydroxide solution to 1 kg of chitin) for 6 hours at an initial starting temperature of 120°C.
2. The liquid was then drained from the reaction tank into the neutralisation tank where it was neutralised with hydrochloric acid under well-stirred conditions.
3. The chitosan was washed by stirring for ten minutes in a container with five times the volume of water per volume of chitosan.
4. The chitosan was dried in an oven at 50°C for 3 hours.
5. The chitosan is obtained as flakes

2.3 Commercial chitosan

Next to the locally prepared chitosan, also chitosan flakes were purchased from Biopolymer Engineering, Eagan, Minnesota, United States (the largest producer of chitosan worldwide). This chitosan was studied for the comparison with the locally prepared membranes.

The chitosan materials used for the adsorption process in this work were obtained from two sources. One of them is Cape rock lobster (Jasus lalandii), obtained from South Africa and is mostly used in this study, and the other is Squat Lobster (Pleuroncodes monodon), from El-Savador, which has been studied as reference material. The most important parameter of the biopolymer, the molecular weight and distribution are given in Table 2.1. As shown in this table, the molecular weight of the beads is larger than the flakes they were made from although the flakes particle used were sieved through 100 µm sieve. This increase in the

molecular weight is suspected to be polymerisation in the cause of beads production (Jansen at al., 2002) however, the measured molecular weight is comparable to those reported in literature, see Table 2.2.

Table 2.1: Molecular weight determination using SEC

Sample	M_w (g/mol)	M_n (g/mol)	M_w/M_n
Local chitosan			
Flakes	78400 (4%)	35200 (15%)	2.23 (16%)
Beads-NXL	940000 (4%)	40100 (13%)	2.35 (15%)
Commercial chitosan			
Flakes	70600 (5%)	41800 (11%)	1.69 (13%)
Beads-NXL	11400 (6%)	56200 (9%)	2.02 (12%)

Table 2.2: Molecular weight of chitosan

Method employed	M_w (g/mol)	% degree of deacetylation	Author
Size Exclusion Chromatograph (SEC)	$7.8x\ 10^4$	82	This work
Viscometric (using Mark-Houwink eqn.)	4.1×10^5	87	Juang & Shao, 2002
Viscometric (using Mark-Houwink eqn.)	8.4×10^4	96	Rhazi, et al., 2002
Size Exclusion Chromatograph (SEC)	1.2×10^5	87	Guibal, et al., 1999

3 FORMULATION OF CHITOSAN

If chitin is converted to chitosan, chitosan is obtained in the form of flakes. Flakes, in general have 2 distinctive disadvantages:

- The nature of the flakes makes it rather difficult to work with in e.g. an adsorption column
- Flakes have a rather dense structure, which makes the interior of the flakes impermeable for the metal ions

Therefore, next to chitosan flakes, the following forms of chitosan are studied:

- Chitosan beads
- Chitosan membranes
- Immobilised chitosan

3.1 Chitosan beads

The adsorption capacity is often limited by the diffusion of the ions into the pores of the chitosan particles, when many pores are blocked. One way to improve the accessibility in the pores is to produce chitosan in the form of gel beads. Gel formation is expected to lead to an increase in the polymer network opening and in the accessibility to adsorption sites. Guibal et al. found a larger adsorption capacity for chitosan beads compared to flakes. They contributed this to the expansion of the polymer network. They tested beads with three different diameters (0.95 mm, 1.6 mm and 2.8 mm). There was no difference in sorption capacity for the different bead diameters, but there was a difference in adsorption kinetics. The smallest beads showed the largest rate of adsorption [Guibal et al., 1997].

Guibal and his colleges produced gel beads by dissolving chitosan in an acetic acid solution (4 w/w %) to a final concentration of 4% (w/w). The solution was allowed to stand for 7 days. After this, the solution was filtered onto 0.5 mm sieve. The solution was pumped drop wise into a sodium hydroxide solution (2.5 M) through a 0.6 mm nozzle. To reduce the diameter of the beads air was blown through an annular space around the nozzle. The air causes the beads to fall in the hydroxide solution before they obtain their usual size [Guibal et al., 1997]. In this project, the beads were prepared according to the following procedure:

A 3%(v/v) acetic acid solution in water was made by pipetting acetic acid (99.7+%, Aldrich) in a volumetric flask. Dry chitosan flakes were dissolved in the acetic acid solution to form a 7%(w/w) chitosan solution. After dissolving, the solution was filtered. The solution was pumped through a glass pipette using a peristaltic pump (Watson Marlow 313S) and dropped into a 1.0 M NaOH (Labchem, Edenvale) - solution, while stirring both solutions. After all

chitosan solution was used, the beads were left in the NaOH solution overnight. The beads were washed with distilled water until constant (neutral) pH and stored in distilled water. The average bead diameter could be decreased, by flowing air along the spinnerette (see Figure 3.1)

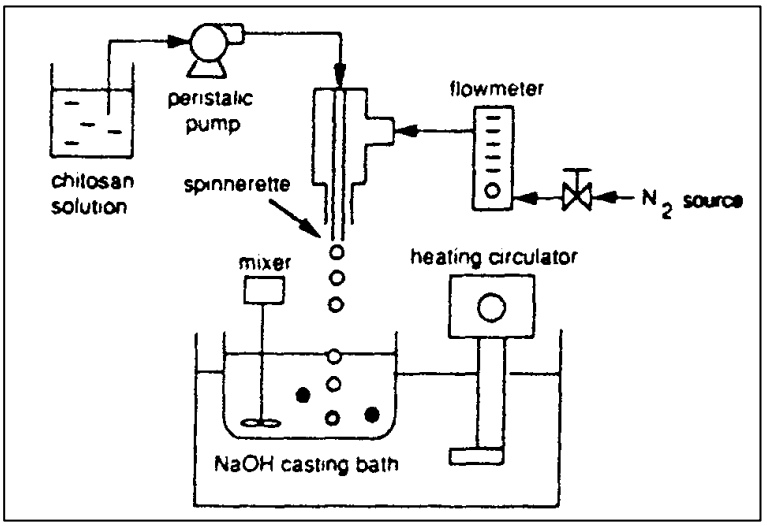

Figure 3.1: Schematic representation of experimental set-up for the production of chitosan beads

Chitosan has the characteristic to be solvable in acidic media. Since the desorption (recovery) takes place at low pH, it is requested that the different forms of chitosan are stabilised. A well-known technique for the stabilisation of chitosan is cross-linking. Cross-linking can be carried out chemically or physically. Chemical cross-linking is usually carried out with glutaraldehyde or epichlorohydrin. When chitosan beads are cross-linked using glutaraldehyde, they are resistant to a pH lower than 3. Cross-linking also improves the mechanical strength. For the preparation of the beads in this study, a 2.5%(w/w) glutaraldehyde solution is prepared from a 50% solution (Aldrich). 1.5 ml of the solution is used per gram of gel beads. The beads reacted with the glutaraldehyde solution for 24 hours at room temperature. After the reaction, the beads are washed several times with distilled water and stored. The gel beads have a white colour.

3.2 Chitosan membranes

In this section, the production of several chitosan membranes is reported. Since the production of chitosan membranes is less reported on than beads, different important process variables for manufacturing the membrane (chitosan-, acetic acid- and NaOH concentration) were varied. The membranes were produced using a phase inversion method as described by Kaminski et al. (1997), and consists of the following steps:

Dissolving chitosan (1-9 mass %) into an acetic acid solution (1-7 mass %) using a magnetic stirrer. A constant speed of 100 rpm and a dissolution time of 24 hours were used. The viscous solution was poured into a mould on a flat surface (glass plate). The mould and chitosan solution was than carefully placed into an aqueous solution of sodium hydroxide (1-9 mass %) for 15 minutes at a constant temperature of 25 °C. After the membranes were formed, they were washed, using flowing tap water for 2 minutes, and the membrane and the mould were removed from the glass plate. The membrane was then removed from the mould and conditioned in demineralised water for 1 hour. After conditioning, the membrane was washed in demineralised water again until a neutral pH was obtained. Throughout the process of manufacturing, the temperature was monitored and remained constant at 25 °C. The average dimensions of the disk shaped membranes obtained after this method were 0.8-mm thickness with a 47-mm diameter.

To prevent chitosan dissolving in acidic media, the membranes were crosslinked, also according to the procedure described by Guibal et al. (1999). In this method, the membranes were crosslinked with a 2.5 mass% solution of glutaraldehyde for a period of 6 hours at 25 °C. A volume of 1.5-cm^3 glutaraldehyde solution per gram of wet membrane was used. After crosslinking the membranes were washed thoroughly to remove all glutaraldehyde.

After varying the different process conditions, the viscosity of the chitosan solution was the most important factor in producing the membranes. A low chitosan concentration results in a low viscosity solution and a mechanical weak membrane is obtained. Those membranes also have low chitosan contents resulting in a low adsorption capacity per volume membrane. A high chitosan concentration forms mechanical strong membranes up till a chitosan concentration of 8.0 %. At higher chitosan concentrations, the membranes form locally holes that can act as shortcut roads for the wastewater to be treated, and is therefore undesirable. The production route was optimised in terms of a maximum adsorption and flux, and the optimum conditions were found to be a 7.0% chitosan solution dissolved in a 4.0% acetic acid solution and precipitated in a 4.0% NaOH solution. The optimised cross-linking time was 6.0 hours.

3.3 Immobilised chitosan

Another formulation technique for chitosan is to immobilise the chitosan on a support. The motivation behind this formulation technique is to obtain a thin layer of chitosan, which is easily accessible (compared to flakes and beads) for the wastewater to treat. In this section, ceramic (alumina) cylindrical supports have been used as support.

3.3.1 Support Preparation

The α-Al_2O_3 powders for the manufacture of the supports were AKP-30 and AKP-15 (Sumitomo Chemical Company, Ltd., Japan), with a mean particle size of 0.40 and 0.62 μm and a BET surface area of 6.2 and 3.5 $m^2.g^{-1}$ respectively. A 50:50 % w/w mixture of the two types of powders was used. To obtain tubes with 2 mm wall thickness and ~20 mm diameter, 120 g of the starting powder was mixed with different amounts of APMA (Ammonium PolyMethAcrylate aqueous solution, Darvan C, R.T. Vanderbilt Company, Inc., Norwalk, USA) and distilled water. For the AKP-15, AKP-30 and supports of the powder mixtures, 10 ml, 20 ml and 15 ml of APMA were used respectively due to the difference in surface area of the powders. The mixture of water and APMA, 120 ml in total was set at pH = 9.5 by adding (~1.5 ml) concentrated ammonia. The resulting suspension was ultrasonically treated for 15 minutes using a frequency of 20 kHz and a transducer output power of 100 W (Model 250 Sonifier, Branson Ultrasonics Corporation, Danbury, USA). With this suspension, tubes of 6 cm in length were prepared in a home-built apparatus using steel moulds. Before pouring the suspension into the mould, the inside of the mould was coated with a solution of Vaseline in petroleum ether (boiling range 60-80°C) to ensure easy mould release. The tubes were centrifuged for 20 minutes at 20.000 rpm and afterwards the remaining liquid was poured out of the moulds. The green tubes were horizontally dried inside the moulds for one day at 30°C. After drying, the green tubes were removed from the moulds and sintered horizontally for 1 hour on a flat surface at 1050°C, 1150°C and 1200°C respectively. The heating/cooling rate was 1°C/min (For more details, see Steenkamp et al., 2001).

3.3.2 Preparation of the chitosan coating

Four different types of coatings were investigated:

<u>Standard chitosan membrane (Chi membrane)</u>

A solution of chitosan was prepared by dissolving 1 g of commercial chitosan flakes (Aldrich Chemical Company, Inc., High molecular, with a minimum degree of deacetylation of 75 %) in 100 ml of a 1 vol % aqueous acetic acid solution.

An AKP-30 (1050°C) support was cut to a length of 5 cm (Area = 26.7 cm^2). The support was filled with the chitosan solution. The excessive solution was then removed so that only a thin chitosan layer remained on the inside of the support. This procedure was repeated before drying, and the acetic acid solution on the inside of the support was allowed to evaporate.

In order to prevent shrinkage of the membrane during drying, it was immersed in a 20 vol % aqueous glycerol solution (softening agent) before drying for 30 min at 30°C. Subsequently, the excess glycerol solution was removed before the composite membrane was dried at room temperature for 1 hour (Chi membrane).

The three other methods were used to increase the porosity and to improve the stability of the chitosan coating.

Chitosan membrane treated with sodium hydroxide (Chi-NaOH membrane)

The same procedure was used as before. Afterwards the dried support with the chitosan layer was immersed in a 5 wt % aqueous NaOH solution for 2 hours at 80°C. Subsequently the wet membrane was immersed in an aqueous glycerol solution for 30 min to prevent shrinkage. The system was then dried at room temperature for 1 hour.

Macroporous chitosan membrane (Chi-Si-NaOH membrane)

The preparation of this membrane was based on the phase inversion method using silica as a porogen to create pores in the coated chitosan layer (Zeng and Ruckenstein, 1996). One gram of chitosan was dissolved in 100 ml of a 1 vol % aqueous acetic acid solution, then 1 g silica particles (Riedel-de Haën, Silica gel 60 (0.063-0.200 mm)) was added to this solution, followed by vigorous stirring to ensure a uniform dispersion. The AKP-30 (1050°C) ceramic support was filled with the chitosan-silica solution and the liquid was allowed to evaporate. The dried membrane was immersed in a 5 wt % aqueous NaOH solution for 2 hours at 80°C in order to dissolve the silica particles to generate a porous membrane. The heat treatment accelerated the dissolution of silica and also improved the mechanical properties of the membrane. Finally, the porous membrane was washed with distilled water to remove the remaining NaOH. In order to prevent shrinkage during drying, the membrane was immersed in a 20 vol % aqueous glycerol solution (softening agent) for 30 min and, after the excess glycerol solution was removed, dried at room temperature for 1 hour.

Macroporous chitosan membrane cross-linked with epichlorohydrin (Chi-Si-NaOH-Cross membrane).

The membrane was prepared in the same way as the macroporous membrane in the previous section. The macroporous membrane was cross-linked under mild alkaline conditions using epichlorohydrin as the cross-linker. The chitosan membrane was immersed in 1 x 10^{-2} M epichlorohydrin solution containing 0.067 M NaOH (pH = 10) for 2 hours at 50°C. The membrane was taken out of the solution and rinsed with distilled water until all NaOH had been neutralized.

4 CHITOSAN BEADS

4.1 Relevant theory for adsorption and desorption in chitosan beads

This project is related to the adsorption (and possible recovery) of heavy metals from wastewater on different forms of chitosan. Therefore, relevant theory concerning adsorption (and desorption) is shortly presented here. Since chitosan, due to its nature, behaves different than traditional adsorbents, a relative new theory has been derived and tested (quantified) in this work. This information is later used to predict the behaviour of chitosan in full-scale applications (e.g. a chitosan bead adsorption column). Chitosan membranes have also been studied in this project, and relevant theories, concerning membrane technology, will also be presented. Since the proposed adsorption model is relative new, this will be presented separately. Other relevant theory will be discussed during the presentation of the model.

4.1.1 Proposed equilibrium model

The study of adsorption is traditionally carried out via, so called, isotherms. An isotherm gives the relation between the amount of adsorbed species as a function of the concentration of that specie in the surroundings (gas or liquid) at a constant temperature. In the case of chitosan, the adsorption of heavy metals is accomplished with the release of hydronium ions (change of pH). Generally, in such cases, the isotherms are studied at constant pH, which is experimentally troublesome. In this project, it is attempted to take the effect of pH into account, so that it is not strictly necessary to keep the pH constant for different experiments. Rhazi et al. (2002a) showed that for chitosan NH2-groups and hydroxide ions are involved in the adsorption of heavy metals, and suggested the following equilibrium:

$$Cu^{2+}(aq) + R\text{-}NH_2 + H_2O \leftrightarrow ((Cu(NH_2))OH)^+ (= Cu_{ads}) + H^+ \qquad 4.1$$

With the following equilibrium constant

$$K_{ads} = \frac{[(Cu(NH_2)OH)^+] \cdot [H^+]}{[R-NH_2] \cdot [Cu^{2+}(aq)]} \qquad 4.2$$

Since chitosan is also a base, the following acid-base equilibrium reaction is also taking place simultaneously:

$$R\text{-}NH_2 + H^+ \leftrightarrow R\text{-}NH_3^+ \qquad 4.3$$

With the following equilibrium constant, Ka:

$$K_a = \frac{\left[R-NH_3^+\right]}{\left[R-NH_2\right]\left[H^+\right]} \qquad 4.4$$

This reaction can be studied independently via a titration curve and e.g. the degree of protonation can be determined as a function of the pH. The acid/base character of chitosan has a pronounced effect on the adsorption characteristics. Since amino groups are the active groups for both adsorption of heavy metals and protonation, there is a competition between the metal ion and the hydronium ion for the amino group. It is therefore to be expected that the adsorption of metals is favoured at high pH. So, the amino groups can be in its free form, attached to a heavy metal or in its acid form. The total number of amino groups is therefore:

$$\left[R-NH_2\right]_{\text{total}} = [R-NH_2]+[R-NH_3^+]+[Cu_{ads}] \qquad 4.5$$

The important constants, K_{ads}, can be obtained from a combination of both equilibrium equations together with the mass balance for the amino groups:

$$K_{ads} = \frac{[Cu_{ads}][H^+]}{[Cu_{aq}]([R-NH_2]-[Cu_{(ads)}])} \cdot \frac{\left(K_a+[H_3O^+]\right)}{K_a} \qquad 4.6$$

where [R-NH_2] is calculated from:

$$[RNH_2] = ([RNH_2]_T - [Cu_{(ads)}]).\left(\frac{K_a}{K_a+[H_3O^+]}\right) \qquad 4.7$$

The total number of available NH_2 sites per gram chitosan can also be obtained from titration experiments.

4.1.2 Particle model

Next to the adsorption equilibrium constants, the dynamics of adsorption are also important for practical implications (e.g. the design and operation of an adsorption column will greatly depend on the kinetics of adsorption). Firstly, a particle model is presented and in the next section, this particle model is included in a column model.

In an article by Swan et al. (1975) a particle theory is presented for the adsorption of metal ions unto spherical particles. A shrinking core model is assumed (see Figure 4.1). When the adsorption starts with fresh beads, adsorption is assumed to take place in the outer layer of the beads. As the adsorption proceeds the outer metal loaded shell becomes bigger and the active, unloaded core becomes smaller. The model is based on the assumption that the rate of

diffusion through the outer fully loaded shell is equal to the rate of adsorption in the active core and that the diffusion is rate limiting, not the adsorption itself. Another assumption is that the equilibrium constant is high enough to ensure maximum adsorption loading in the loaded shell, for every concentration in the solution.

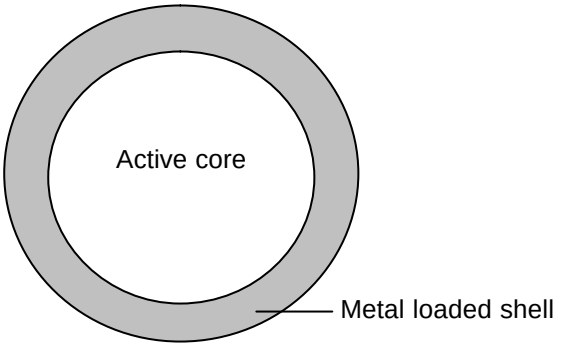

Figure 4.1: Schematic representation of shrinking core model

An electron microscope picture of a 3.8 mm diameter bead taken after one hour of adsorption actually shows a metal loaded shell around the inner unloaded core (see Figure 4.2). It can be seen from this figure that the outer skin of the bead already has adsorbed copper ions, while the inner parts of the bead is still unutilised, supporting the shrinking core theory.

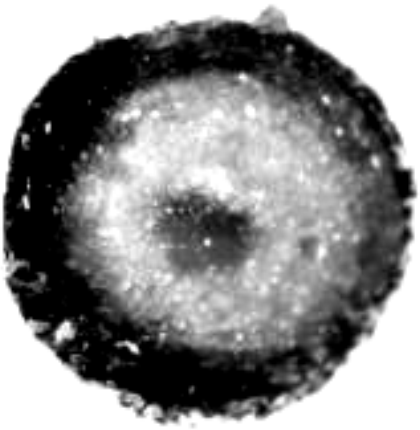

Figure 4.2: Photo of bead. (After 1 hour adsorption, 300 ppm, diameter 3.8 mm)

With the above-mentioned set of assumptions, the following rate equations can be derived:

$$\frac{\partial Q}{\partial t} = \frac{3D_{eff} \cdot C_S}{R_s^2 \cdot r\left(\frac{1-(1-q)^{1/3}}{(1-q)^{1/3}}\right)} \qquad 4.8$$

With:

C_S	metal concentration at the bead surface	mol/m^3
D_{eff}	effective diffusivity of metal ion within the bead	m^2/s
Q	adsorption loading	mol/kg
R_S	bead radius	m
t	time	s
?	fractional adsorbent loading (Q/Qmax)	-
?	bead density (dry mass/wet volume)	kg/m^3

For the maximum adsorption capacity, the adsorption loading that is in equilibrium with the bulk metal concentration is calculated using the proposed equilibrium model.

When a batch experiment is performed in which the Erlenmeyer is shaken properly, external diffusion has a negligible effect on the rate of adsorption (Grant). The metal concentration at the particle interface is equal to the concentration in the bulk. If this dynamic experiment is carried out, the diffusion coefficient can be fitted from the linearised adsorption time figure, schematically given in the following figure.

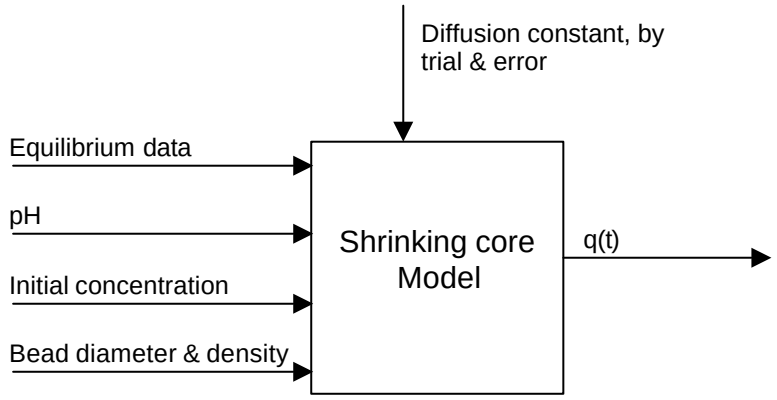

Figure 4.3: Shrinking core model overview

4.1.3 Column breakthrough simulations

An industrial application of chitosan beads could be the treatment of wastewater in an adsorber column. The column is loaded with chitosan beads and the wastewater is passed through it. After a certain adsorption loading has been reached, the copper concentration at the column exit will be too high and the column has to be regenerated. Regeneration can be done using an acid.

When designing an adsorber column, predictions have to be made about the behaviour of the column. The exit concentration as function of the time, a so-called breakthrough curve, has to be predicted.

If external diffusion contributes to the rate of adsorption the single particle model can be extended to:

$$\frac{\partial Q}{\partial t} = \frac{k_L a \dfrac{3D_{eff}}{R_s^2 \cdot r\left(\dfrac{1-(1-q)^{1/3}}{(1-q)^{1/3}}\right)}}{k_L a + \dfrac{3D_{eff}}{R_s^2 \cdot r\left(\dfrac{1-(1-q)^{1/3}}{(1-q)^{1/3}}\right)}} C_B \qquad 4.9$$

With:

a	specific surface area	m^2/kg
C_B	bulk metal concentration	mol/m^3
D_{eff}	effective diffusivity of metal ion within the bead	m^2/s
k_L	external mass transfer coefficient	m/s
Q	adsorption loading	mol/kg
R_S	bead radius	m
t	time	s
?	fractional adsorbent loading (Q/Qmax)	-
?	bead density (dry mass/wet volume)	kg/m^3

All variables are known and the change in adsorption loading can be calculated.

For the external mass transfer coefficient the following equation is applicable [Bird et al., 1960]:

$$\frac{k_L \cdot d}{D_{water}} = 2.0 + 0.60\left(\frac{d \cdot v_\infty \cdot r_f}{m}\right)^{1/2} \cdot \left(\frac{m}{r_f \cdot D_{water}}\right)^{1/3} \qquad 4.10$$

With:

D_{water}	diffusivity of metal ion in water	m^2/s
d	bead diameter (twice the radius)	m
v_∞	bulk fluid velocity	m/s
µ	viscosity	kg/m·s
$?_f$	fluid density	kg/m^3

4.1.4 Adsorber column simulation

A simulation is made of an adsorption column packed with chitosan beads. The column was divided into 35 slices (see Figure 4.4), each slice considered to have a uniform bulk concentration (35 CISTR's in series). All beads in one slice were assumed to be identically loaded with copper. Changes in the column were calculated in discrete time steps equal to 1/35 of the residence time.

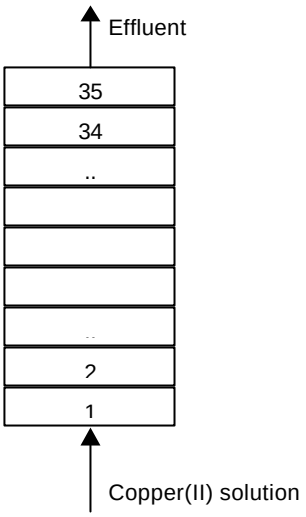

Figure 4.4: Schematic representation of column

The presented particle model equation (Equation 4.9) was used to calculate the derivative of the adsorption load. The change in adsorption load in one step in time can then be calculated using the following formula.

$$\Delta Q = \frac{\partial Q}{dt} \cdot \Delta t \qquad 4.11$$

?Q is the change in adsorption loading and ?t is the length of one step in time (1/35 of the residence time).

Each step in time consisted of the moving of the bulk solution one slice onward and a diffusion and adsorption step (see Figure 4.5). The diffusion and adsorption was calculated using the previously developed particle model. When the change in bulk concentration was more than 25%, the time step was split up in smaller parts, so that the change in concentration did not exceed 25%. This was done to improve the accuracy.

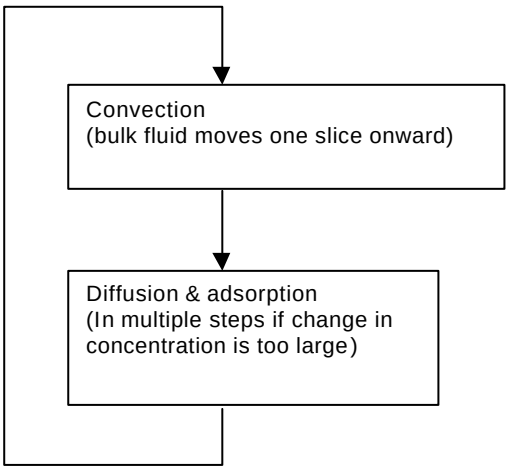

Figure 4.5: Excel simulation overview

4.2 Characterisation of chitosan beads

4.2.1 Chitosan stability/water content

The stability of non-crosslinked and crosslinked chitosan gel beads was measured in terms of solubility in acid solutions. Table 4.1 shows the solubility of non-crosslinked and crosslinked in acetic and hydrochloric acid solutions. The concentration shown on the table is the initial acid values; which also gives the initial pH. The equilibrium pH was slightly higher after 24 hours.

Table 4.1: Solubility of chitosan in acidic solutions

Beads	Hydrochloric acid		Acetic acid	
	0.01 M	0.001 M	0.01 M	0.001 M
0.00 % XLB	Soluble	Insoluble	Insoluble	Insoluble
0.5 % XLB	Partially soluble	Insoluble	Partially soluble	Insoluble
2.5 % XLB	Insoluble	Insoluble	Insoluble	Insoluble

When chitosan is crosslinked with glutaraldehyde the structural transformation is shown in Figure 46. This modification makes the material to withstand acidic pH environment, the higher the concentration of the crosslinking reagent, the more stable the material under that same pH condition. The crosslinking reagent was measured such that 1.5 ml of percent crosslinking reagent was mixed with 1g of wet bead. Thus under these analytical procedures, crosslinking reagent equal to or higher than 2.5 % will make chitosan to be insoluble at pH as low as 2.

The major component of chitosan gel bead is water and, the water content of the beads differs slightly depending on whether the beads are crosslinked or not, and also the size of the crosslinked beads influences the water content. For the bead used, the non-crosslinked beads contain 96% water and the crosslinked beads had water content ranges from 91-95 % mostly depending on the diameter of the bead. These measurements were based on the average value of several samples taken. The calculated water content for 0.9, 1.84 and 3.88 diameter beads were 91, 94 and 95 % respectively.

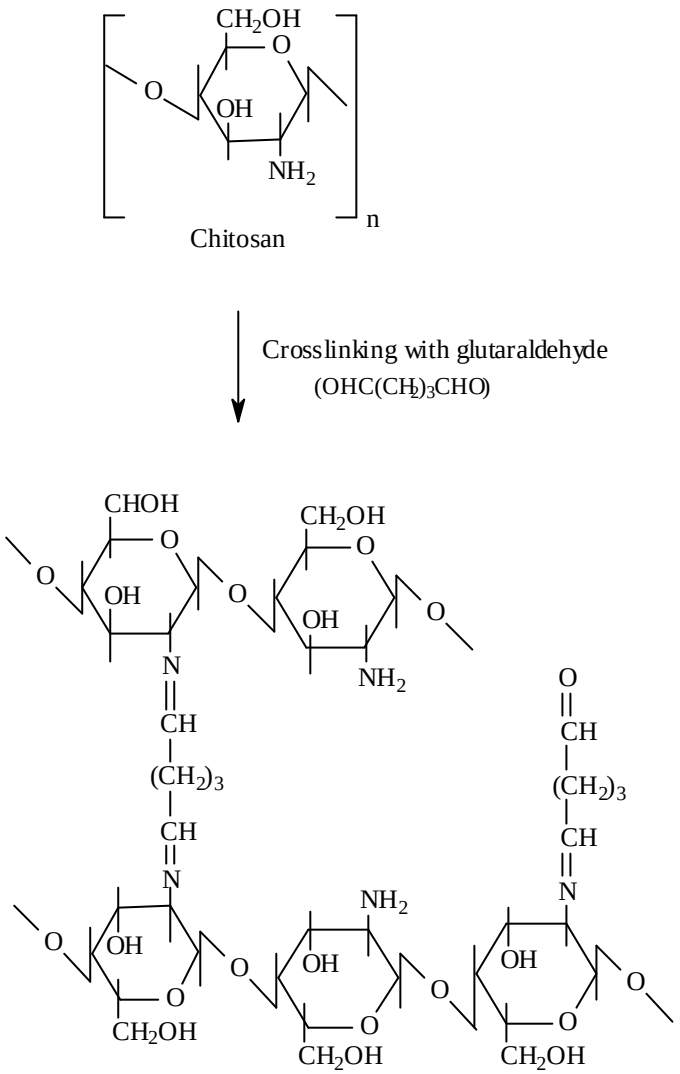

Figure 4.6: Crosslinking mechanism of chitosan with glutaraldehyde

4.2.2 Accessibility of metal ions in gel bead

It has been reported that sodium and alkaline metal ions do not adsorb on chitosan's active sides (Muzzarelli, 1974). In order to know the percent accessibility of the water in the chitosan bead, a sodium ion solubility experiment was done. A solution of sodium ion in wet chitosan beads shown to have 100 % accessed into the bead, this is shown in Table 4.2. This makes us to conclude that metal ions can diffuse into 100 % of the water in the bead.

Table 4.2: % metal ion accessibility in chitosan gel bead

Mass of wet beads (g)	16.6626	16.6620
Mass of dry beads (g)	0.8820	0.8927
Volume of solution (l)	0.025	0.025
[Na^+] begin (mg/l)	1000	1000
[Na^+] final (mg/l)	611.6	616.9
% H_2O accessible for diffusion	100	98.0

4.2.3 Protonated Amino Sites

The adsorption ability of chitosan for metal ions such as copper, lead, cadmium, zinc, and nickel is mainly due to the amino groups (-NH_2) on the chitosan chain. Therefore, the extent of metal adsorption depends strongly on the number of amino groups present in the chitosan source, which in turn is a function of the degree of deacetylation, the nature of metal ions and the solution conditions such as the pH. The metal and hydrogen ions compete for the amino sites. The degree of protonation is a function of the concentration of hydrogen ions in the environment of chitosan solution and the pKa of the chitosan material. Protonation degree was established with titration methods. Figure 4.7 shows the titration curves for the crosslinked and non-crosslinked chitosan.

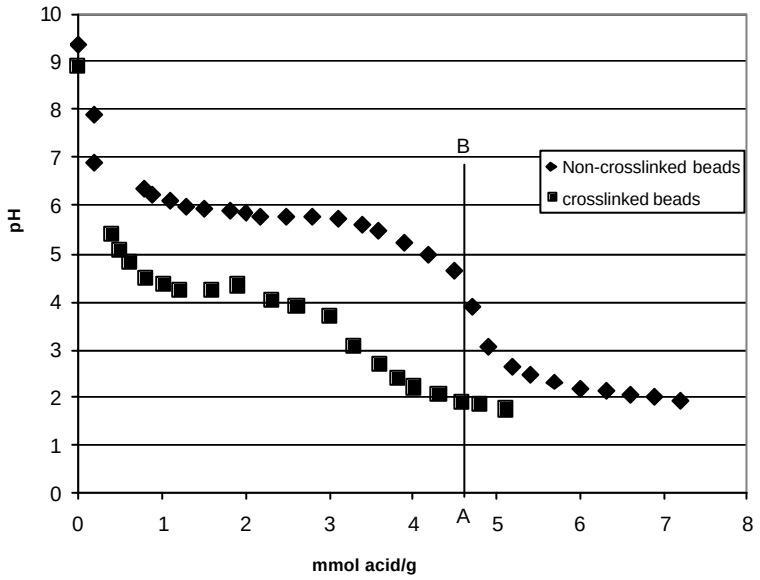

Figure 4.7: Titration curves for the crosslinked and non-crosslinked chitosan

The pKa for the non-crosslinked chitosan solution for the local and commercial non crosslinked materials is 5.9 and 6.2 respectively. This is similar to what has been reported in literature (Muzzarelli, 1974). The pKa were also determined after crosslinking, for the local chitosan we measured 4.3. It was observed that crosslinking of chitosan reduced the number of amino concentration available for adsorption. The total amino concentration from titration

data, for the local crosslinked chitosan bead of 1.84 mm diameter, is 3.4 mmol/g beads. From the analysis of IR spectra for the corsslinked and non-crosslinked, more transition was revealed in the region of 1655 cm-1 for the crosslinked chitosan as shown in Figure 4.8, which is a characteristic of amide I (C=O). With this, we can definitely say that glautaraldehyde partake in chitosan crosslinking (Monteiro and Airoldi, 1999; Guibal, et al. 1999; Jeon & Holl, 2003).

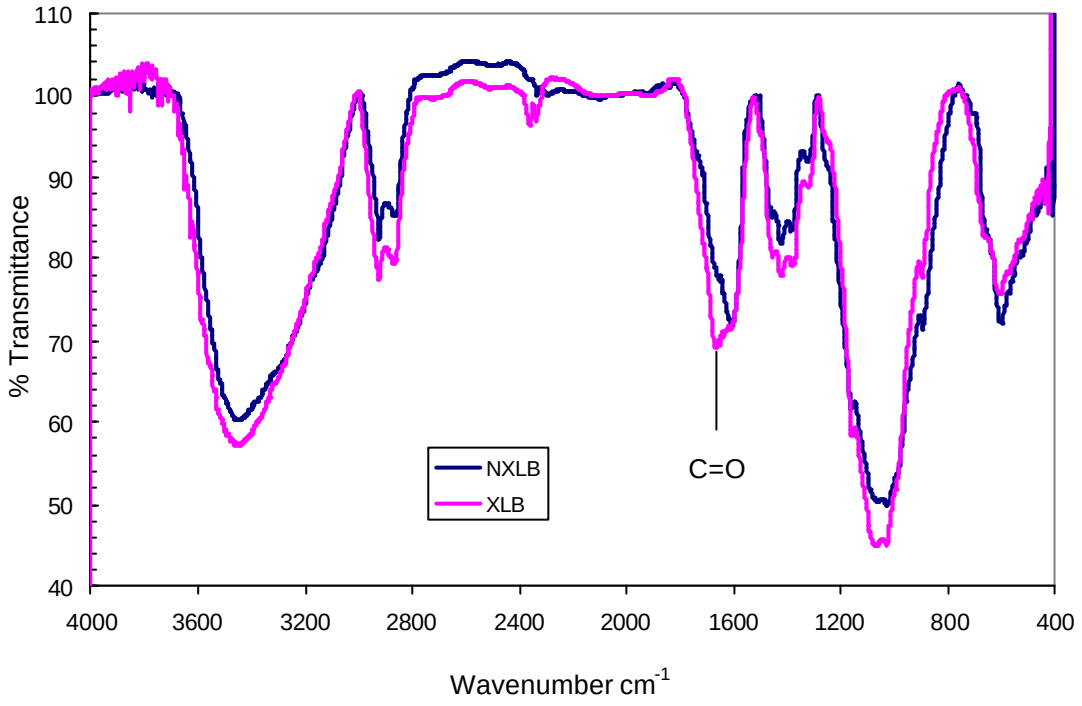

Figure 4.8: IR spectra of non-crosslinked chitosan bead (NXLB) and crosslinked chitosan bead (XLB)

After crosslinking treatment, the beads are normally stored in distilled water at pH near-neutral. After about 8 weeks, a gradual change is observed in the colour of the beads, from whitish to greyish and remains at that colour. This makes us to suggest probably that there might be some changes in the inherent material properties. In that case, the crosslinked beads made a year earlier were titrated to see if there are any significant changes in the chitosan properties as a result of bead's ageing. As shown in Figure 4.9, the pKa of the old and new beads is 4.3. Most significantly, the total concentration of chitosan in both samples were found to be identical. The value of the pKa from titrations done with bead crosslinked at different crosslinking time and different glutaraldehyde concentrations are reported in Table 4.3. From the table it can be seen that different sizes of crosslinked beads has the same or slightly different pKa. The pKa of all the crosslinked chitosan and their concentrations is smaller than that of the non-crosslinked.

Table 4.3: Characterised chitosan parameters

Chitosan type	pKa	Total $-NH_2$ mmol/g	DDA (Titration)	DDA (dye absorbance, UV measurement)	DCL
Local chitosan					
Non-crosslinked	5.9	4.9	0.80	0.85	0.0
Crosslinked in 2.5 % glutaric acid for 24 hr					
0.9 mm dia beads	4.3	3.3	-	-	0.33
1.8 mm dia beads	4.3	3.4	-	-	0.31
3.8 mm dia beads	4.7	4.2	-	-	0.14
8 hr cross linked in 2.5 % glutaric acid (3.8 mm)	5.01	3.4	-	-	0.31
2 hr crosslinked in 2.5% glutaric acid (3.8mm)	4.3	3.1	-	-	0.37
0.5 % glutaric acid (3.8mm) in 24 hr	5.34	4.4	-	-	0.10
4.0 % glutaric acid (3.8mm) in 24 hr	4.3	3.2	-	-	0.35
Commercial chitosan					
Non-crosslinked	6.00	4.1	0.66	0.83	-
24 hr crosslinked in 2.5 % glutaric acid	3.82	3.9	-	-	0.05

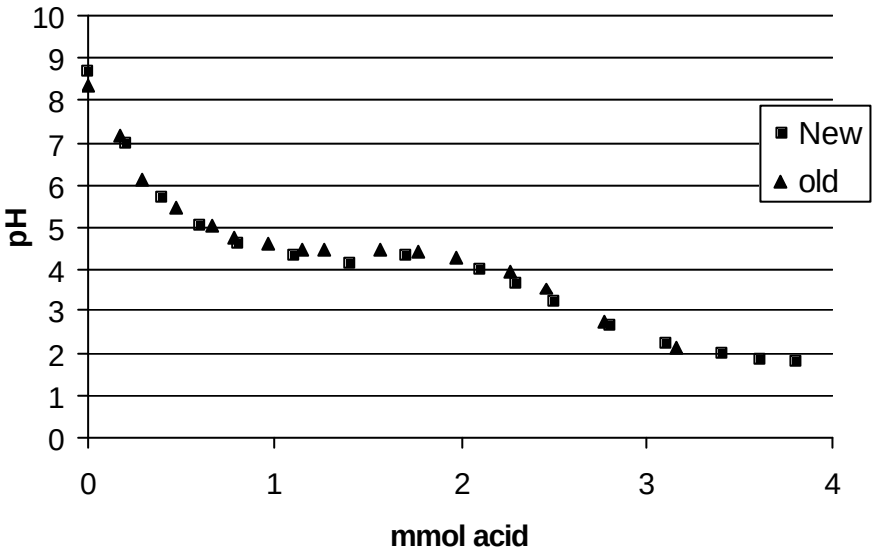

Figure 4.9: Titration curves for new and aged beads.

Since the hydrogen ion competes for the amino sites as the metal ion at the prevailing solution conditions, it is important to know the degree of pronation at that pH condition. The degree of protonation is the ratio of protonated amino concentration to the total amino concentration.

Theoretically, the degree of protonation has a direct relation to the pH and the pKa of the material solution. The degree of protonation(DOP) values were estimated from the titration data, the following expression was used:

$$DOP = \frac{(H^+ \ added) - (H^+ \ needed \ \ for \ \ pH \ \ change \ of \ the \ solution)}{(H^+ \ \ at \ \ equivalent \ \ po\,\text{int})} \qquad 4.12$$

Knowing that chitosan is weak base and the base dissociation equation is

$$\underset{(1-a)C_{(-NH_2)}}{-NH_2} + H_2O \Leftrightarrow \underset{aC_{(-NH_2)}}{-NH_3^+} + OH^- \qquad 4.13$$

Where C(-NH_2) is the total concentration of amino groups in the solution and α is the percent protonation degree (DOP). The equilibrium acid dissociation constant is::

$$k_a = \frac{(1-a)[H_3O^+]}{a} \qquad 4.14$$

and the theoretical degree of protonation is obtained by rearranging the above expression to give

$$a = \frac{[H_3O^+]}{K_a + [H_3O^+]} \qquad 4.15$$

The graph of the degree of protonation for crosslinked beads of 1.84 mm diameter made from local chitosan material is shown in Figure 4.10. The theoretical derived DOP from Equation 4.12 is plotted with that of DOP obtained from the expression of Equation 4.13. The theoretical curve coincide with the data points obtained from the calculated expression of Equation 4.13 The pKa used for estimating the DOP from Equation 4.15 was that obtained from the titration curve for that same material.

4.2.4 Total amount of amino sites obtained from titration data

Sometimes judging the equivalent amount of acid neutralizing amino groups is difficult possibly because chitosan is a weak base. From Figure 4.7, for the non-crosslinked chitosan, the equivalent amount of acid as shown by the line AB is approximately around 4.5 mmol acid/g chitosan. This can also be found by the use of experimental data, equating Equations 4.12 and 4.14 gives;

$$DOP = \frac{H^+ added - H^+ needed\ for\ pH\ change\ of\ the\ solution}{H^+ at\ equivalent\ point} = \frac{[H_3O^+]}{K_a + [H_3O^+]}$$

4.16

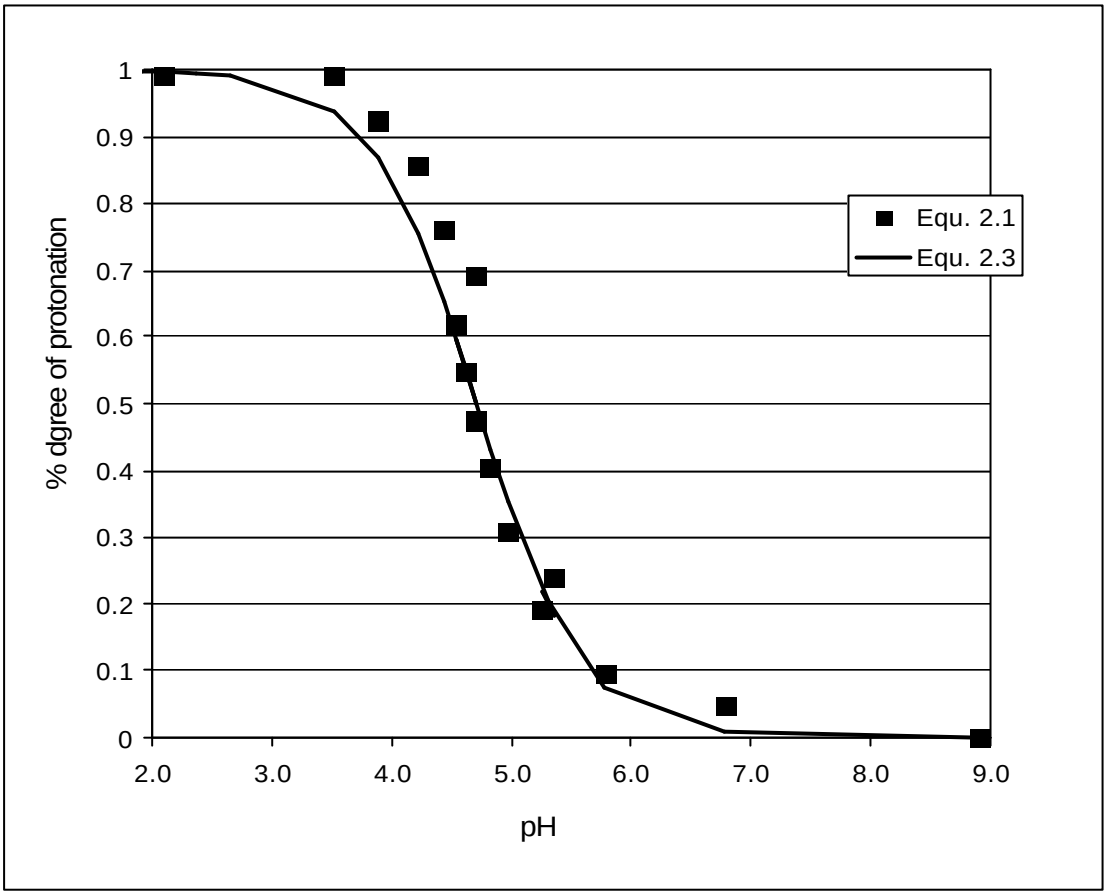

Figure 4.10: The degree of protonation obtained from the titration data.

When beads are produced in their various forms they are crosslinked, and homogenized to form chitosan solution then titrated with standard HCl. In most cases, beads are used for adsorption in their solid form. Solid beads were put in a flask containing a solution of standard hydrochloric acid of different concentrations in the same amount as that for suspension titration. The pH changes of the HCl acid solution with the beads and with suspension at equilibrium is shown in Figure 4.11. It can be seen, that the pKa of the grinded beads titrated with standard HCl is the same as that of the beads in acid solutions. This shows that even in bead form, the total amount protonated is the same at equilibrium. In a binary mixture of metal ions, the sorbate capacity toward the sorbent is the same as that for a single metal ion under that same condition (Muzzarelli, 1974); this similarity was also drawn for metal and hydrogen ions. Figure 4.11 shows the graph of copper solution in chitosan suspension titrated with 1.0 M HCl acid (Standard). It can be seen from the graph that the

initial pH for copper chitosan solution is lower than that with chitosan suspension alone. This can be attributed to the release of hydrogen ion during adsorption of copper, but at a very low pH values almost all the sites are protonated, and between the pH 5 to 6, used for adsorption experiment, the DOP is the same for both with copper solution and without copper solution. Figure 4.12 shows that the copper has no influence on the titration curve.

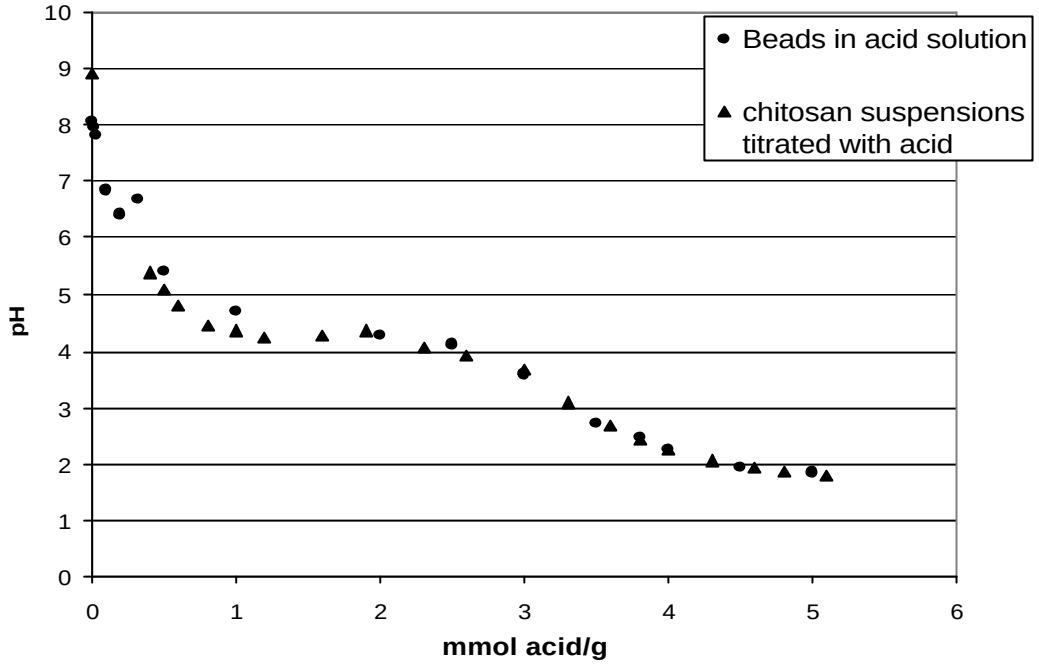

Figure 4.11: Curves for chitosan suspension and chitosan beads in acid solution

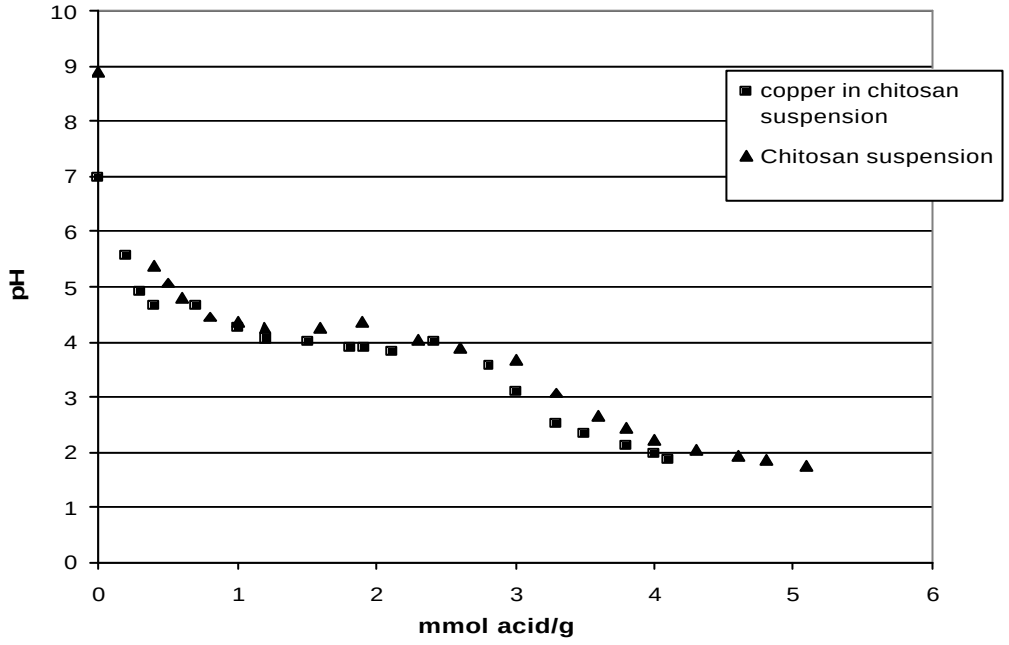

Figure 4.12: Curves of pH changes titrated with 1.0 M HCl against chitosan solutions without copper and with copper

4.2.5 Degree of deacetylation

The degree of deacetylation is an important characteristic of chitosan as it helps to estimate the binding capacity. In the determination of the degree of deacetylation, the method proposed by Roberts (1997) was used. This method makes use of a dye ion adsorption by the protonated amino group in a solution of acetic acid. The extent of adsorption is measured by ultraviolet visible spectrometer that could measure the adsorbance value at 484 nm. The degree of deacetylation as measured by this method for the local and commercial chitosan is 85 and 83 % resectively.

From the titration results we find that for the non-crosslinked chitosan the total amount of the amino concentration of the chitosam material is 4.9 mmol/g. This value also enables us to find the degree of deacetylation. In simple terms the degree of deacetylation was estimated using the expression below:

$$\frac{[-NH_2]_{total}}{g} = \frac{dry\ mass\ of\ chitosan\ x\ DDA}{Mw\ of\ monomeric\ unit\ of\ chitosan} \ x \ \frac{1}{dry\ mass\ of\ chitosan\ material}$$

$$therefore\ the\ \deg ree\ of\ deacetylation\ is,$$

$$DDA = \frac{[-NH_2]_{total}}{g} \ x \ \frac{Mw\ of\ monomeric\ unit\ of\ chitosan}{1}$$

4.17

The molecular weight of monomeric unit of chitosan based on chitosan structure, also as used by others (Tan, et al., 1998; Khan, et at., 2002), is 161 mg/mmol. The use of this value with titration data allowed us to calculate the DDA of this chitosan material to be 80% which is very close to the value obtained when UV method was used to measure DDA. The results from both methods are shown in Table 4.2.

4.3 Experimental Procedures (methodology)

In this section, the different experimental procedures, relevant to this study are presented.

4.3.1 Determination of metal-ion concentration in the water samples

The adsorption characteristics of chitosan are calculated from the difference of metal-concentration in the studied sample. The adsorption (q_{ads} in mg metal/g dry chitosan) in the chitosan is than calculated by:

$$q_{ads} = \frac{(c_{initial} - c_{final})V_{solution}}{m_{drychitosan}} \qquad 4.18$$

Initially, all samples have been analysed using Atomic Absorption Spectroscopy. It is important to note that the adsorption capacity is based on the dry mass of chitosan in the gel-material.

4.3.2 Adsorption studies at lab scale

A salt stock solution of copper sulphate (analytical grade) with a concentration of 1000,0 mg/l was made. For each adsorption experiment a certain quantity of this solution was diluted to the required concentration.

After the production of the beads, the beads are vacuum filtrated. The required amount of beads is weighed and brought into a 500 ml Erlenmeyer flask for dynamic studies or into a smaller flask (10-25 ml) for equilibrium studies. From the stock solution, the required salt solution is prepared in a volumetric flask and added to the Erlenmeyer. For the adsorption studies, the Erlenmeyers / flasks were put in an incubator to establish equilibrium. The incubator was shaking at 120 rpm and keeping the temperature constant. If required, the pH was adjusted with a 0.1 M HNO3 or a 0.1 M NaOH solution. The pH of the solution was measured (by putting the pH meter (Hanna instruments HI 8314) in the incubator for a while, until the displayed pH was constant). A sample of the solution was taken and filtered using a 0.45µm filter (Millipore). The metal concentration in the samples were analysed with an atomic absorbance spectrometer (Varian SpectrAA-10).

After preparation the non-cross-linked beads are white, the cross-linked beads are slightly darker. During adsorption of copper(II) ions the cross-linked beads turn greenish, the non-cross-linked beads turn blue.

4.3.3 Desorption

Immediately after the adsorption experiment the beads were vacuum filtered and rinsed with distilled water. The beads were put in a clean 100 ml or 250 ml Erlenmeyer. A specific volume (20.00 – 25.00 ml) of a hydrochloric acid solution (prepared from a 1N HCl standard solution (Across)) was measured with a pipette and added to the Erlenmeyer. The Erlenmeyer was put in the incubator for 24 hours at 25°C and 120 rpm. For those experiments indicated the pH was kept constant by adding some acid every few hours. After 24 hours the Erlenmeyer was weighed to determine the mass of the contents. A sample was taken and

filtered using a 0.45µm filter. The metal concentration in the sample was analysed with the atomic absorbance spectrometer. The pH of the sample was measured. The beads were vacuum filtrated, rinsed and put in a clean 100 ml beaker. The beaker was covered with a watch glass and placed in an oven for 24 hours at 80°C to remove all the water from the beads. The beaker was weighed to determine the dry mass of the beads.

4.3.4 Multiple adsorption – desorption cycles

After desorption the beads were vacuum filtered and put in a sodium hydroxide solution for ½ to 1 hour. Enough hydroxide was added to obtain a pH between 5.2 and 5.7. After that, the beads were vacuum filtered again and a new adsorption was started. During the adsorption the pH was adjusted with a 0.1 M NaOH solution. Four adsorptions and three desorptions were performed with the same beads for copper. The initial copper concentration was 100 mg/l.

4.3.5 Adsorption in a column with chitosan beads

The column used was made locally at the Potchefstroom University. The column has an internal diameter of 24.5 mm and height of 264 mm. The column can be filled with approximately 90 g beads. The column was fed from the bottom by a peristaltic pump at a flow rate of 8.5 ml/min. The pump was calibrated by measuring the amount of volume per time. The copper solution was pumped through the column and samples were taken at different intervals. The concentrations of the samples were analysed with the AAS. Figure 4.13 shows the used column set-up.

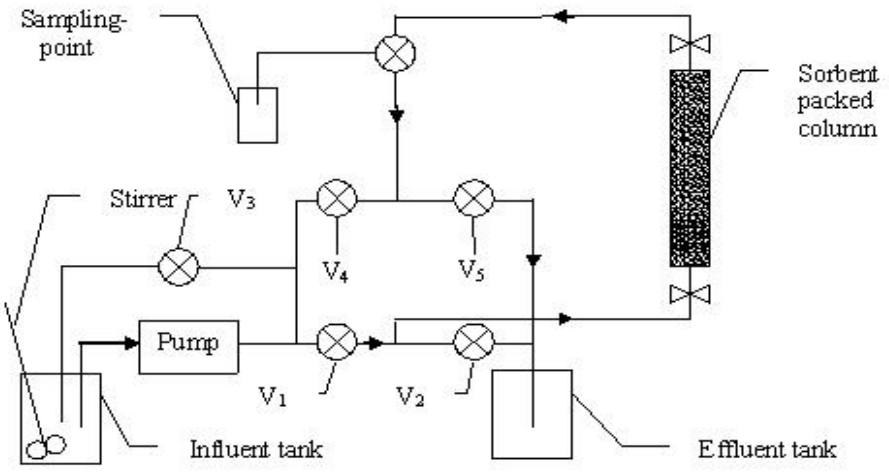

Figure 4.13: Schematic representation of the used column set-up

4.3.6 Desorption in a column with chitosan beads

After adsorption the column and the tubes were washed with water. The desorption experiment was done with a required concentration of HCl solution. The solution was pumped through the column and samples were taken at regular intervals. The concentrations of the samples were analyzed with the AAS.

4.4 Results and discussion

This chapter gives the most important experimental findings from this project. For a proper study of the adsorption characteristics of chitosan is it essential to work outside the precipitation limits of the various metal hydroxides. The following figure (Figure 4.14) gives the precipitation levels at various pH. This is also the reason why copper cannot be studied at a pH higher than 6.5.

Chitosan beads have both been studied batch-wise as well as continuous wise. The novel developed adsorption theory was tested in detail using copper and later compared with other metal ions of interest.

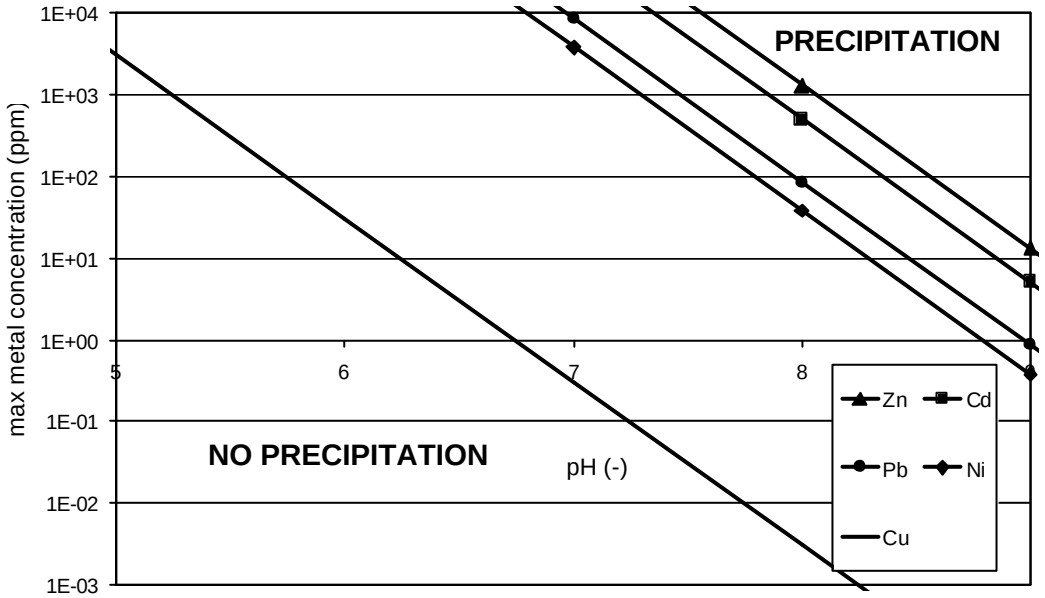

Figure 4.14: Precipitation interval for the different metal ions studied

4.4.1 Batch experiments

4.4.1.1 Determination of the adsorption coefficient

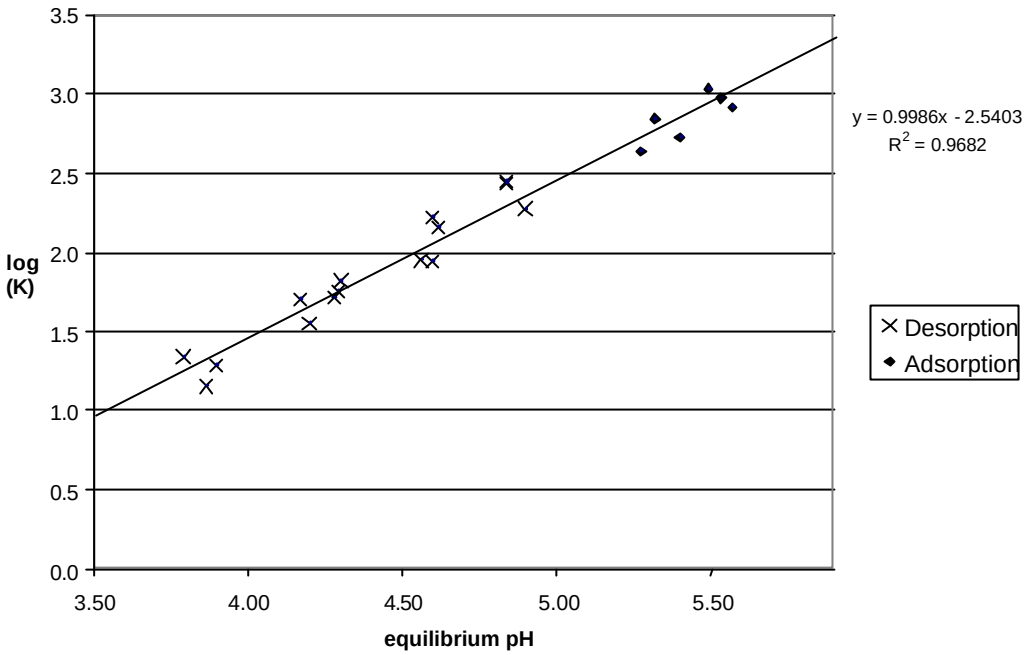

Figure 4.15: The logarithm of the adsorption constant (K or K_{ads}) as a function of pH (both adsorption and desorption have been taken into account here)

According to the proposed model, a figure of log (K) versus the pH should result in a straight line with a slope of unity. Figure 4.15 gives this relation and a slope of unity is approached for all three metals under investigation. For copper, both adsorption and desorption have been taken into account. Form these experiments, it can be concluded that both adsorption as well as desorption are described well by the proposed model.

4.4.1.2 Desorption

Adsorption-desorption experiments with performed with 16.70 g beads and 250 ml 50 mg/l Cu2+ solution (CuSO4). After adsorption, desorption was performed with 25.00 ml of different acid concentrations. During desorption, the pH was not adjusted for most experiments. For a few experiments the pH was kept constant (see legend in the graph). Figure 4.16 shows the percentages of desorption as a function of the pH at the end of the desorption process, the equilibrium pH.

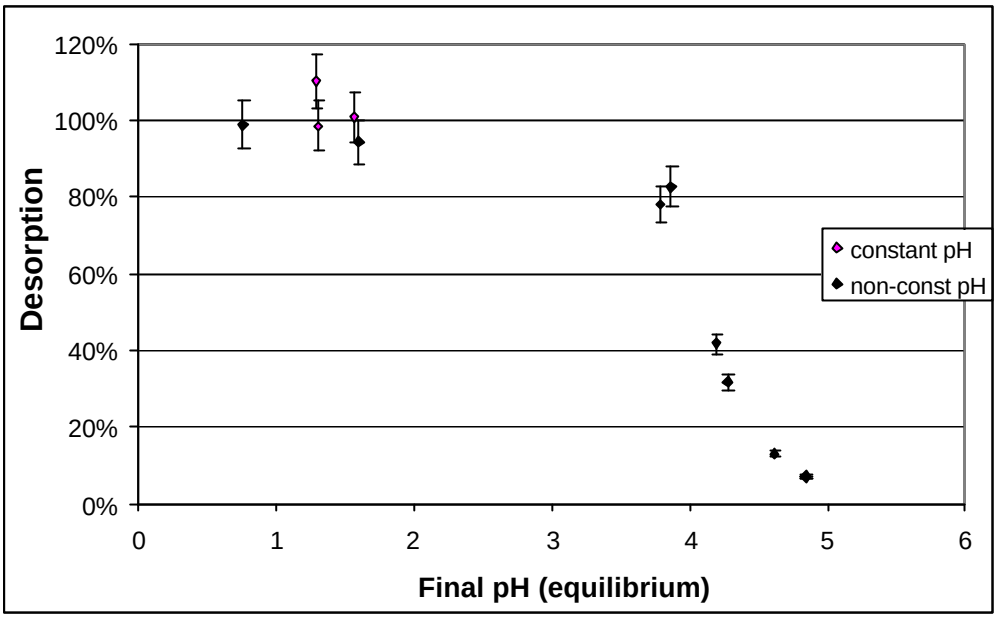

Figure 4.16: Percentage of desorption as a function of pH

From this figure it can be seen that above pH 4.5 there is only little desorption, below pH 4.0 desorption is almost complete. It seems that desorption is possible as long as enough acid is added to the solution to maintain the pH well below 4. The titration curve for chitosan showed a pKa of approximately 4.2. Therefore, around pH 4.2 most NH_2-groups are protonated to NH^{3+}-groups and Figure 4.16 shows that around pH 4.2 most desorption is taking place.

4.4.1.3 Desorption Multiple adsorption – desorption cycles

It could be possible that chitosan beads decrease in adsorption capacity after several adsorption and desorption cycles. To find out whether this occurs after a few cycles, four adsorption experiments with desorption in between were carried out consecutively with the same beads. This experiment has been performed with 3.8 mm beads. After the second desorption the colour of the beads is more orange than after the first time. The pH was not exactly the same for all experiments. It uses quite an amount of acid to bring the beads back from the desorption pH to a pH suitable for adsorption. Not always the exact same amount of acid was added, which resulted in different pH's at different adsorption cycles. The results are given in Table 4.4.

Table 4.4: Results multiple adsorption cycles

	1st measurement		**Duplo**	
	pH	*Adsorption load*	*pH*	*Adsorption load*
1st adsorption	5.84	51.3 mg/g	5.80	48.1 mg/g
2nd adsorption	5.06	33.0 mg/g	5.09	28.2 mg/g
3rd adsorption	4.84	36.9 mg/g	4.64	25.6 mg/g
4th adsorption	5.65	47.1 mg/g	5.65	34.4 mg/g

From this table, it can be seen that for the first experiment there is hardly a difference between the adsorption load after the first adsorption and the fourth adsorption. The pH is slightly lower, which will give a lower adsorption capacity. For the duplo experiment there is a difference in adsorption. However, comparing the adsorption loadings is not the best way to compare the capacities. The copper concentration in the solution at equilibrium was different for the different experiments. (Because there was some copper left in the beads after desorption, the adsorption loading for the second and later experiments was larger than for the first experiment, when the equilibrium concentration is the same). Nevertheless, when the results are used to calculate the equilibrium constant and are plotted in a graph, they can be compared (see Figure 4.17).

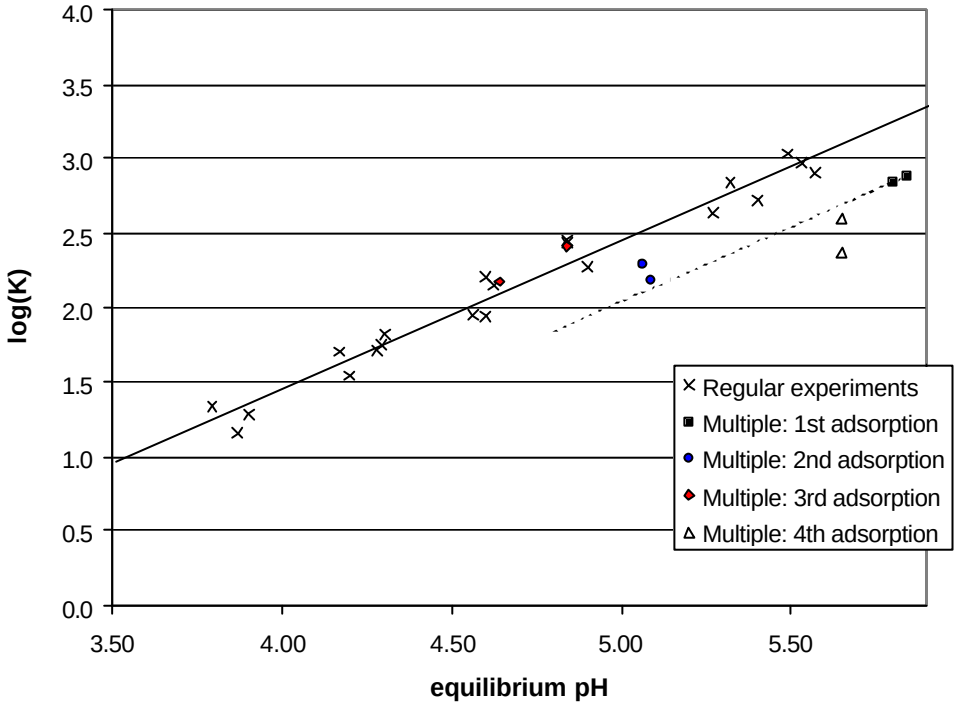

Figure 4.17: Equilibrium constant multiple adsorption cycles

4.4.1.4 The equilibrium model for different metal ions

Identical experiments, as presented in Section 4.4.1.1 were carried out for Pb, Ni, Zn and Cd ions. The results, together with the results for Cu ions, are given in Figure 4.18. From the figure, it can be seen that all salts, except for Ni, follow the developed adsorption model adequately. The deviation of Ni is unclear and no comparing information could be obtained from literature. Qualitatively, it can also be seen from the figure, that the adsorption increase from Cu>Pb>Ni>Zn>Cd. The obtained adsorption constant are given in Table 4.5 (the data for Ni was not obtained, since this metal did not follow the proposed adsorption mechanism.

Table 4.5: Adsorption constant for different metal ions

Metal ion	Log (Kads)
Cu^{2+}	- 2.54
Pb^{2+}	- 3.27
Ni^{2+}	could not be obtained
Zn^{2+}	-4.50
Cd^{2+}	-4.61

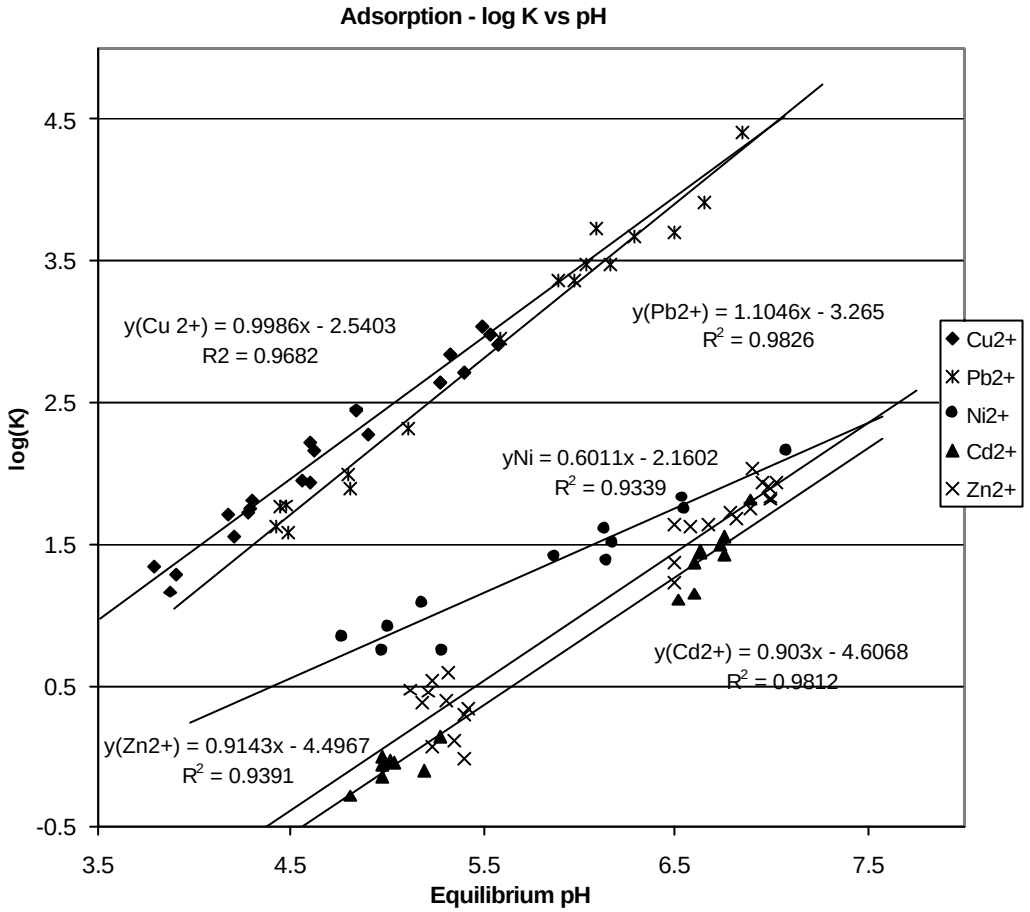

Figure 4.18: Equilibrium constant measurement for Cu^{2+}, Pb^{2+}, Zn^{2+}, Cd^{2+}, & Ni^{2+} ions

4.4.1.5 Selectivity

If the study of water contains more than one metal-ion, selectivity is an important factor. Binary mixtures of Cu and Zn and Cu and Cd have been studied. Figure 4.19 and 4.20 give the adsorption of the Cu/Zn and Cu/Cd mixture respectively. The adsrption of the various metals is not given as the final (equilibrium) concentration, since the selectivity ids the important parameter here. It can be seen from both figures that chitosan has a higher affinity to copper than for Zn and Cd. This is in line with the adsorption data for the single components, as given in Figure 4.18 and Table 4.5.

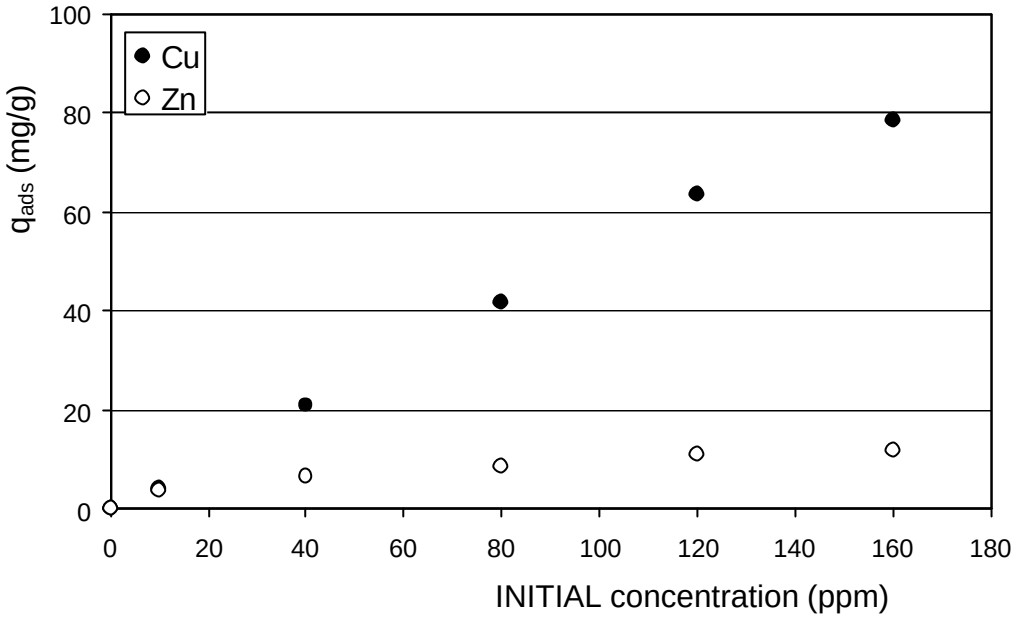

Figure 4.19: The adsorption of copper and zinc on in a binary mixture at pH = 5

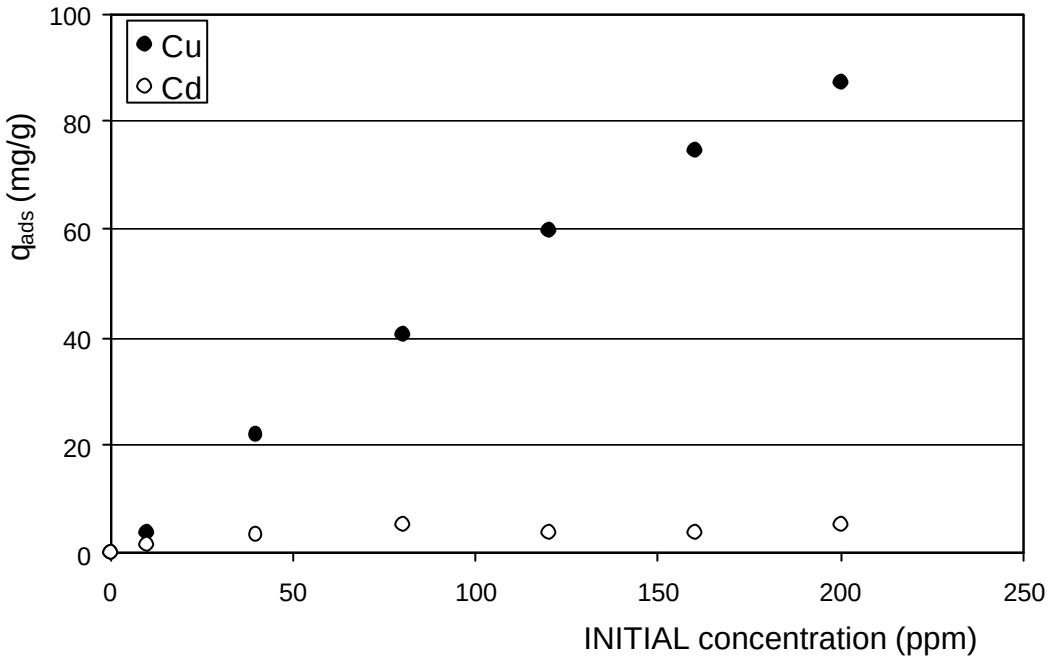

Figure 4.20: The adsorption of copper and cadmium on in a binary mixture at pH = 5

4.4.1.6 Dynamics of adsorption

As reported earlier, next to the equilibrium properties, also the kinetic properties of chitosan beads are of importance. Therefore, the adsorption of copper on chitosan beads has also been studied dynamically. The following figures give the time dependent adsorption on chitosan beads, and the fitted values according to the model presented in section 4.1.2.

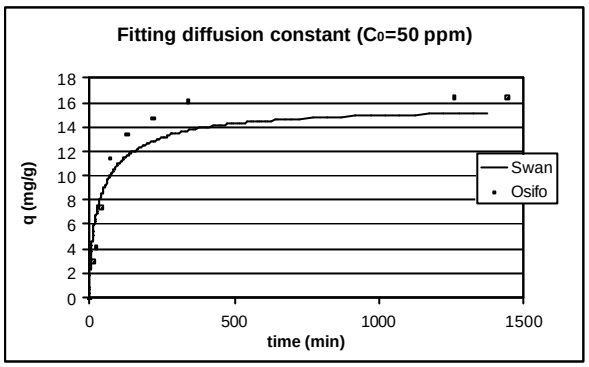

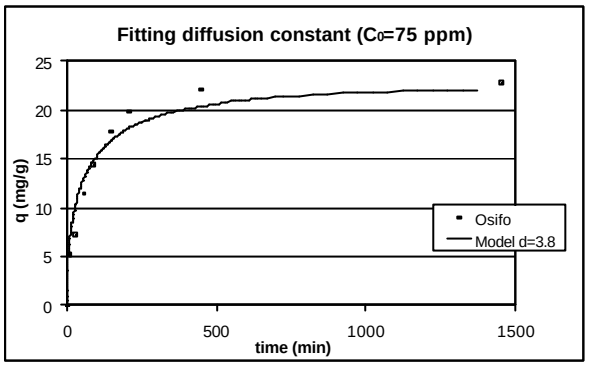

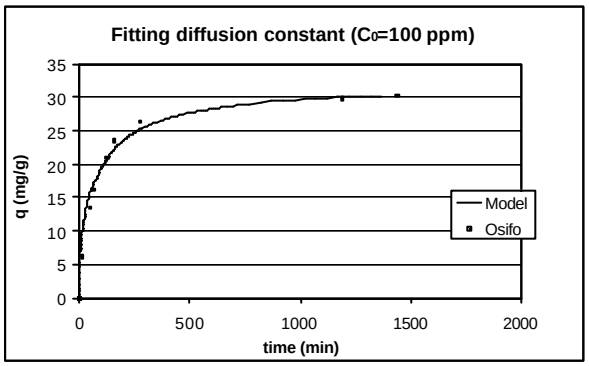

20.00 g wet beads
300 ml solution
$[Cu^{2+}]$= 50, 75, and 100 mg/l
pH approx. 6.0
bead diameter 3.8 mm

Figure 4.21: Adsorption of Cu^{2+} on beads as a function of time using a diffusion constant 6×10^{-11} m2/s (initial concentration is varied from 50 – 100 ppm)

In these figures, the dots represent the experimental values and the lines represent the Swan-model with a (fitted) diffusion constant 6.0·10-11 m^2/s. In general, a good agreement of the model with the experimental points can be concluded. So it can be concluded that the adsorption kinetics can be described using the Swan model when the diffusion constant is assumed to be 6.0·10-11. This value is comparable to what Ko et al. [2001] found for a similar model for adsorption of copper(II) on bone char particles. They found values ranging from 3.19·10-11 to 8.27·10-11 m^2/s.

4.4.2 Column experiments

Initially, two column experiments were carried out with a 10 mg/l copper solution. Constants for the first and the second experiment are given in the following table.

Table 4.6: Experimental settings

Column height	0.26	m
Column inner diameter	0.0245	m
Mass chitosan beads	90.15	g
Flow rate	8.5	ml/min
Vbed	62	ml
pH	5.8	-

The breakthrough figure is given in Figure 4.22. It can be seen from this figure that the breakthrough starts occurring after 35 bed-volumes have been passed. The column model as presented in Section 4.1.3 predicts the behaviour of the column reasonably well. A disturbing effect on the experiments is that the pH will change during an experiment (see Figure 4.26); the pH of the effluent and the column has not been measured in these experiments.

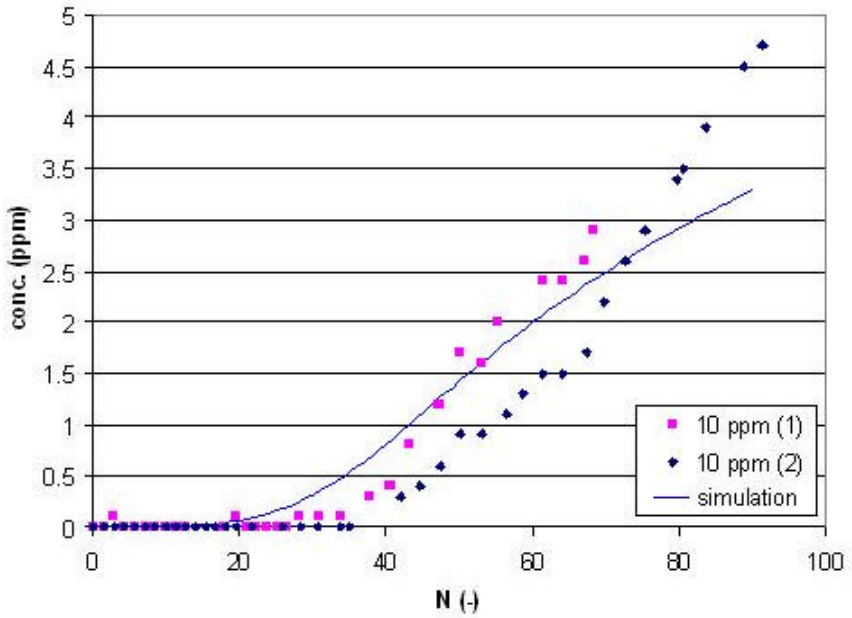

Figure 4.22: Breakthrough: 10 ppm, c vs Bed Volumes

A summary of the 2 breakthrough experiments is given in Table 4.7.

Table 4.7: Summary of initial column results

	1st experiment, 10 mg/l	2nd experiment, 10 mg/l	
90 % removal	45	56	Bed volumes
Volume after 90 % removal	2.79	3.36	l
100 % removal	26	35	Bed volumes
Volume after 100 % removal	1.61	2.1	l

4.4.2.1 Desorption

After the adsorption experiment, the packed column that was saturated with copper ions is regenerated with an acid. The desorption experiments were carried out after a column adsorption with a solution of 50 mg/l. Desorption was done with 0.2 M and 0.02 M HCl solutions. The desorption experiment with 0.2 M is shown in Figure 4.23 and the experiment with 0.02 M is shown in Figure 4.24.

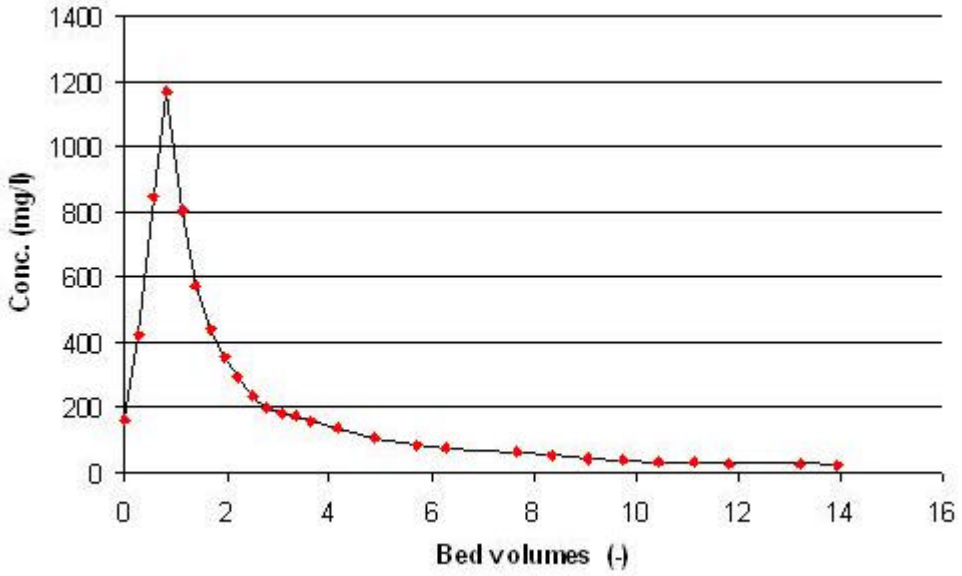

Figure 4.23: Desorption with 0.2 M HCl

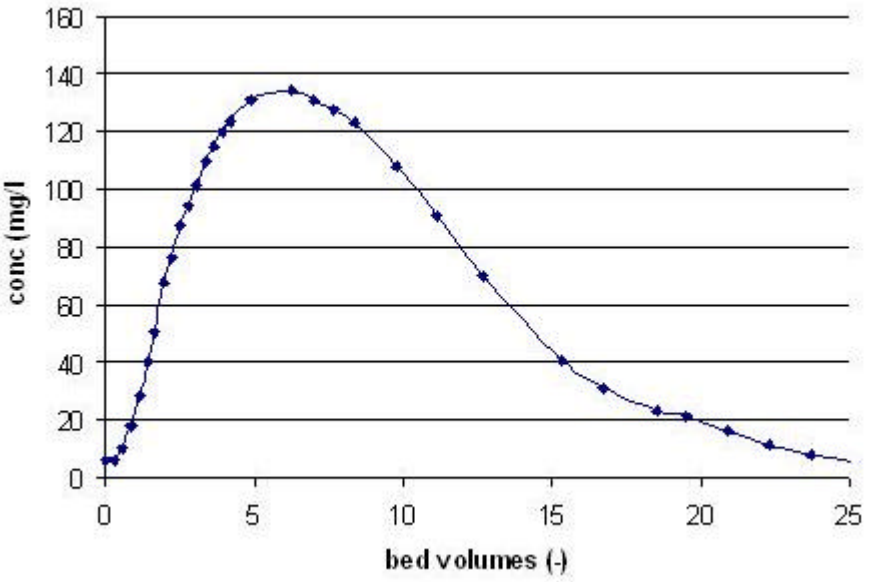

Figure 4.24: Desorption with 0.02 M HCl

From the desorption figures, it can be concluded that HCl can desorb the copper-ion very efficiently (up to 1200 mg/l copper-solutions are obtained using a 0.1 M HCL-solution). After a desorption experiment the bed shrunk up to a total of 6%.

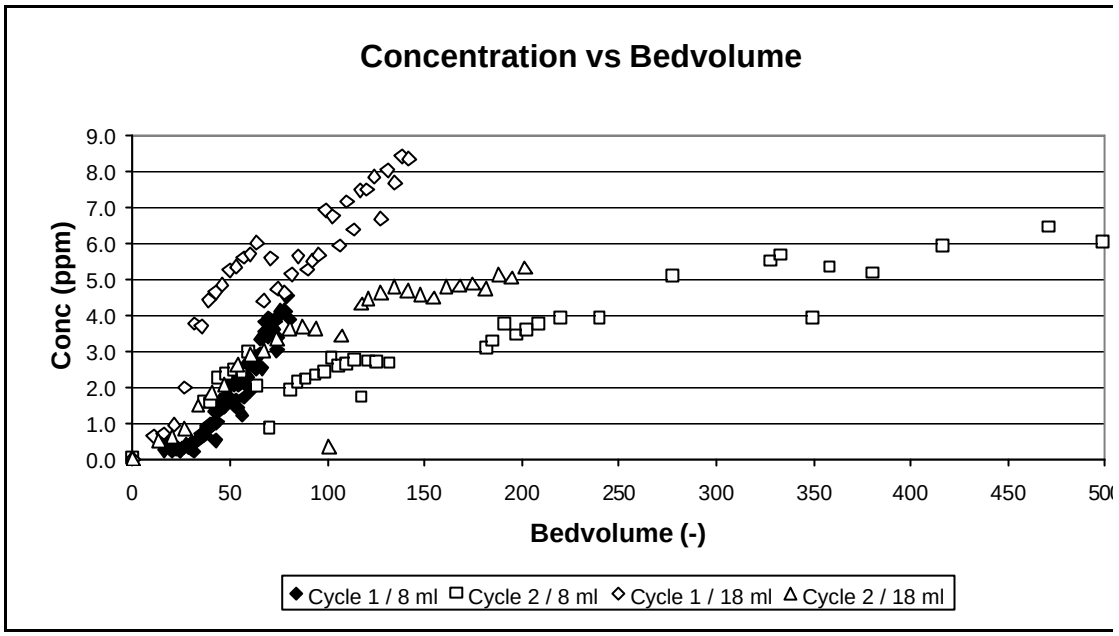

Figure 4.25: Breakthrough curves for 2 cycles at different flow rates

4.4.2.2 Cycle adsorption desorption measurements:

Adsorption and desorption experiments were carried out for two different flow rates (8 and 18 ml/min). For the adsorption experiments, a change in bead colour could be visibly observed. As soon as the beads start to adsorb the copper ions, the beads get a light blue colour. The colour change starts at the bottom of the column and rises upwards in time (column is fed from the bottom). Two cycles were carried out for both flow rates. One cycle is defined as one adsorption experiment followed directly with a desorption experiment. The results are summarised in Figure 4.25.

It can be seen from the figure, that the second cycle gave a better adsorption (lower concentrations after a number of bed volume) than the first cycle. This could possibly be explained by the effect of the acid on the beads after desorption. A faster breakthrough is observed for the higher flow rate, indicating that the diffusion into the beads is determining the adsorption rate, as already was explained by the diffusion controlled shrinking core mechanism. The following additional data, concerning these experiments are given in Table 4.8 (for the 8 ml/min experiments) and in Table 4.9 (for the 18 ml/min experiments)

Table 4.8: Additional adsorption parameters at 8 ml/min

	Cycle 1	Cycle 2	Units
Mass of wet beads	96.8	80.4	g
pH (feed)	4.58	4.60	-
Flow rate	8	8	ml/min
Feed concentration	9.86	10.1	ppm
Desorption efficiency	95	91	%

Table 4.9: Additional adsorption parameters at 18 ml/min

	Cycle 1	Cycle 2	Units
Mass of wet beads	98.7	78.1	G
pH (feed)	4.61	4.94	-
Flow rate	18	18	ml/min
Feed concentration	10.16	10.21	ppm
Desorption efficiency	95	91	%

It can be concluded from these tables that there is a significant loss of bead material from cycle to cycle and that the desorption efficiency decreases for cycle 2, compared to cycle 1.

4.4.2.3 Multi-cycle adsorption experiments

Figure 4.26 shows the breakthrough curves when 10 mg/l Cu^{2+} (a typical contaminant concentration where chitosan could be used) was run through a column of wet chitosan gel beads for 5 cycles. The curves in the figure depict the repeated use of the gel beads in a cycle of multiple adsorption-desorption. The first breakthrough curve achieved with the fresh bead was steeper at 70 bed volumes when considering effluent concentration of 1.3 mg/l. For the second and third cycles of adsorption, the breakthrough point was the same at 240 bed volumes (again a better adsorption was obtained in cycle 2 and 3, compared to 1). The forth adsorption cycle could not be analysed due to a technical problems encountered during experimental procedures. The breakthrough point during the fifth cycle occurred around 6 bed volumes, after which the beads were visible physical damaged.

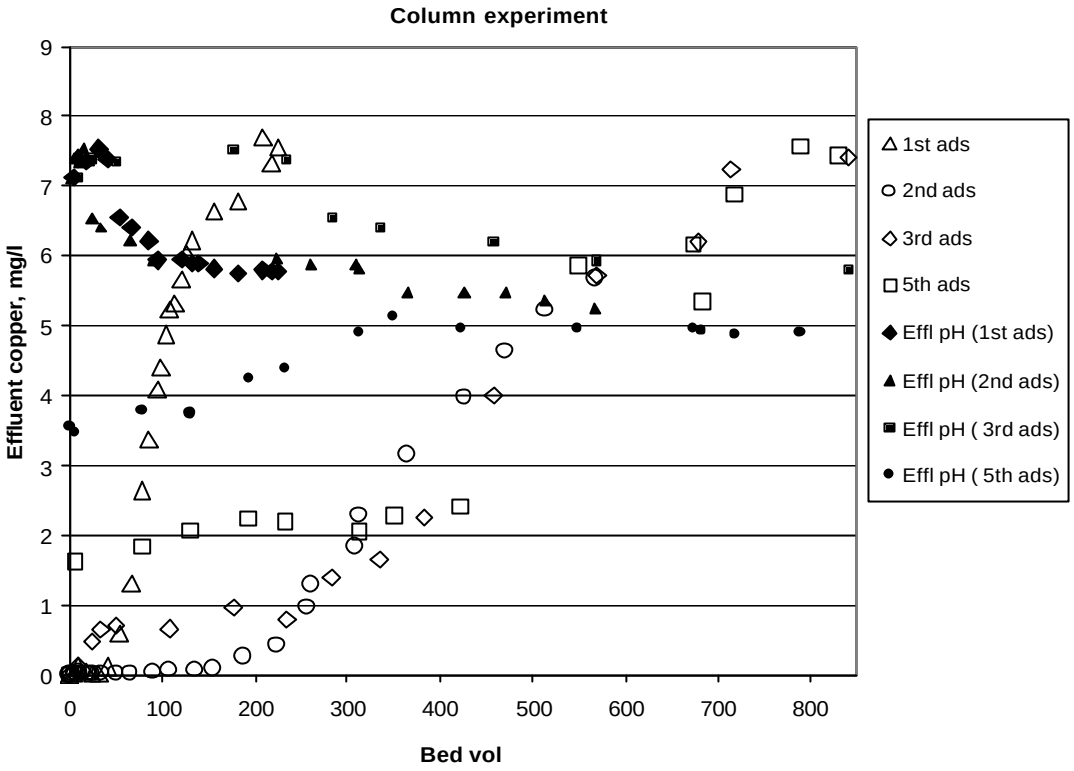

Figure 4.26: Breakthough curve for copper adsorption for 5 cycles of adsorption and desorption

The desorption curves for the 2nd and 3rd cycle are given in Figure 4.27. From this figure, it can be seen that the copper ions obtained in the acidic solution (pH = 1), have about an average concentration of 1000 and 1250 mg/L, which is about a factor 100 more than the treated solution. Another technique can now be used to recover the metals in its pure form from the solution.

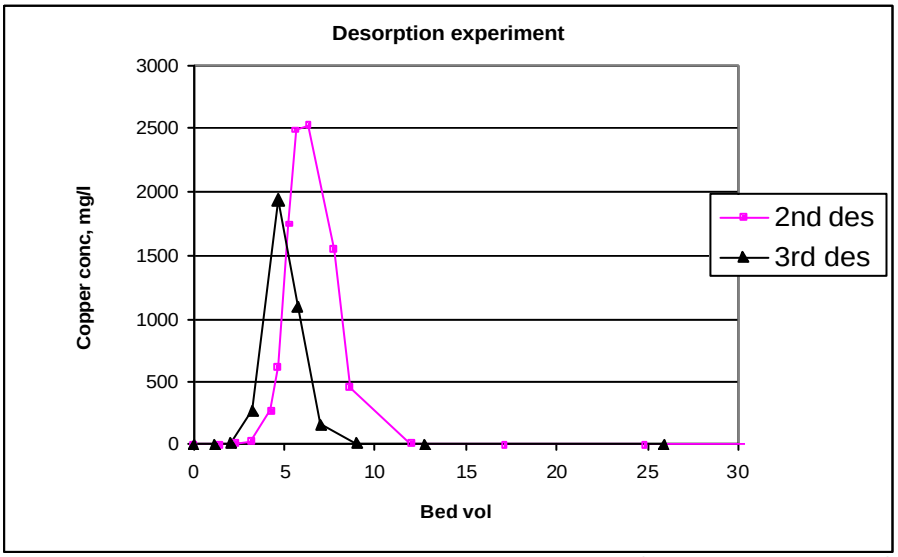

Figure 4.27: Copper concentration in the acid solution after desorption as a function of the bedvolume

4.4.3 Comparison with other adsorbents

An attempt was made to characterize other sorbent in this work, commercial chitosan purchased from biopolymer, USA and ion exchange resins, Amberlite 200CNa, supplied by RHOHM and HAAS, France, were used, as leader in the technology of adsorption of heavy metals from wastewater (The Amberlyte was advised by Mr Perter Cable of RHOHM and HAAS for the specific metal and pH of the solution). The characteristics of the Amberlyte material is given in the table below.

Table 4.10: Specifications of Amberlyte 200C Na, as delivered by RHOM and HAAS

	Amberlite 200C Na
Diameter (μm)	<50
Water content	39-53
Specific gr	1.1
Solubility	Insoluble

The adsorption capacities of copper was carried out identically as to the home made chitosan and the results are given in Table 4.11 together with other sorbents as reported in literature (only maximum values have been used). It can be seen from this table that the locally made chitosan displayes a high adsorption capacity toward copper, both for the maximum adsorption capacity (Q_{max}) as for the affinity parameter (b), which indicates the strength of a bond between the adsorbent and adsorbate at zero occupation.

Table 4.11: The adsorption characteristics of different adsorbent for copper

Adsorbent	Q_{max} (mg/g)	b (l/mg)	pH	Sources
XLB (Local chitosan)	159	0.07	6.0	This work
Prawn shell flakes	17.2	0.00082	6.0	Chu et al
Commercial chitosan, NXL	118	0.04	5.5	This work
Ion exchange Amberlite 200	105.3	0.05	5.9	This work
Activated carbon	122.2	-	4.61-4.81	Dastgheib & Rockstraw

4.5 Conclusions

The prepared beads have a water content of about 95%, slightly depending on the bead size of the material. The crosslinked beads are stable until a pH of 1. The pK_a of the produced beads was 5.9 and an amino concentration of 4.9 mmol per gram of chitosan was obtained. A drop in pK_a and also a decrease in the amino concentration was obtained, when chitosan beads were crosslinked (pK_a is 4.3 and amino-side concentration is 4.2 mmol/g when 2.5 % crosslinking reagent was used for 3.8 mm diameter bead). The total amount of residual amino concentration differs slightly with the size of bead used during crosslinking. The residual amino concentration for the 1.84 mm diameter is 3.4 mmol/g as compared with 0.9 mm diameter bead having 3.3 mmol/g. The smaller value in residual amino concentration of the

0.9 mm diameter bead may be due to the fact that its larger surface area of its useful sites exposed to the outer surface were used for used for crosslinking. The degree of deacetylation is 85%. A novel adsorption model has been developed in which the adsorption of heavy metals is described combined with the acid-base characteristics of the chitosan. This model describes the adsorption of Cu, Zn, Cd and Pb accurately, but fails to predict the adsorption of Ni. A maximum adsorption of 160 mg Cu/g is obtained, which is superior to other adsorbents, known from literature. The chitosan has the highest affinity to Cu, followed by Pb, Ni, Zn and Cd. Since chitosan is intended to be used at low concentrations (below 100 mg/L), the affinity parameter, b, is more important and is was also found to be larger than other adsorbents. Adsorption column experiments have been carried out with a 10 ppm Cu simulated waste stream and 550 bed-volumes could be produced with a Cu level below 1 ppm (WHO limit), where chitosan was recycled three times. After the fifth recycle, the chitosan beads showed a very fast breakthrough, indicating that the beads were not usable anymore. The beads were desorbed in high acidic solutions (pH = 1), in order to obtain a high concentration of Cu in the desorption solution (up to 1200 mg/L), for easy recovery.

5 CHITOSAN MEMBRANES

In this chapter, the characterisation and adsorption characteristics of the membranes, prepared according to the procedure given in Section 3.2, is given. In Section 5.1, a thorough characterisation of the chitosan membranes is given, while in Section 5.2, the transport through the membranes is studied. In Section 5.3, the relevant theory used for the adsorption experiments is described. Section 5.4 deals with the used experimental procedures and the most important results and discussion are given in Section 5.5. Finally, the conclusions of this experimental work are listed in Section 5.6.

5.1 Characterisation of membranes

5.1.1 Introduction

There are two main groups of membranes, porous and nonporous. Porous membranes contain fixed pores, in the range of 2 nm to 10 μm. The selectivity is mainly determined by the dimensions of the pores, thus discriminating between the size of different molecules. Nonporous membranes are used in gas and vapour separation and pervaporation and are capable of separating molecules of approximately the same size (Mulder, 1996).

It is often very difficult to relate the structure related parameters directly to permeation-related parameters because the pore size and shape is not very well defined. The configuration of the pores used in simple model description deviate sometimes dramatically from the actual morphology. Nevertheless, a combination of well-defined characterisation techniques can give information about membrane morphology, which can be used as a first estimate in determining possible membrane modelling. So, for membrane applications, it is important to relate the manufacturing conditions to the structural properties of the membrane. These structural properties include density, porosity, pore size distribution, average pore size and specific surface area.

In Section 5.1.2, the different techniques, relevant to chitosan membrane characterisation are presented. The results of these characterisations are given in Section 5.1.3.

5.1.2 Characterisation techniques used

In order to determine the structure of the manufactured chitosan membranes, different experiments have been carried out, as described in the following sections. For all experiments, chitosan membranes were manufactured in triplicate and the data present the average of the three values. The error was determined statistically and the maximum error for the characterisation of the membranes (according to a 95% confidentiality interval) was 12%.

5.1.2.1 Determination of membrane density

The wet density of the membranes was determined by a method as described by Kawamura et al. (1997) . Since the membranes were stored in deionised water, before weighing, the membranes were vigorously shaken in air, to remove the cohesive water from the edges of the membrane. The volume of the membrane was determined from the membrane diameter and thickness. Finally, the density was calculated with:

$$r_{\text{membrane}} = \frac{m_{\text{membrane}}}{V_{\text{membrane}}} \qquad 5.1$$

5.1.2.2 Determination of water content

The water content was determined from the difference between the mass of a wet and a dry membrane. A wet membrane is hereby defined as the membrane obtained after manufacturing and after removing the cohesive water from the edges (see Section 3.2.2.1). A dry membrane is defined as the structure that remains after removing all the water from the membranes (after heating the membrane at 60 °C in a ventilated oven for at least 24 hours). The water content (xw) is calculated with:

$$x_w = \frac{m_{wet\ membrane} - m_{dry\ membrane}}{m_{wet\ membrane}} \qquad 5.2$$

The chitosan content (x_c) can subsequently be calculated with:

$$x_c = 1 - x_w . \qquad 5.3$$

5.1.2.3 Determination of porosity

Gel type membranes are generally classified as being non-porous membranes. Since the produced chitosan membranes have a relative large water content (up to 95%, see Section 5.1.2.2), the transport of a liquid through the membranes can be described respective to the solid (chitosan) matrix that forms the membrane. While pressing e.g. water through the membranes, part of the water that forms the membranes is continuously replaced, so not all water is forming an integrated part of the membrane. In this way, the produced membranes can be modelled accordingly to porous membranes. The “porosity” of the membrane can however not be based on the mass difference between a wet membrane and a dry membrane, but can be determined using a method reported by Kawamura et al. (1997) by assuming that the pore volume was equal to the free water, which filled the pores of the membrane. The free water in the membrane is determined by the spinning of a wet membrane in a centrifuge and the collection and weighing of this water. The “porosity” can then be determined from:

$$e = \frac{\text{Volume of free water in the pores}}{\text{Volume of wet membrane}} \qquad 5.4$$

5.1.2.4 Determination of maximum pore size

The maximum pore size of the membrane was determined using the Bubble-point method as described by Mulder (1998). The method is based on measuring the minimum pressure needed to blow a gas through a water filled membrane. In this way, the maximum pore diameter can be determined using thee Young equation:

$$r_P = \frac{2 * ?}{? P} * \cos ? \qquad 5.5$$

where ? is zero, since the radius of the gas bubble is equal to the pore radius, at the point of completely penetrating the membrane.

The apparatus used for determining the maximum pore size is shown in Figure 5.1. As a gas, nitrogen was used, and the pressure is gradually increased until gas bubbles are visually present in the water on top of the membrane.

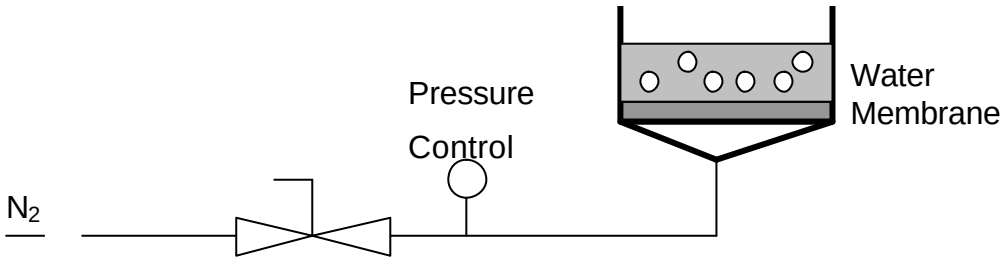

Figure 5.1: Schematic drawing of a bubble-point test apparatus

5.1.2.5 Determination of the surface area

The total surface area of the dried membrane was determined using the iodine adsorption number as described by Pawlowski (1971). In this method, the amount of iodine adsorbed by the dry membrane is measured via the difference in iodine concentration before and after adsorption (iodine concentration is determined by titration using a sodium thiosulphate solution). The amount of adsorbed iodine per gram adsorbent is than correlated to the surface area as described by Pawlowski (1971).

5.1.2.6 Determination of chitosan membrane structure after drying

Chitosan membranes were dried and the solid structure was examined using a Scanning Electron Microscopy (SEM, FEI Quanta 200 ESEM).

5.1.3 Results and discussion of characterisation

5.1.3.1 The effect of Chitosan Concentration on Membrane density

The density is an important property of the membrane, since it frequently directly relates with some membrane properties (e.g. porosity) and so with the transport properties of the membrane. In Figure 5.2, the density of the membrane is given as a function of the chitosan concentration in the acidic solution, used for the preparation of the membrane.

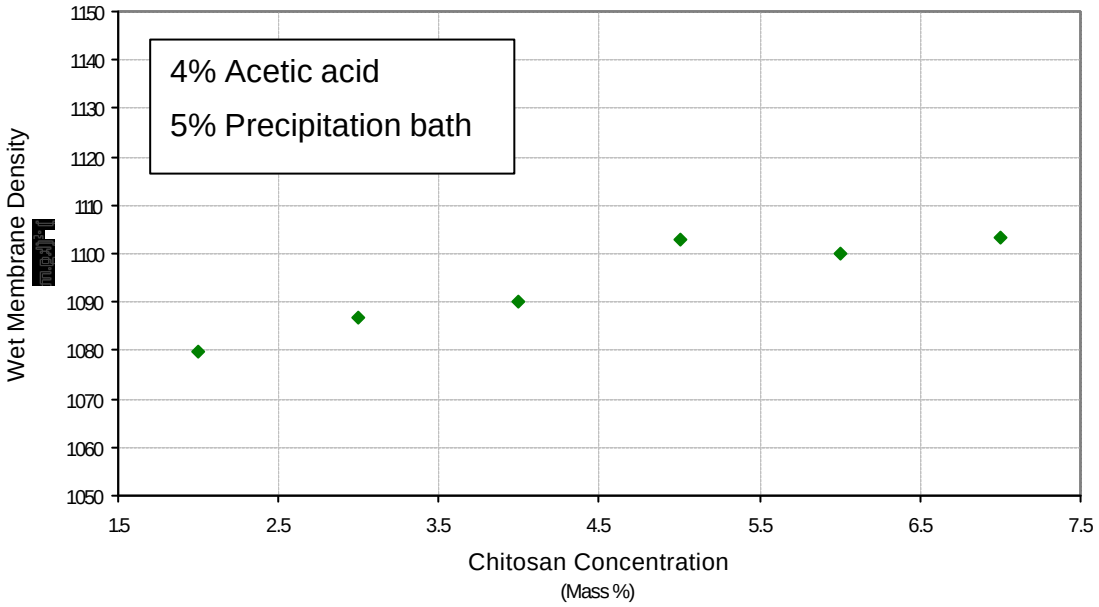

Figure 5.2: Effect of chitosan concentration (Chitosan A) on the wet membrane density

It is clear from Figure 5.2 that the density slightly increases with an increase in the chitosan concentration. As expected only a slight change in density is observed due to fact that approximately 95% of the membrane consists out of water (see Section 3.3.2). The increase in wet membrane density is a result of higher chitosan concentration. Kawamura et al., 1997, also observed this phenomenon.

5.1.3.2. The effect of Chitosan Concentration on the Water content

In Figure 5.3, the chitosan content (x_c) is given as a function of the chitosan concentration in the 4% acetic acid solution, before the manufacturing of the membrane. It can be concluded that the chitosan content will increase with increasing chitosan concentration. Generally, it

can be seen that the water content of the membranes is high (95 - 98%), values that are in good agreement with Kawamura et al. (1997).

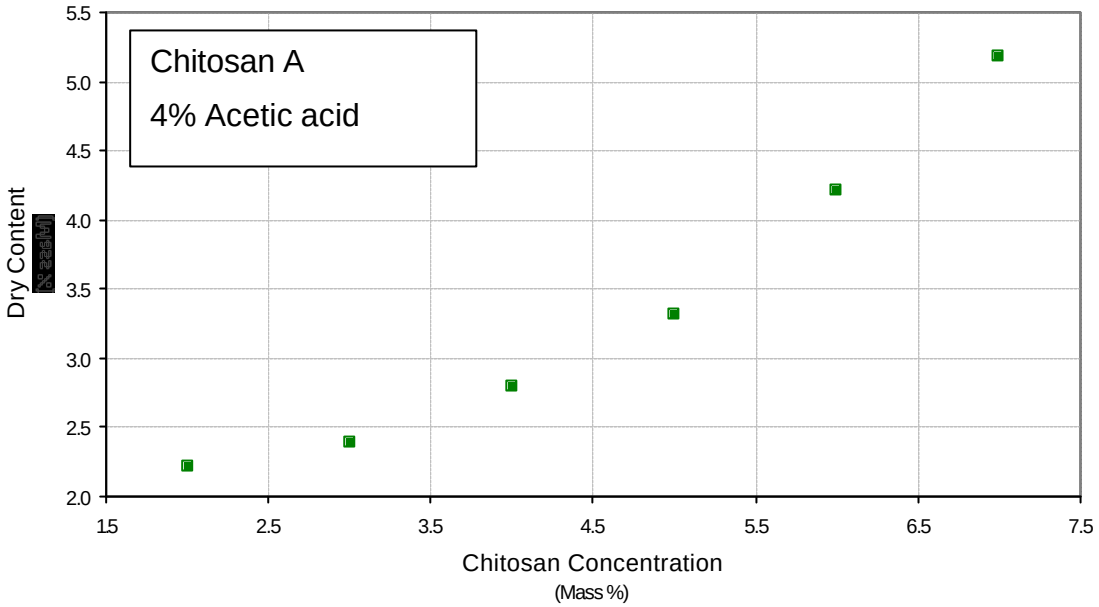

Figure 5.3: Effect of chitosan concentration on the chitosan content (the % dry material in a membrane) of the membranes

5.1.3.2 The effect of Chitosan Concentration on the "Porosity"

In Figure 5.4, the porosity (as defined in Section 5.1.2.3) is given as a function of the chitosan concentration in the 4% acetic acid solution, before the manufacturing of the membrane. It can be seen from this figure, that this porosity is only a slight function of the chitosan concentration and that its value is between 0.65 and 0.67. This value is significant lower that the total water content (see Section 5.1.3.2), indicating that some of the water in the chitosan membrane is part of the integral structure of the membrane, this water is termed fixed water in this study. From Section 3.3.2 and 3.3.3, it can thus be concluded that a membrane, manufactured from a 7% chitosan solution consists of the following composition:

Table 5.1: Composition of chitosan membrane

Fixed Chitosan	5 %
Fixed water	30 %
Free water	65 %

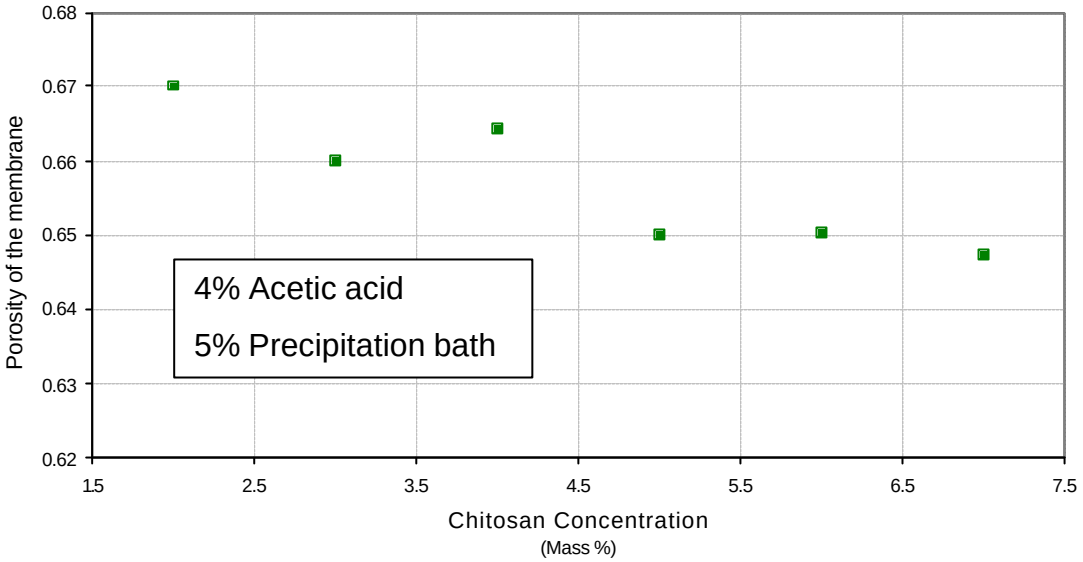

Figure 5.4: Effect of chitosan concentration on the porosity of wet chitosan membranes

5.1.3.3 The effect of Chitosan Concentration on the Maximum pore radius

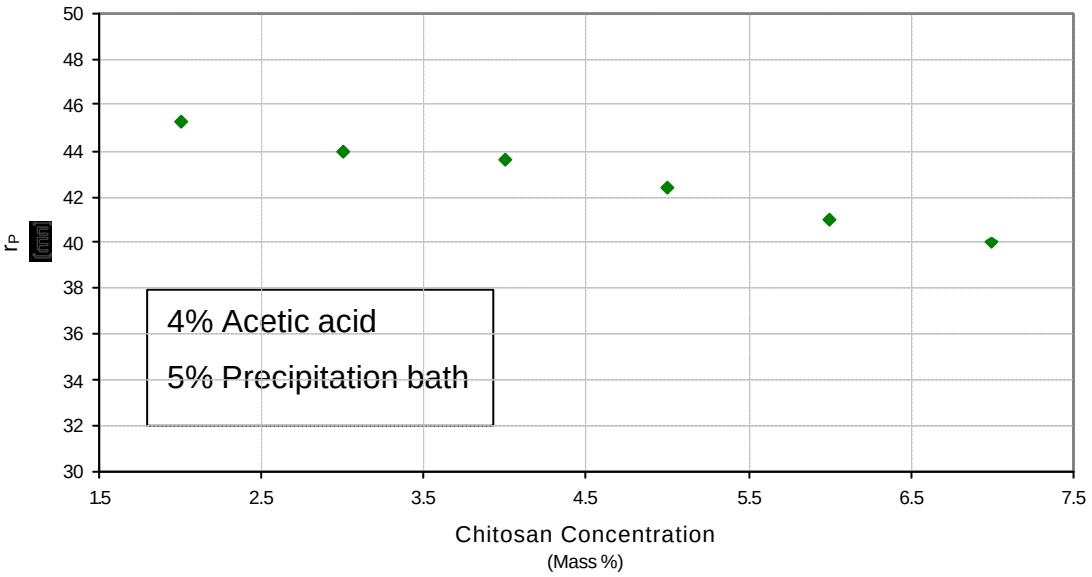

Figure 5.5: Effect of chitosan concentration (Chitosan A) on the maximum pore radius of the wet chitosan membranes

Figure 5.5 gives the effect of the chitosan concentration in the 4% acetic acid solution, before the manufacturing of the membrane on the maximum pore radius. The increase in chitosan concentration leads to a slight decrease in the maximum pore radius. This could be attributed to the fact that more space is occupied by chitosan macromolecules, resulting in a smaller "pore size". The maximum pore size is in the range of 40-45 nm, which is comparable to ultrafiltration (UF) membranes.

5.1.3.4 The effect of Chitosan Concentration on the Surface area

Figure 5.6 gives the relationship between the chitosan concentration and the total surface area of the membrane (For experimental data and calculations see Appendix C-1.3). From this Figure, a similar trend as for the maximum pore size (Figure 5.5) is observed. The increased chitosan concentration leads to a lower "porosity" and thereby also to a lower surface area. This is however not a very strong effect. The surface area ranges from 1.175 – 1.195 m2/kg.

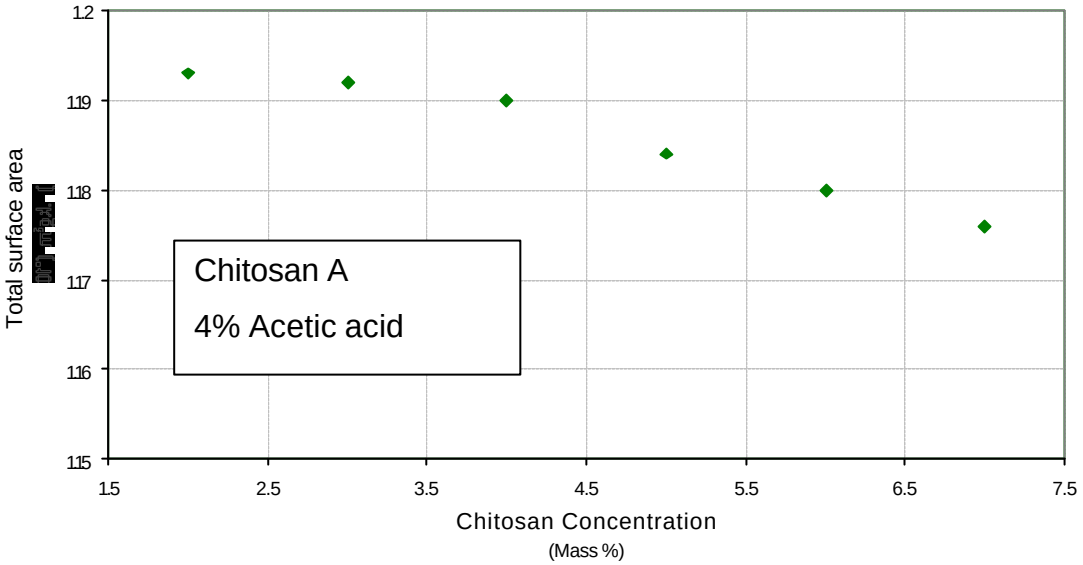

Figure 5.6: Effect of chitosan concentration (Chitosan A) on the total surface area of dried chitosan membranes

5.1.3.5 Scanning Electron Microscope results

A Scanning Electron Microscope analysis revealed that the dried chitosan membrane has a honeycomb structure (Figure 5.7). The matrix structure of the dried chitosan seemed not to be affected by the adsorption of zinc.

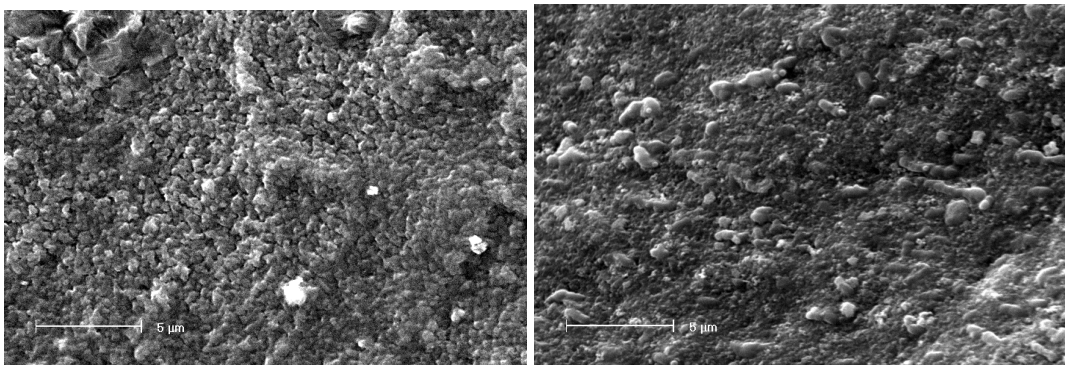

(a) (b)

Figure 5.7: Dried Chitosan Membrane structures (Chitosan A) before zinc adsorption (a) and after zinc adsorption (b) (Surface view)

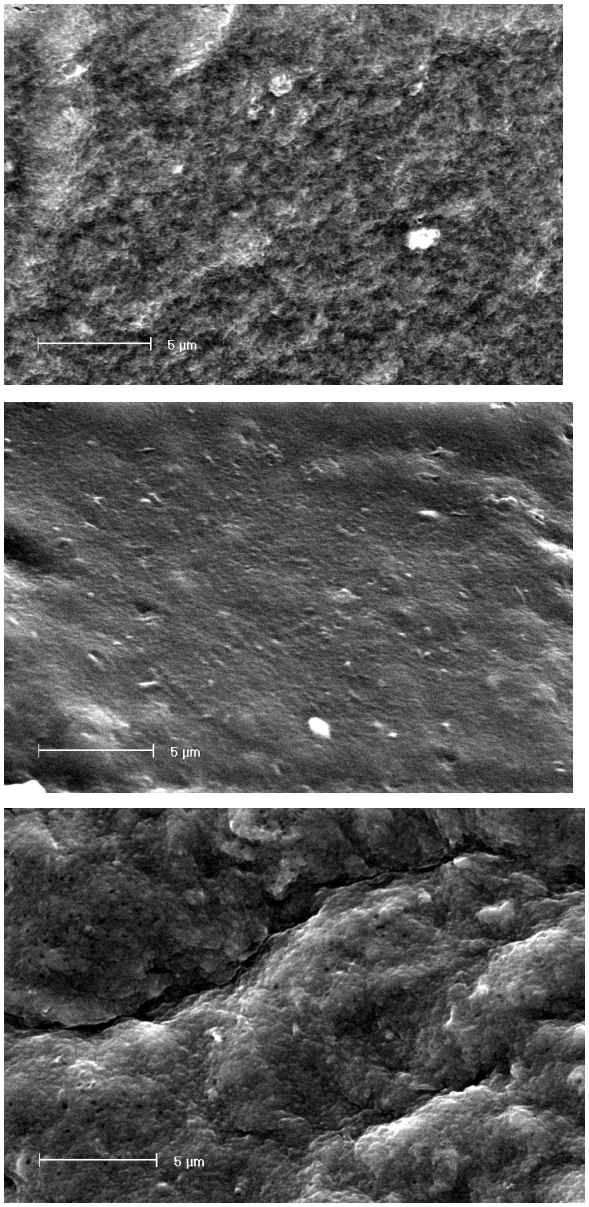

Sample	Chitosan concentration (Mass %)	Acetic Acid concentration (Mass %)	Precipitation Bath Concentration (Mass %)
top	2.5	2	2.5
middle	7.5	2	2.5
bottom	8.22	2	2.5

Figure 5.8: Effect of Chitosan Concentration (Chitosan A) on the dry membrane characteristics

Figure 5.8 gives SEM-micrographs for different prepared membranes. Membrane a, prepared from a relative low chitosan-acetic acid solution, shows a not well formed (loose) structure (see Figure 5.8). This was later confirmed by the low mechanical strength the membranes

had, after applying a pressure difference over the membrane. As the membrane density increases with increasing chitosan concentration, at concentrations between 6.5 and 7.5 mass % a (mechanically) very strong membrane is produced (see Figure 5.8). Above a chitosan concentration of 8.0 the membrane seems to have "cracks" (see Figure 5.8). From the SEM-study, it was concluded that a mechanical strong membrane is obtained as a chitosan concentration of 6.5 to 7.5 is used.

5.1.3.6 Proposed structure for chitosan membranes

After a thorough inspection of the manufactured chitosan membranes, the following structure for the chitosan is proposed. The membranes consist of a large fraction of water (93 – 96 %). If the membrane is dried, a structure as given in Figure 5.9 is obtained from SEM. It can be seen from this figure, that a porous structure is present. It is now assumed that in the wet (gelly) membrane the water is situated in that spaces, where after drying pores appear. Water can be present as free water or as fixed water.

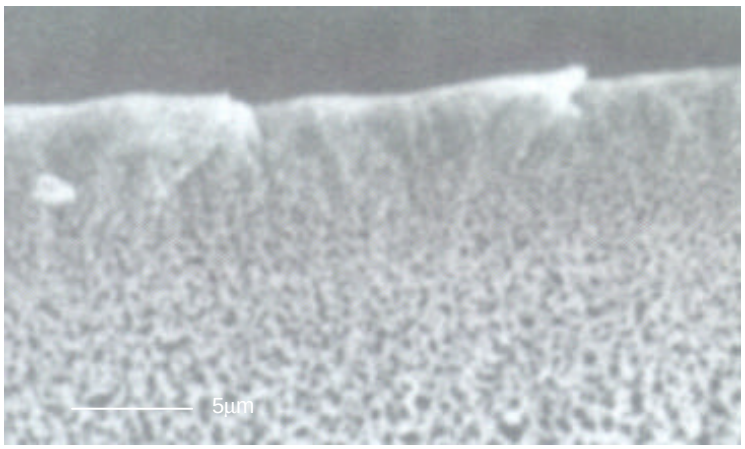

Figure 5.9: Side view of chitosan membrane structure

When applying a pressure difference over the membrane, the free water can be transported through the porous network, as with traditional MF and UF membranes. The fixed water, together with the chitosan forms the skeleton of the membrane.

The bubble point method gives additional evidence that the chitosan membranes can be modelled as porous membranes. The maximum pore diameter of approximately 80 nm classifies this membrane in the category of ultrafiltration (UF). This is also confirmed visually looking at the pore sizes in Figure 5.9.

5.2 Transport through chitosan membranes

The manufactured chitosan membranes were firstly characterized by pressing clean water through the membranes. The volumetric flux (Jp) was measured as a function of the pressure difference (ΔP) as given in Figure 5.10

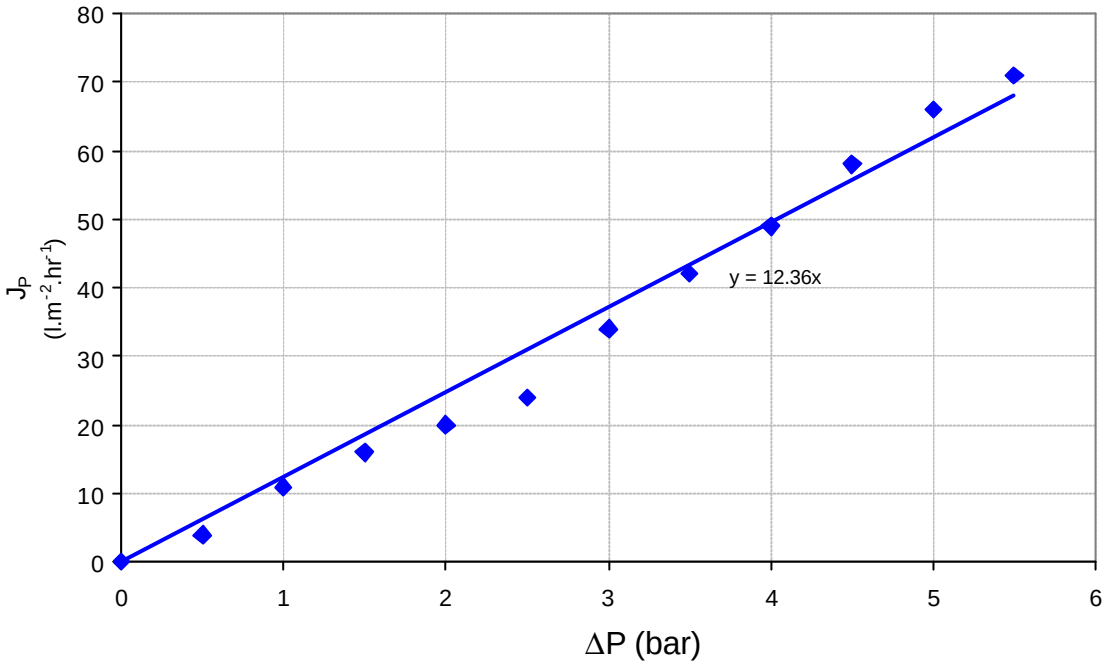

Figure 5.10: Pure water flux as a function of the pressure difference (membrane thickness = 0.8 mm and T = 298K)

The hydrodynamic resistance (Lp) was calculated from the slope of this figure. For pure water at 298K the LP value was 12.36 $l.m^{-2}.hr^{-1}.bar^{-1}$ and for pure water the viscosity is 0.001 Pa.s or $2.77*10^{-12}$ bar.hr, therefore the hydrodynamic resistance is $2.9*10^{10}$ $m^2.l^{-1}$. Using the Hagen-Poiseulle equation, the (average) pore size was determined to be 47 nm. The transport coefficient and pore size proves that the membrane is within the ultrafiltration region.

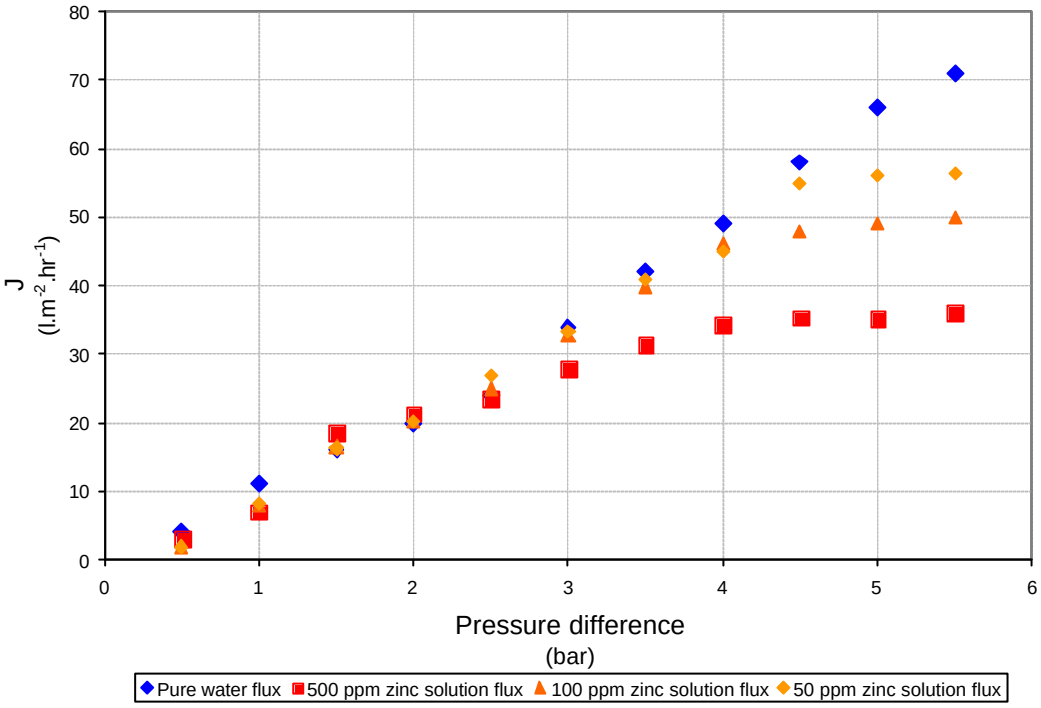

Figure 5.11: Schematic drawing of the relationship between flux and applied pressure for different zinc concentrations (Membrane thickness = 0.8 mm)

Figure 5.11 gives the flux trough the membrane for different salt solutions. Due to concentration polarisation, the flux at a certain pressure difference does not increase anymore if the pressure difference is increased further. This flux is called the limiting flux. The limiting flux (Mulder, 1998) depends on the concentration in the bulk of the feed, cb and on the mass transfer coefficient k

$$J_{limiting} = k.\ln \frac{c_f}{c_i} \qquad 5.6$$

This equation can be written in a linear form as shown in equation:

$$J_{limiting} = k.\ln c_f \quad -k \ln c_i \qquad 5.7$$

If the results depicted in Figure 5.11 are plotted as J versus $\ln(c_i)$, a straight line is obtained. This is shown in Figure 5.12. From this figure the transfer coefficient can be obtained from the slope of the plot and $\ln(c_f)$ is the value where the plot cuts the x-axis.

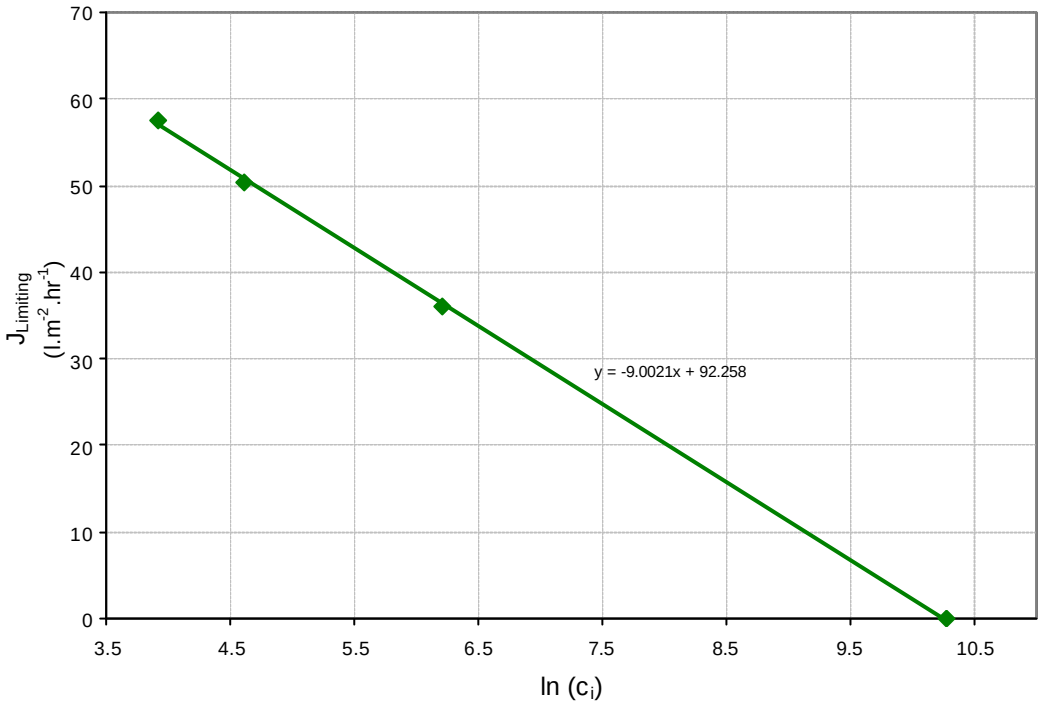

Figure 5.12: Limiting flux J plotted as a function of the logarithm of the bulk concentration

Thus the equation describing the limiting flux is

$$J_{limiting} = 9.002 * \ln \frac{28282}{c_i} \qquad 5.8$$

In summary, it can be stated that the manufactured chitosan membranes behave like conventional ultrafiltration membranes, although the separation mechanism between chitosan membranes and ultrafiltration membranes differs.

5.3 Relevant adsorption theory

A brief summary of the adsorption theory used in the study of membrane adsorption is given in the following sections. Since the actual adsorption is fundamentally not different from adsorption on other media, general adsorption theories are used.

5.3.1 General adsorption theory

Adsorption is defined as the process where an adsorbate attaches to the surface of an adsorbent. Molecules can either bind to the surface via chemical (covalent bond) or physical adsorption (normally van der Waals bonds). Chemical adsorption is associated by a larger heat of adsorption and is generally an exothermic process (Tien, 1994). The strength of the bond with the adsorbent is an important factor for the adsorption process (Swart et al., 1999). The stronger the bond is, the easier the adsorbate will be adsorbed, but also the more difficult

it is to recover (desorb) the adsorbate. Since the objective of this study is to evaluate the adsorption- and recovery of heavy metal ions from wastewater, both adsorption and to a lesser extend desorption are studied.

Mechanistically, it has been suggested by Tien (1994) that the adsorption of an adsorbate from a solution (e.g. metal ions) on an adsorbent occurs in three consecutive steps:

1. Sorption at the surface of the adsorbent
2. Diffusion of adsorbate into the pores of the adsorbent
3. Sorption on the internal surface of the adsorbent

Generally, the first and second step are rate-determining and the third step is fast.

In the specific case that ions are adsorbed from an aqueous solution onto an adsorbent, the equilibrium of the adsorbate separated between the two phases can be determined from the partition of the solute concentration in the solid phase as a function of the solute concentration in the liquid phase, and is called an isotherm. There are two widely accepted adsorption isotherm models available in literature, which were proposed by Langmuir and Freundlich (Tien (1994)). The most popular way to describe metal ion adsorption is with the Langmuir isotherm model (McKay et al., 1989).

The Langmuir model assumes uniform energies of adsorption on the surface and no transmigration of sorbent in the plane of the surface (McKay et al., 1989). This model is valid for monolayer sorption on a surface containing a finite number of sites (Volesky, 1989), and is represented by:

$$q_e = \frac{K_L.C_e}{1+b.C_e} = \frac{b.C_e}{1+b.C_e} q_m \qquad 5.9$$

The second isotherm model, the Freundlich model (Tien, 1994), is a semi-empirical relation between the adsorbate-concentration and the adsorbed concentration. The general form of this model is:

$$q_e = K_F * C_e^{1/n} \qquad 5.10$$

The equilibrium characterisation of the biosorbent material is crucial for a quantitative assessment of the performance of the adsorbent and for process design (Volesky, 1989).

Factors that influence the adsorption characteristics in the case of the adsorption of heavy metals on a specific adsorbent are temperature, presence of other ions, oxidation number of

the metal-ion and the pH of the solution (Maruca et al., 1982). One of the more widely used methods to describe the effect of temperature on the adsorption parameter b in the Langmuir equation, is the van der Waals equation:

$$b = b_o \exp(-\frac{?H}{R.T}) \qquad 5.11$$

5.3.2 Adsorption on chitosan

Adsorption techniques, specifically those using chelating resins, have been widely demonstrated and promoted as being feasible technology (Yang et al., 1984) for the removal of heavy metal ions from wastewater.

The active groups of chitosan that are involved in the binding with heavy metals are both amino and hydroxyl groups (Nam et al., 1998). These groups act as the chelating ligands (Kondo et al., 1996), using the three-dimensional structure of the groups, with a release of hydrogen ions, causing the pH to decrease with adsorption (see, Figure 5.13, Kaminski et al., 1997).

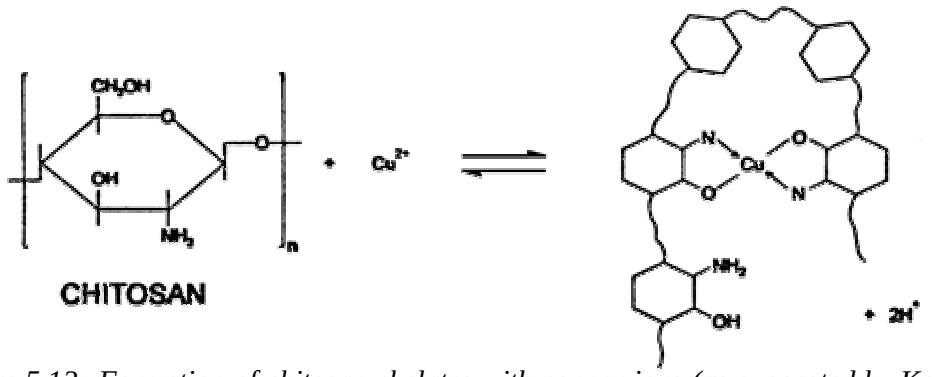

Figure 5.13: Formation of chitosan chelates with copper ions (as suggested by Kaminski et al., 1997

This adsorption theory is supported by the following:

1. A comparison of Fourier transform infra-red spectra of chitosan and chitosan doped with rare earth metals, indicated complex formation between the metal ions and the amino groups of the chitosan (Grant, 2002).
2. X-ray photoelectron spectroscopy analysis support this (Jiang et al., 1997), and indicate that these bonds are weak and possible ionic in nature.
3. Carbon nuclear magnetic resonance studies (Jansson-Charrier et al., 1995) shows that the amino sites are the main adsorption sites for uranium adsorption onto chitosan.

The adsorption of zinc-ions on chitosan follows the same mechanism as given in Figure 6.1 (Kaminiski et al., 1997). Note that the released hydronium ions originate from the –OH groups and that the hydrogen atoms of the amino function are not shown. The chitosan molecular weight and the degree of deacetylation are therefore important factors when determining the maximum theoretical capacity. Involvement of other groups in the adsorption process cannot, however, be excluded, as the adsorption loading capacity sometimes exceeds the concentration of available amino sites (Grant, 2002).

The adsorption mechanism will be influenced by the membrane and solution pH, speciation of metal ions (Guibal et al., 1999a) and ionic strength (Udaybhaskar et al., 1990). A decrease in adsorption takes place with ionic strengths in excess of 10-2M, indicating the importance of electrostatic attraction in metal adsorption (Chen, 1997 and Yiacoumi, 1997). Increase pH provides increased metal adsorption capacity. This is due to the decrease of surface charge of chitosan with increasing pH. The surface charge approaches zero near pH 6, with maximum adsorption capacity between pH 6 and pH 7 (Grant, 2002).

Because chelants possess acid-base characteristics, and chelation is an equilibrium reaction, the equilibrium can be shifted and altered by species such as protons and hydroxide ions that interact with metals and chelants (Nam et al., 1998). If protons are introduced into a metal containing solution, the hydrogen ions will compete with the metal ions and at sufficient low pH, the metal ions will be desorbed from the chitosan (Conway et al., 1999).

The fact that chitosan is relatively inert to alkali metals and alkaline earth metals makes it superior to the other polymers tested for transition metal recovery in alkaline or saline waters (Ghandi et al., 1997). The addition of organic acids also reduces chitosan adsorption performance (Bassi et al., 1999).

The nature of the anions present in the solution carrying the transition metal ions to be collected is also of importance (Inoue et al., 1996). It is known from literature for chitosan beads that chloride ions can depress the collection extent, while sulphate ions can enhance it, due to the modifications of chitosan introduced by the presence of anions. The increase of adsorption capacity due to sulphate is explained by the increased degree of crystallinity (Muzzarrelli, 1977). However, Kurita (1998) found that calcium, magnesium, bicarbonate and chlorides present in tap water did not influence cadmium uptake by chitosan flakes.

Bassi et al. (2000) proved that in commercially available chitosan (chitosan flakes supplied by Sigma, with a DDA of 85%) the order of metal ion adsorption decrease from Cu^{2+} to Zn^{2+} as

follows: copper (1 $mg.g^{-1}$) > lead (0.20 $mg.g^{-1}$) > cadmium (0.113 $mg.g^{-1}$) > zinc (0.06 $mg.g^{-1}$). The metal adsorption uptake was found to be pH-dependant, with a maximum of 1 mg.g-1 zinc ions between pH 6 and pH 7. The equilibrium studies correlate well with the Langmuir isotherm equation with a maximum adsorption capacity of 11.66 mg.g-1 and an adsorption equilibrium constant of 0.97 $L.mg^{-1}$ for the zinc ions.

Chui et al. (1996) investigated the removal of copper, chromium and nickel from solutions using crude shrimp chitin and crab chitosan (powder). The performance of the shrimp chitin and crab chitosan as expressed by the order of its metal affinity was Cu (1 $mg.g^{-1}$) > Cr (0.98 $mg.g^{-1}$) > Ni (0.4 $mg.g^{-1}$) and Cu (1.1 $mg.g^{-1}$) > Cr (0.9 $mg.g^{-1}$) > Ni (0.8 $mg.g^{-1}$) respectively. The adsorption of Cu^{2+} and Ni^{2+} on pelletised chitosan was investigated by Huang et al. (1995). Results showed that the calcium-alginate beads had an adsorption capacity of 17 $mg.g^{-1}$ and 2.5 $mg.g^{-1}$ for copper and nickel respectively.

Kawamura et al. (1997) investigated the breakthrough curve for adsorption of Hg2+ on polyaminated highly porous chitosan beads. The beads were prepared to the following properties: An average dry pore diameter of 100 nm and a total porosity of 0.779. Results indicated a Langmuir type isotherm with a maximum adsorption capacity of 210 mg.g-1.

Equilibrium studies (McKay et al., 1989) for the sorption of metal ions onto chitosan flakes showed that the monolayer sorption capacity was 815, 222, 164 and 75 $mg.g^{-1}$ chitosan for mercury, copper, zinc and nickel ions respectively, at room temperature and at a particle size in the range of 710-1000 μm. Langmuir adsorption isotherms for zinc ions in the range showed a maximum adsorption capacity of between 98 to 120 $mg.g^{-1}$ and an adsorption equilibrium constant of 1.2 $L.mg^{-1}$ for the zinc ions. Temperature studies indicated that the maximum adsorption capacity increased with increasing temperature, and resulted in an adsorption enthalpy value of –17.7 $kJ.mol^{-1}$.

Activated carbon is another low cost material that can be used for metal ion adsorption. It has a metal ion adsorption for zinc of 25 $mg.g^{-1}$ according to Atkinson et al. (1998) and for mercury 120 mg.g-1 according to Namasivayam et al. (1998).

Wan Ngah et al. (2001) investigated the removal of copper ions from aqueous solution onto chitosan beads and crosslinked chitosan beads. Beads were crosslinked using glutaraldehyde, epichlorohydrin and ethylene glycol diglycidyl ether. The adsorption capacity was 39.8, 11.9, 17.5, and 6.2 $mg.g^{-1}$ respectively at a pH of 6.

5.3.3 Desorption of ions from chitosan membranes

Desorption of the metal ions from the saturated adsorbent translates into an economic advantage. The adsorbent does not have to be replaced that often and the adsorbed material can be recovered (Volesky, 1989). Metals are most often removed from chelating molecules by pH manipulation. Since ligands are frequently only active when ionised, a pH shift can be used to remove the active form of the ligand and remove the metal ligand complex (Volesky, 1989).

Most biomass-based systems, however, will not withstand long-term recycling. Loss of activity of ligands is of particular interest in relation to solid substrate bound ligand systems. Expected activity losses occurs as follows:

1. Chemical degradation
2. Chemical fouling
3. Thermal degradation
4. Mechanical destruction

Both chemical degradation and mechanical destruction were studied on chitosan beads (Jha et al, 1988). Jha et al. (1988) reported the following on cadmium desorption, that 88% desorption was observed in 0.01 N HCl. After two cycles, the adsorption capacity of chitosan was reduced to 69%, whereas the recovery of the cadmium with 0.01N HCl reduced from 91.2% in the first cycle to 81.3% in the third. The chitosan weight reduced after each acid treatment.

5.4 Experimental procedures

The study of membranes was focussed on the metal Zinc. The flux and adsorption through the membranes were tested by using a 50 - 500 $mg.l^{1}$ solution of zinc in demineralised water. The solution was continuously stirred above the membrane to prevent concentration polarisation and the pH of the zinc solution was controlled. The membrane was clamped in a membrane holder and the zinc solution was pumped through the membrane at 25°C. The flux and separation were tested under at various pressure differences. The pressure was applied to the cell using pressurised nitrogen from a gas bottle. The pH of the heavy metal salt solution, was adjusted using sulphuric acid to obtain acidic conditions and sodium hydroxide for alkaline conditions. The temperature was controlled using a hotplate. The solution was poured into the membrane holder. The hotplate was set on the needed temperature. The temperature was monitored until a constant temperature was reached, thereafter the nitrogen supply was opened for the start of an experiment.

Above a pressure difference of 100 kPa a support was used to prevent destruction of the membrane. For adsorption experiments, the solution was recirculated three times to reach equilibrium (it was proved that equilibrium already was attained after two cycles of recirculation).

Zinc samples were collected in acid washed plastic bottles. The pH of the solutions was measured with a Metler pH meter. A quantitative determination of elements present in the filtrate was made by Atomic Absorption Spectrophotometer analysis.

During the adsorption experiments, the solution was re-circulated to reach equilibrium. The concentration of the metal ion after the first cycle is denoted as the final concentration (C_{final}). The metal ion concentration did not change significantly between the second and third cycle, indicating that equilibrium was reached. The metal ion concentration after the solution was re-circulated three times to reach equilibrium is denoted as the equilibrium concentration (C_e).

During the adsorption experiments, equilibrium conditions were used for all experiments except where indicated. The adsorption loading of the membranes was calculated in mg of zinc adsorbed per gram of membrane (using the mass of the membrane on a dry basis) using:

$$q_e = \frac{(C_{in} - C_e) * V}{m} \qquad 5.12$$

5.5 Results and discussion

First, the equilibrium results are presented and then the dynamic properties of the membranes are discussed.

5.5.1 The adsorption equilibrium of zinc ions

The results for the equilibrium capacity (adsorption $mg.g^{-1}$) of chitosan membranes for zinc are shown in Figure 5.14. The conditions are at a pH of 6 and a membrane thickness of 0.8 mm. Experiments were conducted at temperatures of 293K to 313K, with five degree changes. The shape of the adsorption isotherm shows a rapid initial increase in sorption capacity resulting from a high apparent affinity of the chitosan for the zinc anion. The plotted results were tested for both Langmuir-type and Freundlich-type isotherms.

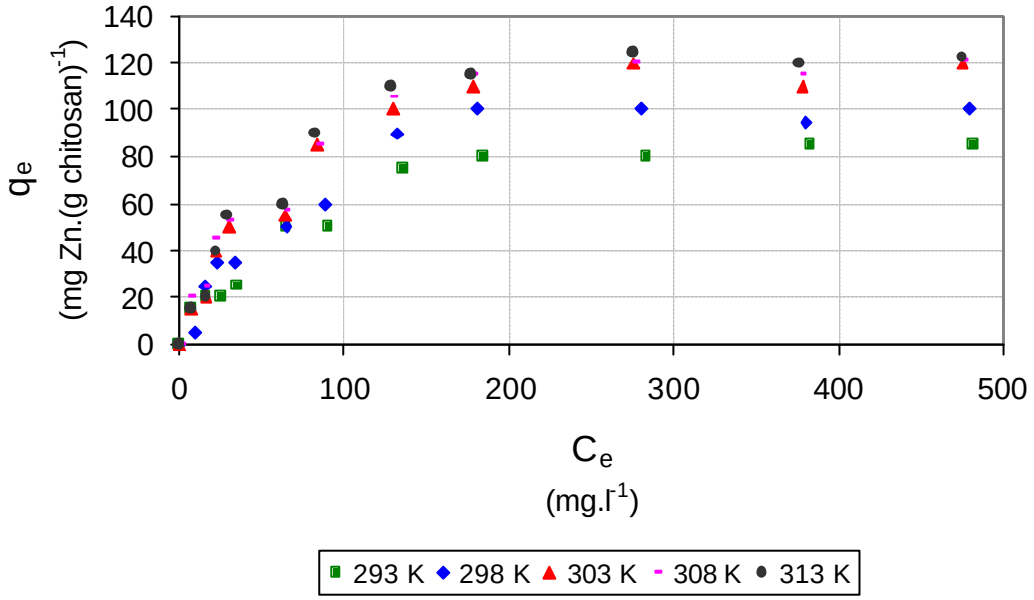

Figure 5.14: Equilibrium capacity after recirculation of zinc sorption onto a 0.8 mm chitosan membrane

The general expression for the Langmuir adsorption isotherm is the amount of metal taken up per gram of chitosan (mg/g). The approach for obtaining the Langmuir adsorption isotherm is to used the linear form of Equation 5.6, thus

$$\frac{C_e}{q} = \frac{1}{K_L} + \frac{b.C_e}{K_L} \qquad 5.13$$

hence a plot of $\frac{C_e}{q}$ versus C_e is linear with intercept-1=K_L and the slope = b*K_L^{-1} (Figure 5.15). The constant b in the Langmuir equation is related to the energy or net enthalpy of sorption.

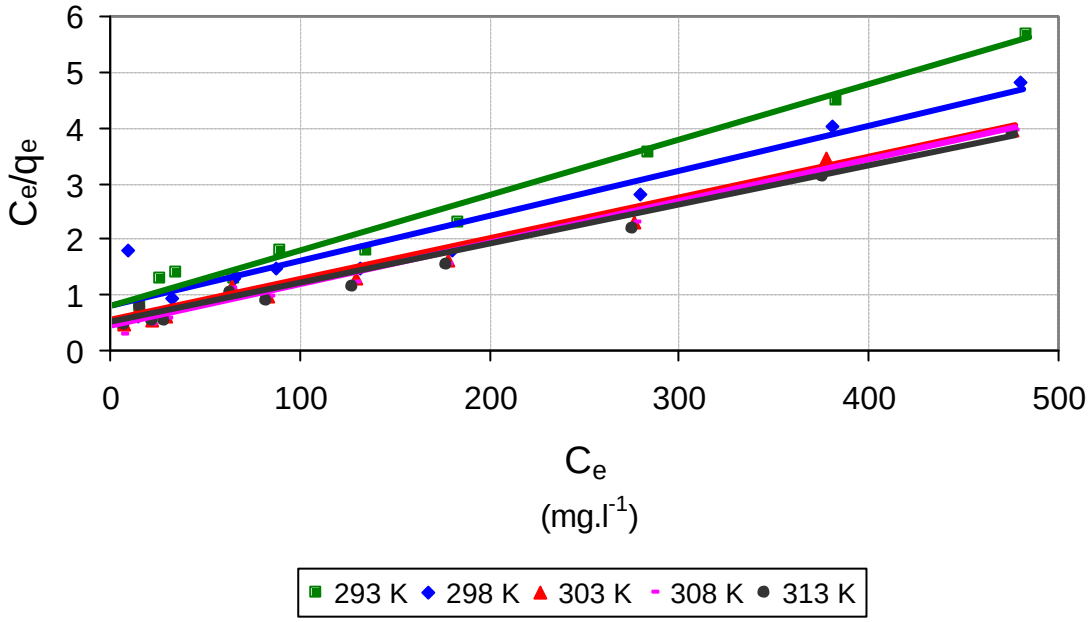

Figure 5.15: Experimental data modelling using Langmuir equation for corrected concentration

The Langmuir constants for corrected concentration were calculated from Figure 5.15 and are given in Table 5.2. The maximum adsorption capacity is the solid-phase concentration corresponding to a condition in which all the available sites are filled. Thus, the isothermal data was used to calculate the maximum adsorption capacity of chitosan by substituting the required equilibrium concentration in the Langmuir equation.

Table 5.2: Langmuir constants for zinc adsorption at different temperatures

Temperature (K)	qmax qmax=KL.b-1 (mg Zn.g chitosan-1)	b (l.mg-1)	KL (l.g-1)
313	135	0.020	2.677
308	136	0.018	2.444
303	135	0.016	2.175
298	122	0.013	1.611
293	105	0.012	1.218

McKay et al., 1989 reports the following Langmuir constants for chitosan beads, a maximum adsorption loading of between 98 and 120 $mg.g^{-1}$, an affinity parameter of 0.013 $l.mg^{-1}$ and a K_L value of 1.3 $l.g^{-1}$ at 298K. Thus, comparing well with the chitosan membranes.

The difference in qmax to temperature is explained due to the fact that chitosan membranes are gel type membranes where free volume plays an important role (Krajewska, 2001). An increase in temperature results in an increase in free volume. This increase in free volume "opens up" the membrane for better contact to adsorption sites, thus resulting in higher adsorption. The effect is only evident to a temperature of 303 K after which the adsorption capacity remains constant. The data shows a very good correlation between the calculated and the experimentally measured values of zinc concentration in the solid phase.

5.5.2 The effect of temperature on adsorption

The influence of temperature on the Langmuir equilibrium constant was studied. The Langmuir constant b, can be used to determine the enthalpy of adsorption, using the Van Waals equation (Equation 5.11), in the linear form:

$$\ln(b) = \ln(b_o) - \frac{?H_{ads}}{R.T} \qquad 5.14$$

Hence a plot of ln b versus (1/T) Figure 5.16, yields a slope of $(-\Delta H_{ads}/R)$ from which ΔH_{ads} is calculated.

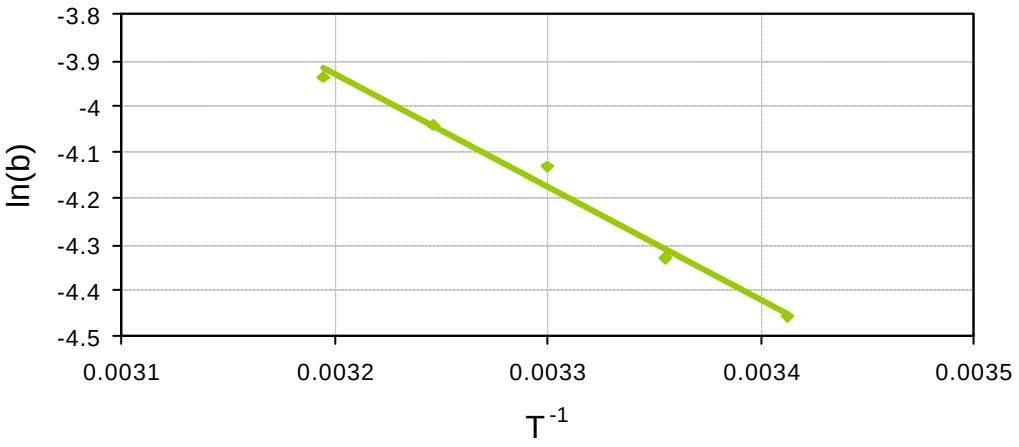

Figure 5.16: Van der Waals plot of Zinc sorption onto a 0.8 mm chitosan membrane

The enthalpy change (ΔH) for zinc was determined from the slope of Figure 5.16 as 20 kJ.mol^{-1}.The ΔH value of zinc suggests an endothermic reaction. A rise in temperature will favour the adsorption in an endothermic adsorption reaction, as oppose to an exothermic reaction. Although adsorption is generally an exothermic process; McKay et al., 1989, who determined the enthalpy change to be 17.7 kJ.mol^{-1}, also found an endothermic reaction.

5.5.3 Dynamics of zinc adsorption by chitosan membranes

In Figure 5.17, the breakthrough curve of a 50 ppm, 100 ppm and 500 ppm zinc solution for an applied pressure difference of 100 kPa is given. The same Figure also compares the breakthrough with the breakthrough curves for copper as obtained by Grant, 2000 and Osifo, 2003. The zinc ions can be removed from the solution below a level of 2 ppm up to a membrane capacity of 50%. After the membrane has reached 40% of its capacity, the removal efficiency drops significantly. Thus, a membrane can treat a 100 mg.l^{-1} zinc solution effectively to 20 times its bedvolume. Compares to packed bead columns that can treat effectively to 15 times its bedvolume for a 50 ppm Cu^{2+} solution (Grant, 2000) and 50 times its bedvolume for a 10 ppm Cu^{2+} solution (Osifo, 2003). Taking into account that the adsorption capacity for copper is higher than the capacity for zinc it is expected that the 50 ppm copper should have a higher bedvolume capacity than the 50 ppm zinc solution, which is not the case. This indicates an advantage of chitosan membranes above other forms of chitosan (chitosan powder, chitosan flakes and chitosan beads).

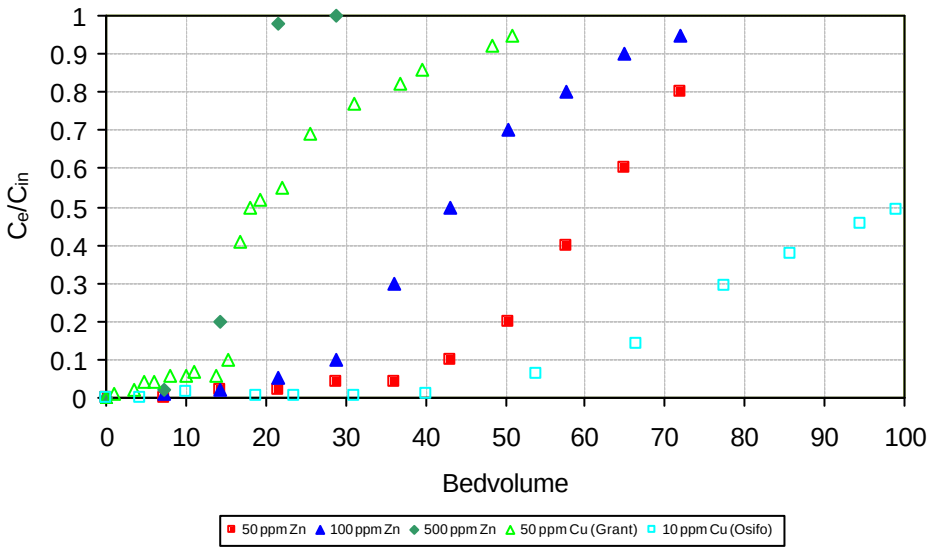

Figure 5.17: The breakthrough profile of zinc solutions (Membrane thickness = 0.8 mm and 100 kPa pressure difference) compared to copper solutions

Figure 5.18 illustrates the effect of membrane thickness on the breakthrough profile for zinc. Thicker membranes produces slightly better breakthrough profiles because of the higher crosslinking at thinner membranes. The similarity in the breakthrough profiles proves that the velocity does not influence the breakthrough curves and therefore proves the absence of internal diffusion limitations which exist with chitosan beads.

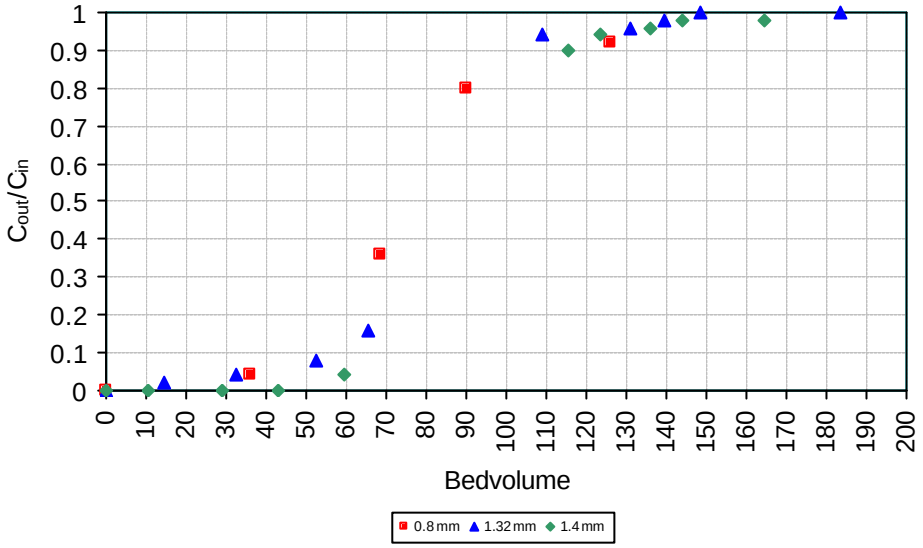

Figure 5.18: Schematic drawing of the breakthrough profile for zinc solutions

5.5.4 Adsorption of other metal ions

The focus of this will be on the metal ions copper, nickel and zinc. Table 5.3 shows the theoretical metal uptake (Equation 5.15) and the experimental uptake for SA produced chitosan. The results are for metal concentrations of 500 mg.l^{1} at a pH of 6. The theoretical adsorption capacity was calculated from the theoretical number of amine sites in chitosan and the assumption that two sites are required to react with one metal ion divalent. The DDA was 0.77 and the degree of crosslinking (DOC) was 0.2.

$$q_{theoretical} = \left(\frac{m_{chitosan}}{Mw_{monomer}} \right) (1 - DOC)(DDA) Mw_{metaladsorbed} \qquad 5.15$$

The metal ion adsorption calculated using this equation is similar to the metal ion adsorption observed by Muzzarelli (1977) and Bassi (2000).

Table 5.3: Theoretical and experimental adsorption capacity for SA chitosan

Metal	Theoretical adsorption capacity (mg/gchitosan)	Experimental adsorption capacity of chitosan membranes (mg/g chitosan)
Zinc	149	122
Copper	147	182
Nickel	135	100

Chitosan membrane adsorption is evaluated by comparison to other adsorption materials. Table 5.4 is a summary of results obtained from literature. This proves that chitosan membranes are comparable (or even better) to other adsorbents and that higher adsorption can be obtained due to forced contact between the adsorbent and the metal.

Table 5.4: Chitosan membrane adsorption compared to the highest adsorption capacities on other adsorbent materials for the metal ion zinc

Material	Adsorption capacity (mg Zinc g-1)	Reference
Chitosan membranes	122	This study
Chitosan powder	75	McKay et al, 1989
Chitosan flakes	83	Levan et al, 1998
Chitosan beads	50	Osifo, 2003
Chitin	18	Chui et al, 1996
Activated sludge	25	Atkinson et al. 1998

5.5.5 Desorption and recovery

The membranes prepared for desorption studies were first subjected to adsorption. During the adsorption process the membrane was treated with 500 $mg.l^{-1}$ zinc solution at a pH of 6. The solution concentration before and after treatment was analysed to determine the adsorption capacity. Desorption was carried out by treating the membranes in separate experiments with distilled water and solutions of hydrochloric acid (pH=2 and 4), and sulphuric acid (pH=2 and 4). A volume of 200 ml acid was used per treatment. Figure 5.19 is a summary of the mass % zinc that was desorbed and the mass % membrane loss during regeneration treatment. The following observations were made during the experiments: There was a significant membrane mass loss after each cycle and the membrane looses adsorption capacity after each cycle.

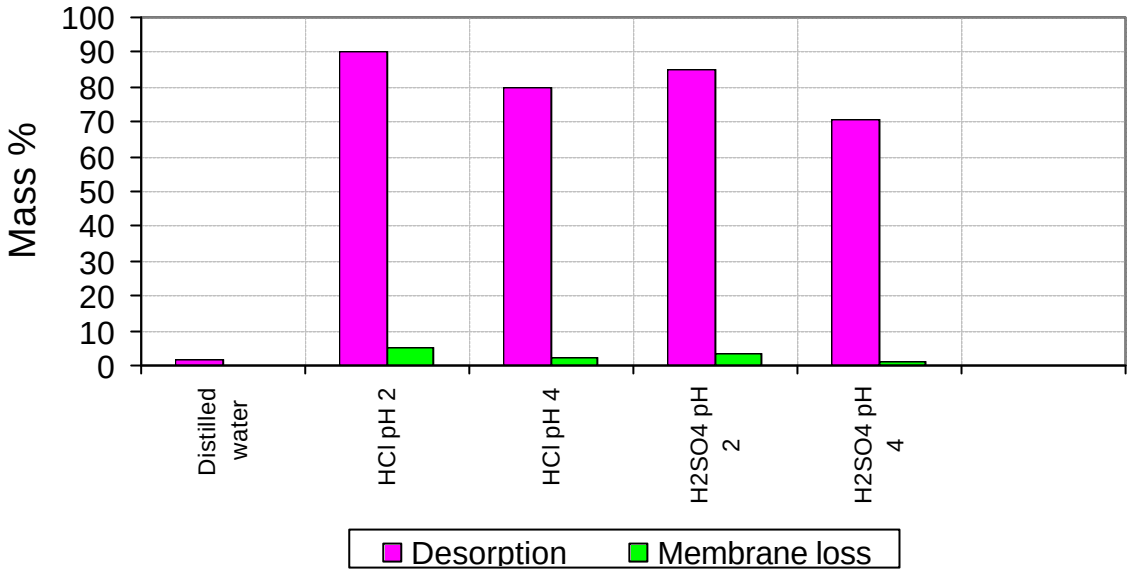

Figure 5.19: Schematic drawing of the regeneration of chitosan membranes using different acids

No significant concentration of ions was desorbed by water. As seen from Figure 5.19 it is clear that sulphuric acid is the best regeneration acid. Although desorption is lower as with hydrochloric acid, the membrane loss is also lower. It has been shown by Milot et al (1997) that chitosan is less soluble in sulphuric acid than in hydrochloric and nitric or organic acids. The effect of a high adsorption decrease during the treatment using hydrochloric acid can be described by the effect of chlorides on the adsorption. During the first cycle, if 165 mg of zinc was adsorbed on a membrane, 140 mg of the zinc will be recovered from the membrane if sulphuric acid at a pH of 2 is used, the acid will contain 700 mg.l^{1} zinc.

To investigate the amount of cycles a membrane can undergo before destruction of the mechanical strength of the membrane, sulphuric acid was used. The reason for using sulphuric acid is the low loss in membrane mass, thus more recycle cycles are possible. Figure 5.20 illustrates the change in adsorption capacity, desorption of zinc, and membrane mass loss as a function of recycle cycles. From this figure, it is clear that at best, the membrane can be regenerated twice, thereafter the membrane forms localised points where the flux is high and very little adsorption is detected.

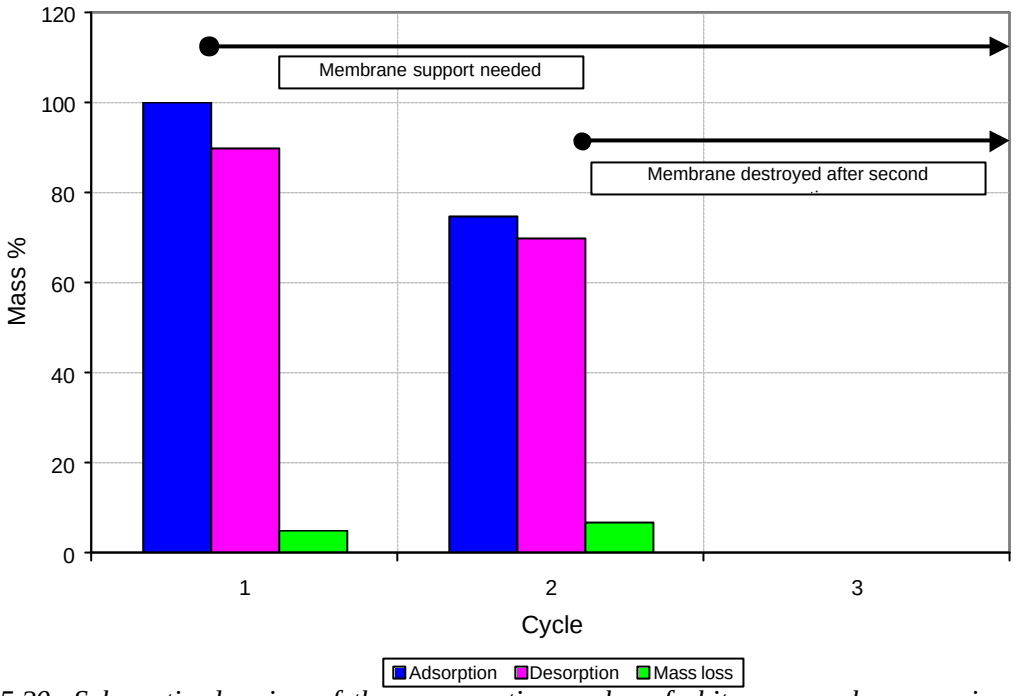

Figure 5.20: Schematic drawing of the regeneration cycles of chitosan membranes using sulphuric acid solution at a pH of 2

5.6 Conclusions

Chitosan membranes were manufactured by controlling the concentration of chitosan in the chitosan/acetic acid solution and the concentration of NaOH in the precipitation bath, followed by crosslinking. The physical properties of the crosslinked chitosan membranes were 1080 < wet membrane density < 1100 $kg.m^{-3}$, 2.2 < Dry content < 5.2 mass %, 0.65 < wet porosity < 0.67, 40 < maximum pore radius < 45 nm, and $1.18*10^5$ < Total surface area < $1.2*10^5$ $m^2.kg^{-1}$.

Both from structural and transport properties it can be concluded that the manufactured chitosan membranes can be modelled as ultrafiltration (UF) membranes with capillary pores. SEM pictures of dried chitosan membranes show a porous structure comparable with UF membranes and justify the average pore diameter. The transport of clean water through the membrane can be described with the Hagen-Poiseuille using an average pore diameter of 47 nm; a value that is also comparable to UF membranes. An osmotic pressure model describes the flux of solvent (water) and solutes (zinc ions) adequately.

Equilibrium isotherm studies reveal that the sorption of zinc onto chitosan can be described by a Langmuir equation. This study has shown that the adsorption of metal ions by chitosan membranes is largely affected by the pH of the solution, and therefore the metal ion identity, contaminants, initial concentration of metal ions, co-ions, reaction time, and the membrane

thickness. The adsorption process is endothermic although adsorption is normally an exothermic process. A maximum adsorption of 136 mg Zn/g was obtained, a value that is influenced by temperature and relative large compared to other adsorbents. After adsorption, a membrane with high zinc concentrations in its structure is obtained, from which metals can be recovered by washing the metal-complexed chitosan membranes with acidic solutions. As the pH of the elution solution was decreased from a pH of 6 to a pH of 3, zinc was removed. This in turn causes a decrease in the adsorption capability of the chitosan. The membranes were stable for 2 cycles, after which the membranes wer not usable anymore. A better crosslinking process is recommended, also to obtain the chitosan in the interior of the membrane to be stable.

6 IMMOBILISED CHITOSAN

Chitosan has been studied in the form of beads and membranes in the previous chapters. In this chapter, chitosan is immobilised, as a thin layer, on a support. By using a thin layer, the chitosan can be used very efficiently, since the transport path is rather small. As a support, ceramic membranes have been used.

6.1 Characterisation of ceramic support and chitosan coating

6.1.1 Strength test of supports

The strength of the support was tested for compressive stresses. A type of 3-point bending test was carried out as described Steenkamp et al. (2001). A force was exerted on the outside of the tube by means of a metal rod on one side of the tube, while two other metal rods supported the tube on the other side. The strength (exerted stress) of the tube was calculated from the force of rupture/breakage, the dimensions of the tube and the distances between the metal sticks.

6.1.2 Structure of support

Pore size and porosity of the support were determined using mercury porosimetry (Autopore III, Micromeretics). The microstructure of a cross section as well as of the inner and outer surface of the ceramic support was examined with SEM (Philips XL 30). The microstructure of the chitosan layer was also examined. The distribution of the Cu^{2+}-ions after adsorption in the composite membrane was examined with the EDX unit of the SEM.

6.1.3 Flux and adsorption experiments

The structure of the membrane support was also characterised with water and N_2 transport at room temperature at pressures ranging from 0.2 to 1 MPa. The water permeability set-up was also used for Cu2+-adsorption measurements at a pressure of 0.6 MPa. A 50 mg/l Cu^{2+}-solution (as $CuSO_4.5H_2O$) was permeated through the membrane until no further adsorption could be detected. A Varian AA 250 atomic adsorption spectrometer was used to analyse the Cu^{2+} - concentrations in the feed and permeate. The inaccuracy of the analysis was ± 0.5 mg/l Cu^{2+}, which was also the lower limit of the analysis.

6.2 Characterisation results

6.2.1 Support characterisation

In Table 6.1, the structure, strength and water transport properties of the casted ceramic supports are shown as a function of the type of powder (mixture) and the sintering temperature. The pore radius is a function of the particle size of the powder and decreases with decreasing particle size. The porosity of all samples sintered at 1050°C was almost equal

(38-41%), but decreased with increasing sintering temperature, especially for the smaller particle sizes.

Table 6.1: Properties of the different types of ceramic tubular supports

Tube Type	Sint. Temp. (^oC)	Pore radius (nm)**	Porosity (%)	Stress (MPa)	Water flux exp. (mol/m^2.s.Pa) x10^6	Water flux calc. (mol/m^2.s.Pa) x10^6
AKP-15	1050	100 (5)	41	320	6.8*	6.4
AKP-15	1150	90 (5)	41	230	6.1	5.3
AKP-15	1200	99 (5)	36	830	4.4	4.8
AKP-30	1050	51(2)	37	470	1.35	1.38
AKP-30	1150	50 (2)	36	840	1.26	1.28
AKP-30	1200	44 (2)	30	1600	1.07	0.67
AKP-15/30	1050	57 (5)	38	440	2.9	3.0
AKP-15/30	1150	59 (5)	32	860	2.7	2.5
AKP-15/30	1200	55 (5)	32	1100	1.5	1.7

* Molar flux of N_2-gas = 2.6 to 4.3 x 10^{-6} mol/m^2.s.Pa for a AKP15/1050^{o}C at pressures ranging from 200 to 1000 kPa

** Standard deviation of pore radius is given in parentheses

A simple qualitative interpretation can be given for this sintering behaviour. For smaller particles, the number of contact points per volume, as well as the driving force for transport is larger, due to larger curvatures of pore surfaces. At lower temperatures, surface diffusion is dominant, which does not lead to a decrease in pore volume. At higher temperatures, grain boundary diffusion plays a larger role, resulting in the decrease of pore volume. This argument can also be used to explain the increase in strength with increasing sintering temperature. Larger amount of contact points per volume, larger contact area and lower pore volume all increase the strength of the porous material.

Water flux through the support is also a function of the structure. The flux J described by the Poisseuille equation

$$J = \frac{e}{t}\frac{r^2}{8h}\frac{\Delta P}{\Delta x} \qquad 6.1$$

was used to calculate the water flux from the structural properties and to compare this flux with the measured flux. A correction was made for the use of cylindrical co-ordinates.

In the equation, ε is porosity (%) and τ (-) is tortuosity, which is estimated as 2.5, a characteristic value for packed beds of spherical particles. The pore radius is r (m) and the driving force is pressure difference ΔP (Pa) over the thickness Δx (m). Almost all calculated flux values are within 10% of the measured values, so the structural parameters can describe

the water transport very well. The N_2 gas transport is a function of the pressure. This transport is a sum of Knudsen diffusion and viscous flow. At higher pressures, the density of the gas is larger and therefore also the contribution of viscous flow (more momentum exchange between molecules). Surprisingly, the value of the molar nitrogen flux is comparable to the value of the molar water flux and if corrected for the Knudsen factor ($(M_{N_2}/M_{H_2O})^{1/2} = 1.25$), it is almost equal.

The inner surface of the tube of an AKP-15 support sintered at 1150°C is shown in Fig. 6.1. The packing is very regular and the surface is very smooth. Tubes of other compositions and sintered at other temperatures are similar in appearance.

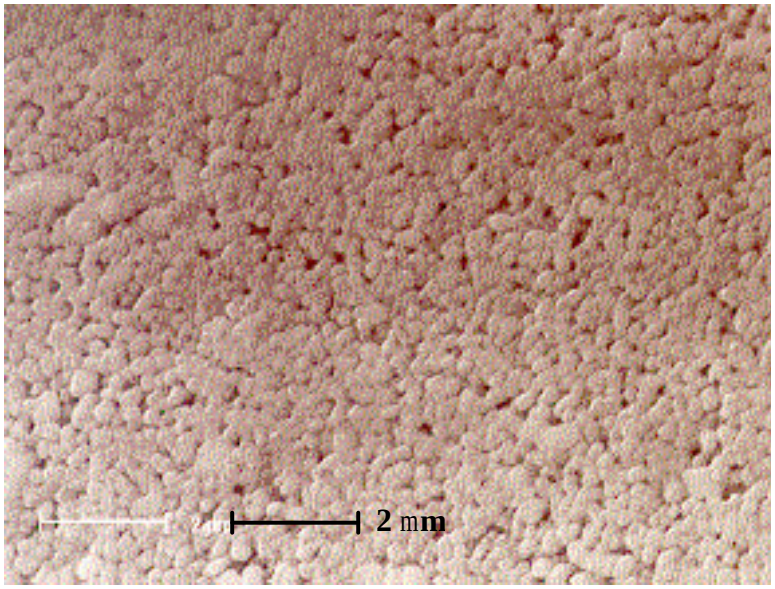

Figure 6.1: SEM picture of an inner surface of a centrifugal casted AKP-15 support sintered at 1150°C

6.2.2 Chitosan layer characterisation

Normal dipping and drying of pure chitosan did not lead to a coherent coating. The adherence with the support was poor. A SEM picture of a CHI-NaOH membrane is shown in Fig. 6.2.

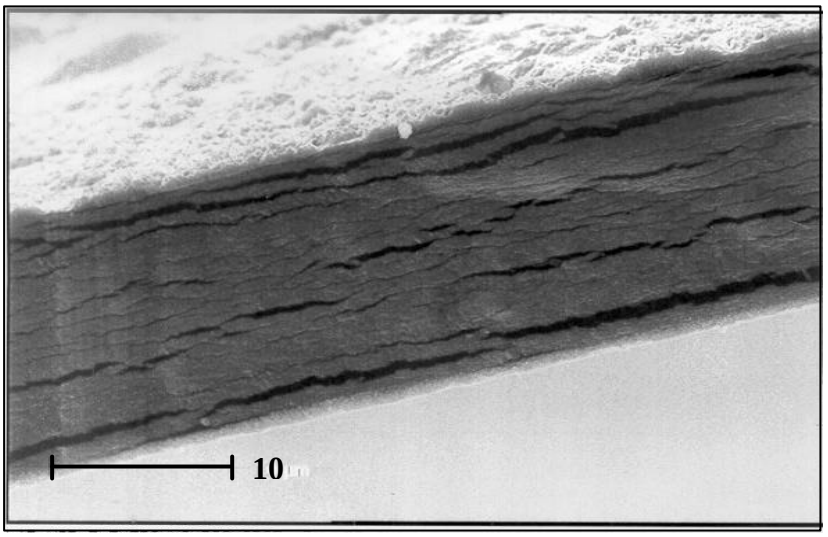

Figure 6.2: SEM micrograph of Chi-NaOH membrane before adsorption of $Cu2^{+}$

The layer is about 14 μm thick and seems to consist of layers parallel to the support surface. Some voids are visible between the layers. The Chi-Si-NaOH chitosan membrane, as shown in Fig. 6.3, is about 17 μm thick and seems to be much more porous than the previous layer. This was expected because silica is used as a porogen, which is dissolved during the NaOH treatment. One other feature has to be mentioned. The surface of the chitosan coating still seems to be rather dense. This can probably give some problems due to fouling. The Chi-Si-NaOH -Cross membrane, as shown in Fig. 6.4, is about 16 μm thick. The structure strongly resembles the one shown in Fig. 6.3, although some voids are visible in the top of this coating as was the case for the Chi-NaOH layer. It seems that with this method, different structured chitosan coatings can be obtained with a thickness of about 15±2 μm.

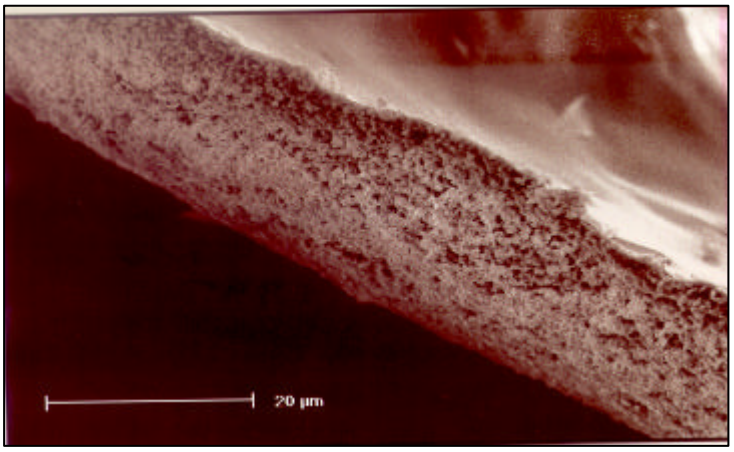

Figure 6.3: SEM micrograph of Chi-Si-NaOH membrane after $Cu2^{+}$ adsorption

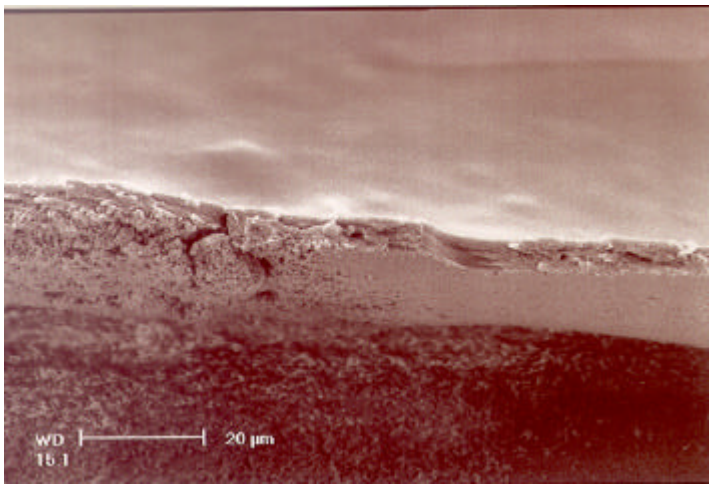

Figure 6.4: SEM micrograph of Chi-Si-NaOH-Cross membrane after $Cu2^+$ adsorption

The pure water transport properties of these composite membranes are shown in Table 6.2. An AKP-30/1050°C was used for the coating process because of the finer structure and the higher strength compared to the AKP-15 supports. The decrease in transport resistance of the coating in the sequence Chi →Chi-NaOH →Chi-Si-NaOH→Chi-Si-NaOH-Cross is clearly shown. It is clear that silica does act as a porogen for the chitosan layer. The resistance of the cross-linked layer is only 22% of the total composite membrane (support + coating).

This means that, in this case, the support determines the total flow rate. An AKP-15/1050°C support has about a 5 times higher permeability and then the total permeability of the composite membrane would be about 3 times higher (3-3.5x10^{-6} mol/m^2.s.Pa). An optimum has to be found between the mechanical strength and transport properties of these membranes. However, from the values found with the force of rupture measurements, the AKP15/1050°C supports seem to be strong enough to withstand pressures of at least 1 MPa.

Table 6.2: Liquid transport data of pure water, the $Cu2^+$-solution and the relative resistance of the chitosan coating for several alumina/chitosan membranes

Membrane	Permeance Clean water (mol/m^2.s.Pa) x10^6	Resistance top layer/total resistance (%)	Permeance Cu^{2+}-solution (mol/m2.s.Pa) x10^6	Resistance top layer/total resistance (%)
Support (AKP-30 /1050°C)	1.35	0	-	-
Support + Chi	0.17	87	-	-
Support + Chi-NaOH	0.76	43	0.37	73
Support + Chi-Si-NaOH	0.93	30	0.35	75
Support + Chi-Si-NaOH-Cross	1.06	22	1.16	14

6.3 Results and discussion adsorption

A 50 mg/l Cu^{2+}-solution (as $CuSO_4$) was permeated through the different types of alumina/chitosan composite membranes. As expected, an α-alumina support and the Chi-membrane adsorb Cu^{2+} -ions only slightly (Fig. 6.5) and were therefore not used any further in the study on Cu^{2+} adsorption. This means that the α-alumina support shows no nanofiltration properties, contrary to the α-γ-membrane system as presented by AlamiYounssi et al. (1995). The other 3 composite membranes can adsorb copper below the level of 1 mg/l as shown in Fig. 6.5, which is below the accepted level of 1.3 mg/l (as Cu^{2+}). These membranes can therefore directly decrease the Cu^{2+}-level without waiting for hours and days for equilibrium, as is the case with beads and flakes. However, for both the Chi-NaOH and the Chi-Si-NaOH membranes, the water flux decreases as a function of time until a constant flux is obtained after about one hour. It seems that some fouling occurs with these membranes. As mentioned before, the thin, dense top layer of these coatings can be responsible for this fouling.

However, with EDX-SEM, no accumulation of Cu^{2+} could be found in this top of the coating. This fouling layer is probably too thin for EDX (penetration depth about 1 µm) and other techniques like Auger or XPS spectroscopy should be used.

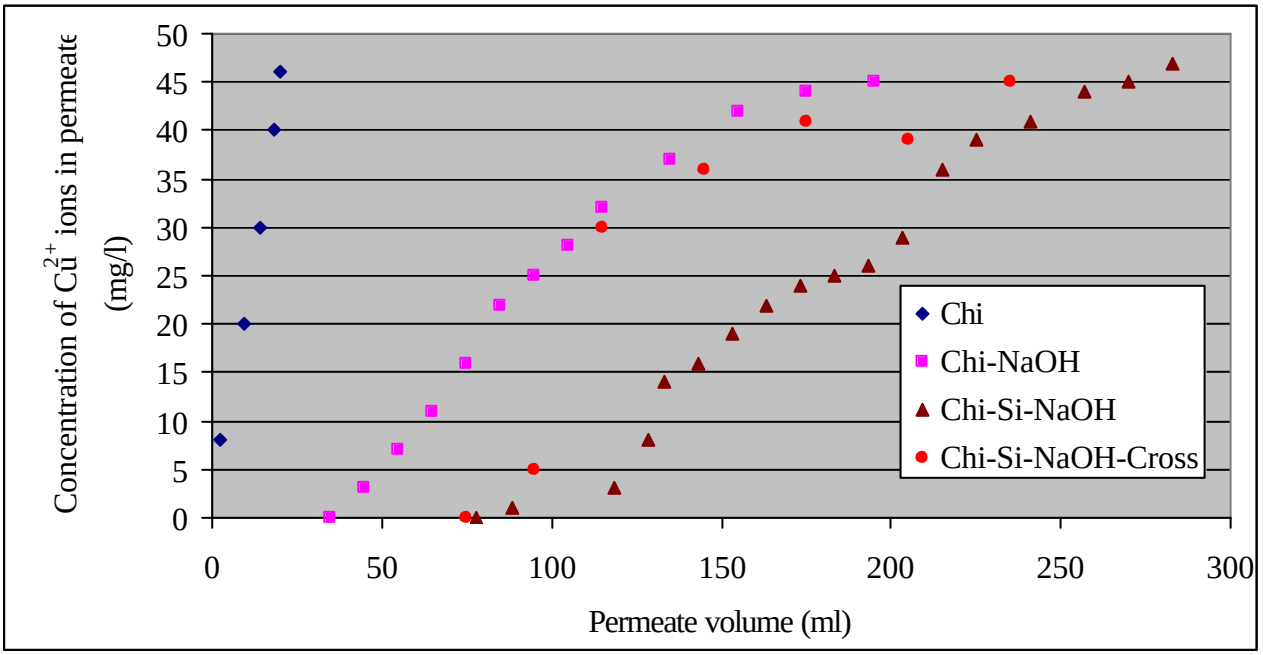

Figure 6.5: Concentration of Cu2+ ions in permeate as a function of the volume in the permeate

Surprisingly the cross-linked layer does not show that fouling. A reason for that is not so clear, but the top of this coating may be more porous. Both Chi-Si-NaOH and Chi-Si-NaOH-cross can remove about the same amount of copper below the level of 1 mg/l.

In Table 6.3 an estimation of the adsorption is shown. In this estimation, a top layer thickness of 15 µm and a porosity of 50% were used. The bulk density of chitosan is estimated as 1 g/cm^3. The amount of chitosan in the coated layer is then about 0.019 g. From this calculation, the Cu^{2+}-adsorption below the level of 1 mg/l is 0.2 ± 0.05 g Cu^{2+}/g chitosan (75±20 g Cu^{2+}/m^2 membrane area), which is surprisingly high even compared to equilibrium studies of other authors (Schmuhl et al., 2001, Findon et al., 1993, Udaybhaskar et al., 1990, McKay et al., 1989). This suggests that, in equilibrium studies with beads and flakes, not all adsorption sites are available even after 2 days of equilibrium.

Table 6.3: Comparison of literature values with the value obtained in this study for the maximum adsorption of Cu2$^+$ ions by chitosan

Source	Cu^{2+} adsorption below 1 mg/l level (mg/g)	Total Cu^{2+} adsorbed (mg/g)
Findon et al., 1993	-	60
McKay et al., 1989	-	29
Udaybhaskar et al., 1990	-	60
Schmuhl et al., 2001	-	80
This study: Chi-Si-NaOH membrane	150 75±20*	300 170±50*
This study: Chi-Si-NaOH-cross membrane	150 75±20*	200 110±35*

* g Cu^{2+}/m^2 of membrane area

In these beads and flakes, the structure can be denser as in our Chi-NaOH coatings. In the adsorption process with beads and flakes only diffusion can occur, while for the composite membranes, the Cu^{2+} flow is forced through the membrane. The structure of the chitosan coating is also more open since a porogen (silica) was used. The Chi-Si-NaOH membrane has a larger total adsorption for Cu^{2+} than the Chi-Si-NaOH-cross membrane (see Table 6.3, 0.45 vs. 0.3 g/g, 170 vs. 110 g Cu^{2+}/m^2 membrane area). This can be due to the differences in the number of adsorption sites or to the differences in the flow rate through the membranes. With cross-linking, some adsorption sites may disappear. The kinetics of adsorption can become slower at higher adsorption values of Cu^{2+} and at higher flow rates, equilibrium of adsorption of Cu^{2+} on chitosan is not reached anymore. This supports the idea in of Schmuhl et al. (2001), that there may be 2 different types of adsorption sites, one type with fast adsorption kinetics and one type with slower adsorption kinetics.

The adsorption part of this study is still far from complete. Other supports with higher permeability can be used. The structure of the porous membrane top layer can still be changed and also the thickness may be a parameter in the adsorption due to differences in capacity and in flow rate. One can investigate the adsorption as a function of the flux and the Cu^{2+}-concentration in the flow may also be changed. This will generate a large amount of new data and will give the possibility of a better understanding of the adsorption mechanism and kinetics. However, this paper shows that these composite membranes are relatively easy to prepare while having a large potential in the adsorption of heavy metals. The desorption step has still to be investigated, but pH changes can probably be used as an indication. However, the chitosan membrane should then be insoluble in low pH environments and therefore cross-linked membranes like Chi-Si-NaOH-cross are preferred.

6.4 Conclusions

Tubular alumina supports with smooth inner surfaces were manufactured with the centrifugal casting method. The pore radii of these supports varied between 45 and 100 nm and the porosity between 30 and 40%. Strength increased from 300 to 1600 MPa with decreasing pore size, porosity and particle size and increasing sintering temperature. The water permeability varied between 1 and 7 mol/m^2.s.Pa, which could also be calculated from the structural parameters using the Poisseuille equation for cylindrical geometry.

The inner surface of the alumina tubes was coated with a porous chitosan layer of about 15 µm thickness. The porosity of this coating was improved using silica as a porogen. A phase inversion method with pH variation as solvent-non-solvent parameter was used to create the porous structure.

The alumina/chitosan composite membrane was used to remove Cu^{2+} ions from a 50 mg/l $CuSO_4$ solution. After permeation, the Cu^{2+} concentration was below 1 mg/l for the phase inversion membranes with an adsorption capacity of about 0.2 g Cu^{2+}/g chitosan. The cross-linked chitosan membrane is preferred because of the larger stability as a function of pH needed for the desorption of the Cu^{2+} -ions.

7 ECONOMIC CONSIDERATIONS

Chitosan is only made at a relative small scale and finds most applications in the pharmaceutical industry. The world market is only about 10 000 ton/year and the largest producer of chitosan (biopolymer engineering) produces about 2000 ton of chitosan annually, in the form of chitosan flakes. The market ranges with volume of purchase; buying a quantity of about 100 kg the price is $55.00/kg and for volume of 2000 kg the price will be $35.00/kg, making the material the determining factor in a potential chitosan treatment plant if chitosan is not produced locally. Rorrer (2002) calculated a production price of chitosan of $ 15.50/kg

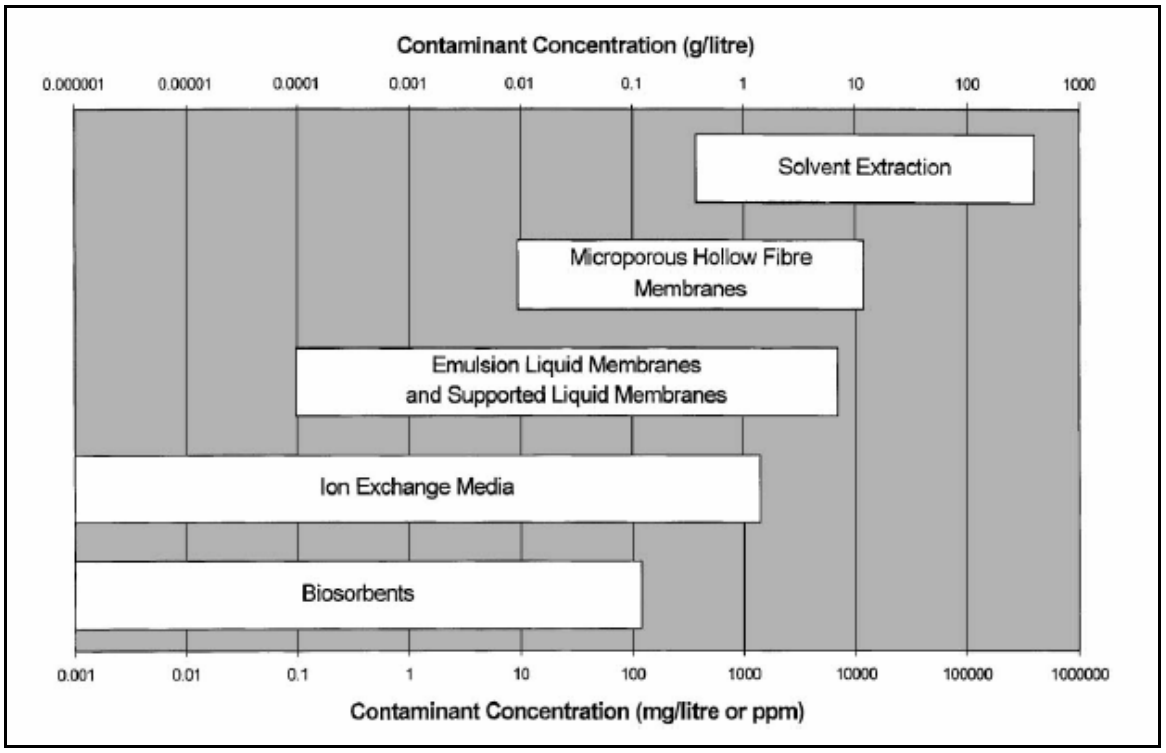

Figure 7.1: Different treatment techniques for different contaminant concentrations

Figure 7.1 shows that biosorbents (including chitosan) can best be used at relative low contaminant concentration (<100 mg/L); so at larger concentrations, different techniques should be used and possibly chitosan treatment can be used as a final step in the total wastewater treatment. It is to be mentioned that electrochemical processes are not mentioned in Figure 7.1, but can also be used over a wide range of concentrations (5 -1000 ppm). In the bead column experiments it was shown that a minimum of 550 Bedvolumes (cycle 1, 2 and 3 together) could result in the production of water with a concentration below 1 ppm (WHO limit). A column with a total mass of beads of about 100 g was used for this purpose (5 gram of chitosan was present in the beads). A total of 55 L of 10 ppm copper could be treated with this column, making the costs for chitosan on about $ 3 per m^3 water (it is assumed that no cost is charged for the waste water), which is still relative expensive in comparison with other

techniques (i.e. ion exhange resins cost about $ 2 – 5, and could also be used in more cycles; activated carbon is relative expensive, having a price of $4-5 (CSIRO, Enecon's webside)).

If the beads are produced locally, the total price to produce chitosan is equal to the costs for manufacturing chitosan from sea food waste consists of the costs for getting the material, producing chitin from this waste material, producing chitosan from the produced chitin and formulation of the chitosan (beads or membranes). The chemicals to produce the final product are NaOH, HCl and aceitc acid.

The bulk-prices of these materials were obtained from www.chemspy.com and are NaOH (50%): $ 0.10/kg and HCl (36%): $ 0.22/kg and acetic acid (98%): $ 0.68/kg.

The total price for cleaning 1 m^3 wastewater is now reduced by a factor 6 to about $ 0.50/m^3 (price of chitosan production is now $ 5/kg. 87% of the costs are the costs needed for the production of chitosan from chitin, since a large excess of NaOH is used (45:1). If a suitable technique will be found to recycle the largest part of the NaOH (stoechiometrically, only a factor of 0.5:1 is necessary), the cost of chitosan will be reduced to $ 0.70/kg and the wastewater to treat to $ 0.06/m^3.

The total price does not include the costs for collection of the raw material. After private communication with several sea-fish restaurants it seems to be troublesome to collect it from these origins. There are mainly two reasons for this:

1. The owners are not really prepared to store the waste material since strict hygienic rules are present in the kitchens of these restaurant (only a daily collection would be appropriate to the owners)
2. The amount of material is very limited, so a daily collection would be troublesome and expensive.

A possible chitosan plant should therefore be located close to the raw material, i.e. large seafood processing industries, or another source of chitosan (e.g. fungi) should be used to produce chitosan. In the cost analysis, the costs of collection of the raw material are not taken into account.

The detailed estimation of the costs for a large scale chitosan adsorber / desorber column fall outside the scope of this study and are estimated to be relatively small compared to the raw materials used; so will not increase the price dramatically.

8 GENERAL CONCLUSIONS

In this study, different forms of chitosan have been prepared from chitin flakes, obtained from rock lobster waste from the seafood processing industry by BioSpec (Cape Town), in order to use the chitosan material for the adsorption of heavy metals from wastewater. Firstly, the chitin flakes were converted to chitosan flakes, and after characterisation of the material, large similarities with commercial chitosan (biopolymer engineering) were found. Since flakes do not have good adsorption characteristics and are difficult to use in large equipment, other formulations (beads, membranes and immobilised chitosan) were prepared for the experimental adsorption studies. All formulations techniques used, were based on the phase inversion method, in which chitosan is dissolved in acetic acid and later precipitated in a caustic soda bath. Using this method, a gel type of material is formed, which contains predominantly water (93-96%) and the balance chitosan (4 – 7%). Initial experiments showed that chitosan in the gel form has much better adsorption characteristics than chitosan flakes (affinity parameter is at least a factor 10 higher for beads compared to flakes).

When using beads, a high adsorption capacity of 160 mg/g for copper was obtained, and the affinity parameter was 0.07 L/mg, values that are larger than reported values for activated carbon and measured values for ion exchange resins (in this study Amberlite 200C was used as reference). During adsorption column experiments using a 10 ppm copper solution, at least 550 Bed-volumes were processed to a < 1 ppm (WHO limit) effluent solution, in three cycles of adsorption and desorption. The copper could be recovered using an acid of pH = 1, obtaining a copper solution of 1200 ppm, which could be processed further to obtain the metal in its pure form back. The beads were stable to only 5 cycles, using the high acid concentration. When milder desorption conditions (pH = 2), the effluent copper solution only contained about 100 mg/g, making further processing more difficult. During the adsorption process, the diffusion inside the beads played an important role in the total mass transfer. An effort was therefore undertaken to reduce the size of the beads, which resulted in beads with an average diameter of 1.8 mm, a size that still results in a negligible pressure difference over the column. The costs for the treatment of water using chitosan beads were approximated at $ 0.06/m^3.

For the chitosan beads, a novel adsorption model has been developed, which take the acid base characteristics of the chitosan into account. The new model can therefore be used at any pH, for both adsorption and desorption. From this model, it could be concluded that the chitosan has the largest affinity to copper, followed by lead, nickel, zinc and cadmium

Chitosan membranes have been prepared according to a method quite similar to the production of beads. The membranes were characterised and it was found that the membranes could be modelled as a porous hydrated membrane and showed large similarities with ultrafiltration membranes, both for the flux of clean water and salt solutions. The membranes showed large affinities to Zn (maximum adsorption capacity 135 mg/g and affinity parameter of 0.02 mg/L at a pH of 6). The adsorption could well be described with a Langmuir isotherm in the region from 20 – 40 °C. The adsorption capacity increased from 20 – 30 °C and remained constant between 30 and 40 °C. The increase of the capacity could be due to a better accessibility of sites, caused by an increase in free volume of the biopolymer. The affinity parameter also increased in temperature, indicating an exothermic adsorption process. The membranes could be recycled effectively (>95%) using sulphuric acid (pH = 2), but after 2 cycles of adsorption and desorption the membranes were damaged and could not be used anymore. This was possibly caused by the acid, which was pumped through the membrane during desorption (SEM analysis revealed that after crosslinking the edges of the membrane were more crosslinked than in the centre of the membrane).

Immobilised beads were prepared by the coating of a thin chitosan layer (around 20 μm) on an alumina support. Very high adsorption capacities (> 200 mg Cu/g) were obtained when a porogen was used. The porogen makes the active sides easily available. Although excellent adsorption characteristics have been obtained, the production of ceramic support is still very expensive (> \$ 200 / m^2), which makes this technique less applicable for water purification.

In general, we can conclude that chitosan (in the gel form) is a very effective adsorbent. It can adsorb the studied metals Cu, Zn, Pb, Ni and Cd to very high values, higher than their economical counterparts, like activated carbon and ion exchange resins. Since chitosan is only produced at a small scale, the prices on the world market are relatively high (\$ 35/kg). Since the market for chitosan is rapidly growing (mainly for the application of fat absorber), price decreases are expected in the future. The production costs for the preparation of chitosan are largely determined by the conversion of chitin to chitosan; a process that uses an excess of caustic soda. Without reuse of the soda, a price of around \$6/kg is estimated. This price can be reduced to an approximated \$ 0.6/kg if the caustic soda is recycled effectively. The cost for cleaning contaminated water is than about \$ 0.06/m^3, not taken into account the investment for an adsorption/desorption plant. A general disadvantage of chitosan is that the stability is not very good. In the case of beads, chitosan could be recycled 5 times and for membranes only 2 times, which makes a long-term use of the biopolymer impossible. The harsh conditions, under which the desorption process takes place, is the main reason for this. Milder

desorption conditions, however, would result in a more dilute metal stream, which again is unfavourable for further processing and recovery of the metal.

In comparing the three formulations studied in this project, the following table can be presented, in which the three different formulations are compared on adsorption, flux, stability characteristics and costs.

Table 8.1: Pros and Cons for different formulations of chitosan

	Beads	Membranes	Immobilised on alumina
Adsorption	+	+	++
Flux	+ / -	+	+
Stability	+ / -	-	Not studied
Costs	+	+	--

Chitosan immobilised on alumina shows excellent adsorption characteristics above beads and membranes, but is rather expensive because of the high production costs involved in the preparation of the ceramic supports; also the low capacity per volume requires large equipment (only a thin layer of chitosan is deposited). Comparing chitosan membranes with beads, it can be concluded that beads are more stable than membranes. However, the advantage of using chitosan membranes is that a pressure difference is used to induce convective flow through the membrane, which in turn results in a higher throughput, compared to the diffusive transport inside the bead, which is the rate determining step in the adsorption column (Also slightly higher adsorption capacities could be obtained with membranes, compared to beads). An improved crosslinking technique for membranes should be found in order to solve the stability problems. If such a technique could not be found, the use of adsorption beads in an adsorption/desorption column would be the recommended process, which can process metal contaminated wastewater at relative low concentrations (< 10 ppm) to disposal water, meeting the most stringent legislation, against a price of about $ 0.06/m^3.

9 REFERENCES

A.A. Adeyiga, L. Hu, T. Greer, *Removal of metal ions from wastewater with natural wastes*, Hampton: Hampton University, www.netl.doe.gov/publications/proceedings/98/98hbcu/liang_hu.pdf

S. Alami-Younssi, A. Larrbot, M. Persin, J. Sarrazin and L. Cot (1995), Rejection of mineral salts on a gamma alumina nanofiltration membrane, Application to environmental processes, *J. Membrane Sci.*, **102**, 123.

R. Bassi and S.O. Prasher (2000), Removal of selected metal ions from aqueous solutions using chitosan flakes, *Separation Science and Technology*. **35(4)**, 547.

T. Becker, M. Schlaak and H. Strasdeit (2000), Adsorption of nickel(II), zinc(II) and cadmium(II) by new chitosan derivatives, *Reactive and functional polymers*, **44**, 289.

R.B. Bird, W.E. Steward, E.N. Lightfoot (1960), *Transport Phenomena*, New York: John Wiley and sons.

G. Cárdenas, P. Orlando, T. Edelio (2001), Synthesis and applications of chitosan mercaptanes as heavy metal retention agent, *International Journal of Biological Macroolecules*, **28**, 167.

K.H. Chu (2002), Removal of copper from aqueous solution by chitosan in prawn shell: adsorption equilibrium and kinetics, *Journal of hazardous materials*, **B90**, 77.

V.W.D. Chui, K.W. Mok, C.Y. Ng, B.P. Luong and K.K. Ma (1996), Removal and recovery of copper(II), chromium(III) and nickel(II) from solutions using crude shrimp chitin packed in small columns, *Environment International*, **22(4)**, 463.

M. Conway, S. Holoman, L. Jones, R. Leenhouts and G. Williamson (1999), Selecting and Using Chelating Agents, *Chemical Engineering*. **March 1999,** 86.

L. Dambies, C. Guimon, S. Yiacoumi and E. Guibal (2001), Characterization of metal ion interactions with chitosan by X-ray photoelectron spectroscopy, *Colloids and surfaces A*, **177**, 203.

C. Faur-Brasquet, Z. Reddad, K. Kadirvelu and P. Le Cloirec (2002), Modeling the adsorption of metal ions (Cu^{2+}, Ni^{2+}, Pb^{2+}) onto ACCs using surface complexation models, *Applied surface science*, **7854**, 1.

A. Findon, G. McKay and H.S. Blair (1993), Transport studies for the sorption of copper ions by chitosan, J. Environ. Sci. Health, **28**, 173.

P. Ghandi (1997), Obtaining Copper-Free Water. *WATER/Engineering and Management*, **February 1997**, 18.

H.W. Grant (2000), Modelling the kinetics of cation removal from simulated waste water using Chitosan Beads, Potchefstroom: PU for CHE. (Dissertation – M.Eng.) 104 p.

E. Guibal, C. Milot and J. Roussy (1997), Chitosan gel beads for metal ion recovery. In: R.A.A. Muzarelli and M.G. Peter (eds.), *Chitin handbook*, Atec: European chitin society, 423.

E. Guibal *et al.* (2001), Competitive sorption of platinum and palladium on chitosan derivatives, *Int. J. of biological macromolecules*, **28**, 401

C. Huang, Y. Chung and M. Liou (1996), Adsorption of Cu(II) and Ni(II) by pelletized biopolymer, *Journal of hazardous materials*, **45**, 265.

K. Inoue, H. Hirakawa, Y. Ishikawa, T. Yamaguchi, J. Nagata, K. Ohto and K. Yoshizuka (1996), Adsorption of metal ions on gallium(III)-templated oxine type of chemically Modified Chitosan, *Separations Science and Technology*, **32(16)**, 2273.

A. Isogai (1997), Molecular mass distribution of chitin and chitosan. In: R.A.A. Muzarelli and M.G. Peter (eds.), *Chitin handbook*, Atec: European chitin society, 103.

K.C. Jansen, S.W. Voster, and H.W.J.P. Neomagus (2002). Adsorption desorption of Cu2+ ions on chitosan beads. Report of internship at the Potchefstroom University for Christian Higher Education.

E. Jansson-Charrier, E. Gulbal, J. Roussy, J. Delanghe and P.E. Cloirec (1996), Vanadium (IV) sorption by chitosan: kinetics and equilibrium. *Water Research*, **30(2)**, 465.

C. Jeon and W.H. Holl (2003), Chemical modification of chitosan and equilibrium study for mercury ion removal. *Water Research*, **37**, 4770.

I.N. Jha, L. Iyengar and A.V.S. Prabhakararoa (1988), Removal of cadmium using chitosan, *Journal of Environmental Engineering.* **114(4)**, 963.

X. Jiang, X., L. Chen and W. Zhong (2003), A new potentiometric titration method for the determination of deacetylation degree of chitosan. *Carbohydrate polymers*, **54(4)**, 57.

P.D.Johnson, M.A.Watson, J.Brown and I.A.Jefcoat (2002), Peanut hull pellets as a single use sorbent for the capture of Cu(II)from wastewater, *Waste management*, **22**, 471.

R. Juang, F. Wu and R. Tseng (1999), Adsorption removal of copper(II) using chitosan from simulated rinse solutions containing chelating agents, *Wat. Res.*, **33(10)**, 2403.

R. Juang and H. Shao (2002), A simplified equilibrium model for sorption of heavy metal ions from aqueous solutions on chitosan, *Water Research*, In Press, Uncorrected Proof, Available online 6 January 2002

A.K. Khan, K.K. Peh and H.S. Ch'ng, (2002), Reporting degree of deacetylation values of chitosan: the influence analytical methods, *Journal Pharm Pharmaceut Science*, **5(3)**, 205.

M. Kandah (2001), Zinc adsorption from aqueous solutions using disposal sheep manure waste (SMW), *Chemical engineering jounal*, **84**, 543.

A. Kapoor and T. Viraraghavan (1998), Removal of heavy metals from aqueous solutions using immobilized fungal biomass in continuous mode, *Water research*, **32(6)**, 1968

W. Kaminski and Z. Modrzejewska (1997). Application of chitosan membranes in separation of heavy metal ions. *Separations Science and Technology.* **32(16)**, 2659.

Y. Kawamura and H. Yoshida (1997), Effects of chitosan concentration and precipitation bath concentration on the material properties of porous cross-linked chitosan beads. *Separations Science and Technology*. **32(12)**, 1959.

Khan, A. K., Peh, K. K and Ch'ng, H. S (2002), Reporting degree of deacetylation values of chitosan: the influence analytical methods. Journal Pharm Pharmaceut Science, Vol 5(3), 205-212

D.C.K. Ko, J.F. Porter and G. Mckay (2001), Film-pore diffusion model for the fixed-bed sorption of copper and cadmium ions onto bone char, *Wat. Res.*, **35(16)**, 3876.

K. Kondo, H. Sumi and M. Matsumoto (1996), Adsorption characteristics of metal ions on chitosan chemically modified by D-Galactose, *Separations Science and Technology*. **31(12)**, 1771.

B. Krajewska (2001), Diffusion of metal ions through gel chitosan membranes. *Reactive and Functional Polymers,* **47**, 37

H. Kyoon No and S.P. Meyers (1997), Preparation of chitin and chitosan. . In: R.A.A. Muzarelli and M.G. Peter (eds.), *Chitin handbook*, Atec: European chitin society, 475.

J.T. Matheickal and Q. Yu (1999), Biosorption of lead(II) and copper(II) from aqueous solutions by pre-treated biomass of Australian marine algae, *Bioresource technology*, **69**, 223.

R. Maruca, B. Suder and J.P. Wightman (1982), Interaction of Heavy Metals with Chitin and Chitosan, *Journal of Applied Polymer Science.* **27**, 4827.

B.J. Mcafee, W.D. Gould, J.C. Nadeau and A.C.A. da Costa (2001), Biosorption of metal ions using chitosan, chitin and biomass of rhizopusoryzae, *Separation science and technology*, **36** (14), 3207.

G. Mckay, H.S. Blair and A. Findon (1989), Equilibrium studies for the sorption of metal ions onto chitosan, *Ind. J. Chem.*, **28**, 356.

C. Milot, J. McBrien, S. Allen and E. Guibal (1997), Influence of physicochemical and structural characteristics of chitosan flakes on molybdate sorption, *J. Appl. Polymer Sci.* **68**, 571.

D. Mohan and S. Chander (2001), Single component and multi-component adsorption of metal ions by activated carbons, *Colloids and surfaces A*, **177**, 183.

D. Mohan and K.P. Singh (2002), Single-and multi-component adsorption of cadmium and zinc using activated carbon derived from bagasse – an agricultural waste, *Water research*, **36(9)**, 2304.

L. Monser and N. Adhoum (2002), Modified activated carbon for the removal of copper, zinc, chromium and cyanide from wastewater, *Separation and Purification Technology*, **26**, 137.

O.A.C. Monteiro Jr. and C.Airoldi (1999), Some studies of crosslinking chitosan-glutaraldehyde interaction in a homogeneous system, *International journal of biologial macromolecules*, **26**, 119.

M. Mulder (1996). Basic Principles of Membrane Technology. 2nd ed. Netherlands: Kluwer Academic Publishers.

R.A.A. Muzarelli (1973), Natural chelating polymers. Alginic acid, chitin and chitosan. In: R. Belcher and H. Freiser (eds.), *International series of monographs in analytical chemistry. Volume 35. natural chelating polymers*, Oxford: Pergamon press

R.A.A. Muzzarelli, R.A.A (1974). Natural chelating polymers: Alginic acid, chitin and chitosan. Pergamon press.

R.A.A. Muzzarelli (1977), *Chitin*, Oxford: Pergamon Press

S.Y Nam and Y.M. Less (1998), Pervaporation performance of surface crosslinked chitosan membranes. *Journal of Membrane Science*, **153**, 155.

B.S. Pawlowski (1971). Determination of the iodine number of activated carbon. (Paper as part of analytical manual for SASTECH.) Sasolburg, 23 p.

M. Rhazi, J. Desbrières, A. Tolaimate, M. Rinaudo, P. Vottero, A. Alagui (2002a), Contribution to the study of th complexation of copper by chitosan and oligomers, *Polymer*, **43**, 1267.

M. Rhazi, J. Desbrières, A. Tolaimate, M. Rinaudo, P. Vottero, A. Alagui, M. El Meray (2002b), In ?uence of the nature of the metal ions on the complexation with chitosan. Application to the treatment of liquid waste, *European Polymer Journal*, Uncorrected proof, available online 5 Feb 2002

G.A.F. Roberts (1997), Determination of degree of N-acetylation of chitin and chitosan. Chitin Handbook. Edited by: Muzzarelli, R.A.A and Peter, M.G. European chitin society. 129.

G.L. Rorrer and J.D. Way (2002), Chitosan beads to remove heavy metals from industrial waste waters, Dalwoo-ChitoSan, ftp://dalwoo.com/chitosan/rorrer.html

M. Ruiz, A.M. Sastre and E. Guibal (2000), Paladium sorption on glutaraldehyde-crosslinked chitosan, *Reactive and functional polymers*, **45**, 155.

R. Schmuhl, H. Krieg, and K. Keizer (2001), Removal of heavy metals using chitosan, *Water SA*, **27,** 1.

G.C. Steenkamp, K. Keizer, H. W. J. P. Neomagus, and H. M. Krieg (2001), Centrifugal casting of ceramic membrane tubes and the coating with chitosan, *Sep. Pur. Tech.* **25**, 407.

G.A. Swan *et al.* (1975), Heavy metal removal from aqueous media. In: I. Zwiebel and N.H. Sweed (eds.), *AIChE Symposium series: Adsorption and ion exhange*, **152 (71)**, 96.

S.C. Tan, E. Khor, T.K. Tan and M.S. Wong (1998), The degree of deacetylation of chitosan: advocating the first derivative UV-spectrometry method of determination, *Talanta*, **45**, 713.

M. Terbojevich and A. Cosani (1997), Molecular weight determination of chitin and chitosan. In: R.A.A. Muzarelli and M.G. Peter (eds.), *Chitin handbook*, Atec: European chitin society, 87.

C. Tien (1994), Adsorption calculations and modelling. USA: Butterworth-Heinemann. 244 p.

P. Udaybhaskar, L. Iyengar and R.A.O. Prabhakara (1990), Hexavalent chromium interaction with chitosan, *J. Appl. Polymer Science*, **39,** 739.

E. Valdman, L. Erijman, F.L.P. Pessoa and S.G.F. Leite, Continuous biosorption of Cu and Zn by immobilized waste biomass Sargassum sp., *Process biochemistry*, **36**, 869.

B. Volesky (1989), Biosorption of Heavy Metals. Boston: CRC Press. 396 p.

W.S. Wan Ngah, C.S. Endud and R. Mayanar (2001), Removal of copper(II) ions from aqueous solution onto chitosan and cross-linked chitosan beads. *Reactive and Functional Polymers.* **50**, 181.

T.C. Yang and R.R. Zail (1984), Absorption of Metals by Natural Polymers Generated from Seafood Processing Wastes, *Ind. Eng. Chem. Prod. Res. Dev.* **23**,168

X. Zeng and E, Ruckenstein, Control of pore sizes in macroporous chitosan, and chitin membranes, *Ind. Eng. Chem. Res.*, **35** (1996) 4169.

Z. Zulfadhly, M.D. Mashitah and S. Bhatia (2001), Heavy metals removal in fixed-bed column by the macro fungus Pycnoporus sanguineus, *Environmental pollution*, **112**, 463.